AD NUMBER
AD829023
LIMITATION CHANGES
TO: **Approved for public release; distribution is unlimited. Document partially illegible.**
FROM: **Distribution authorized to U.S. Gov't. agencies and their contractors; Critical Technology; 30 OCT 1967. Other requests shall be referred to Space and Missile Systems Organization, Attn: SMSD, Los Angeles, CA 90045. Document partially illegible. This document contains export-controlled technical data.**
AUTHORITY
SAMSO ltr, 28 feb 1972

CONVAIR

A DIVISION OF GENERAL DYNAMICS CORPORATION
SAN DIEGO

144

CONVAIR

SAN DIEGO

REPORT ZA-259

DATE 30 October 1957

MODEL

TITLE

CALCULATION OF OPTIMUM SUPERSONIC DELTA WINGS

nationals ... only with prior approval of: Hq.SAMSO, LA., Ca. 90045 Attn: SMSD

Copy #5

J. H. Kainer

H. Yoshihara
Aerodynamics Group Engineer

GROUP Aerodynamics

REFERENCE

APPROVED BY D. H. Bennett
Chief of Aerodynamics

127

71

No. of Equations 285

REVISIONS

			CHANGE	PAGES AFFECTED

TABLE OF CONTENTS

1.0 SUMMARY

This paper presents the distributed and total drag-due-to-lift in closed form by means of linearized supersonic wing theory for delta wings having arbitrary warp described by a symmetrical ten-term power series expansion for which the loading was reported on previously by the author [1-3] and others [4-7]. For both sonic and supersonic leading edges one hundred drag contributions are derived, ninety of which are interference terms induced by the interaction of each loading with each of the non-corresponding downwashes. For subsonic leading edges additional terms are included to account for the suction forces induced by the leading edge pressure singularities.

The mean chord shape required to deflect under aeroelastic load to the desired shape computed herein has been programmed for the IBM 704 Digital Computer by the Dynamics Group.

2.0 INTRODUCTION

With the advent of supersonic operational aircraft during the past decade there has been increasing demand for improved procedures for predicting the distributed and integrated force and moment characteristics of wings, bodies, and complete aircraft configurations.

In regard to warped triangular wings, the steady-state forces (excluding drag) and moments have been fully developed and reported on by the author[1-3] and others[4-7] for a ten-term power-series approximation to the actual downwash. With the exception of a limited amount of additional terms by Roper[10], the excessive labor involved has precluded the analytical consideration of terms more than the first ten of the power series. It is recognized, however, that not only is it possible to obtain any desired number of solutions by means of high-speed digital computing equipment, but that some organizations have already, or are in the process of accomplishing this. For example, at Convair-San Diego the complete design problem has been mechanized for highly generalized planforms comparable to the method discussed herein. The Forth Worth Division of Convair utilizes power series expansions for the downwash which involve oblique Mach line coordinates.

Several noteworthy contributions were made to the development of low-drag delta wings particularly of the subsonic leading edge variety. Baldwin[11] warped subsonic leading-edge delta wings to support some non-singular specified distributions of lift. Tucker[12] presented a method to warp subsonic leading-edge wings. The assumed non-singular pressure distribution was replaced by four terms of a power series, the constants of which were chosen to satisfy the design lift, pitching-moment and the condition of nearly elliptic span loading. Tsien[13] studied subsonic leading-edge delta wings of the conical family cambered to give minimum pressure drag with and without full leading edge suction. Rodriguez, Lagerstrom and Graham[14] extended the drag reduction procedure

developed by Graham[15] whereby use is made of orthogonal loadings. Strand[16] applied the Graham[15] technique to the problem of sonic leading-edge delta wings. Using four terms of a Legendre polynomial representation for the downwash, the method produced nearly 7% drag reduction from the untrimmed flat plate. Grant[17] approximated Jones'[18, 19] criterion of constant downwash in the combined forward and reverse-flow fields by using Lagrangian multipliers to combine four non-singular loadings on delta wings having subsonic leading edges. To date the best wings were developed in a recent paper by Doris Cohen[20]. Generally, six terms of a power-series expansion for the downwash were used to determine the shape of subsonic, sonic and supersonic leading-edge delta wings. For the subsonic leading edges the results include the effect of full-leading edge suction thereby leading to greater reductions than the results of previous methods[11, 12, 13]. For sonic leading edges gains of 8.9% were reported for the series considered. A similar treatment was concurrently reported on by Fenain and Valée[21]. At Convair-Fort Worth Stewart and Danby and Stancil developed procedures for determining the shape of wings having nearly minimum drag-due-to-lift.

In order to achieve the leading-edge suction it is necessary, however, to bend the wing leading edge in the direction of the streamlines to avoid separation. Leading edge conical camber may be used to maintain satisfactory characteristics at subsonic speeds for wing shapes designed to operate at supersonic conditions. The optimum leading edge conical camber is a function of lift coefficient and Mach Number and movable leading-edge controls may be in order.

None of the previous methods* for drag reduction have considered the large trim drag at supersonic speeds for tailless aircraft. In addition to the possible requirement for maintaining straight hinge-lines a further drag savings can be realized if the constraint of trimmed flight is applied at the design lift coefficient.

* except Tucker.

At subsonic and low supersonic speeds (where the component of Mach Number normal to the leading edge is subsonic) a suction force may be realized provided that leading-edge separation is eliminated. Boyd, Migotsky and Wetzel[22] published a method to determine the required leading-edge modification for some restricted flat delta wings. Recently, Falk[23] developed a design procedure to determine the required modification for given warped (as well as flat) delta wings utilizing slender-body theory.

The current paper presents the formulas in closed form for the one hundred distributed and integrated drag contributions resulting from a ten-term power-series expansion for the downwash on delta wings having subsonic, sonic and supersonic leading edges. With the formulas included for the suction forces for subsonic leading edges one may thereby compute the drag for off-design conditions for warped delta wings with undeflected elevons at supersonic speeds when the known mean chord line is expressible by the chosen power series. This procedure has been programmed for the IBM 704 Digital Computer for the determination of the mean chord shape, drag polars and pitching moment for pointed tip wings having swept trailing edges (e.g., arrow and diamond wings). The set-up did not include design for subsonic leading edges since this case is of little practical competitive interest. The drag polar for off-design conditions where the closed form equations for the mean chord shape are modified by either or both elevon deflection and leading-edge camber (not described by the chosen power series for the downwash) are computed by numerical means by an IBM 704 program prepared by the Dynamics Group. This latter procedure requires only the design shape with the numerical modifications. Furthermore, this IBM 704 program will compute the required shape which under aeroelastic load will deflect to the shape predicted herein.

The procedure for determining the mean chord line for delta wings trimmed for level flight at design lift coefficient with two straight hinge-lines is described in the text. The detailed procedure for some illustrative examples are included in the Appendix for

the option of the reader. In order to make the drag expression more tractable for the minimization procedure, the interference drag terms were eliminated at the design condition by constructing orthogonal loadings[15]. (The evaluation of the design drag coefficient thereby requires only ten known orthogonal terms or merely two Lagrangian multipliers instead of one hundred drag terms as required for off-design conditions.)

Several delta wings having sonic and supersonic leading edges were designed and compared to the flat plate value. All designs were carried out for the ten-term power-series expansion for the downwash. For a sonic leading edge delta wing at $C_{L_d} = .136$, about 9.9% drag reduction from the untrimmed flat plate was found without specifying the static margin and with only one straight hinge-line. The penalties mentioned previously nullify the gain, however. A second sonic leading edge wing designed for trimmed level flight indicated about 46% drag reduction from the trimmed flat plate. The third wing of this group designed for trimmed level flight with two straight hinge-lines resulted in about 33% less drag than the trimmed sonic leading-edge flat-plate delta wing.

Similar studies were carried out for delta wings having supersonic leading edges. For the supersonic leading-edge delta wing at design $C_L = .087$, the untrimmed case resulted in about 5.8% drag reduction from the untrimmed flat plate. The second wing of this group designed for trimmed level flight resulted in about 31% drag reduction from the trimmed flat plate. The supersonic leading-edge delta wing designed for trimmed level flight with two straight hinge-lines resulted in 39% less drag than the trimmed flat plate.

No illustrative examples were carried out for wings having subsonic leading edges for lack of interest. However, the procedure outlined for the sonic and supersonic cases applies and all the quantities required for application are included. It is pointed out that the current procedure can include leading-edge suction at the option of the reader.

The conical functions derived herein for the section drag parameters were used to set-up an IBM 704 program to treat pointed tip wings having supersonic swept trailing edges.

The effect on drag reduction of including additional terms up to ten taken one at a time is illustrated for the sonic leading-edge delta wing without restraints.

The drag-due-to-lift is quite sensitive to the shape of the mean chord line. For this reason it is suggested that the next logical step in this direction would be to include flexibility in the drag reduction process. The extension could be made by using a conservative structure and replacing the resulting elastic warp by a power series similar to the one used for the rigid wing downwash.

3.0 SYMBOLS

3.1 FREE STREAM CONDITIONS

V	Velocity
M	Mach Number
β	$(M^2 - 1)^{1/2}$
μ	Mach angle, arc sin $(1/M)$
ρ	Mass density of air
q	Dynamic pressure of free stream $(1/2) \rho V^2$

3.2 WING GEOMETRY

$b/2$	Semispan
c	Local chord
c_r	Root chord
c_{av}	Average chord, $c_r/2$
$\bar{c}$	Mean aerodynamic chord, $(2/3)\, c_r$
S	Wing Area
ϵ	Wing half apex angle
ω	Angle between trailing edge and stream axis
m	$\beta \tan \epsilon$
m_o	$\beta \tan \omega$
x, y, z	Cartesian coordinates of system of axis with origin at leading edge of root chord
$\alpha, \alpha(x', y')$	Wing angle of attack in stream direction, radians
α_i	$(x')^r (y')^s$
x', y', z'	x, y, z non-dimensionalized by c_r, $b/2$, c_r, respectively
α_{rs}	Constants of proportionality

3.3 ANALYSIS PARAMETER

ϕ	velocity potential
ϕ_x	horizontal perturbation velocity ($= \partial \phi / \partial x$)
$\phi_{xx}, \phi_{yy}, \phi_{zz}$	second partial derivatives of velocity potential with respect to x, y, z, respectively
$\phi_n (x, y)$	velocity potential normal to leading edge
V_n	velocity normal to leading edge
x_n, y_n	coordinates perpendicular and parallel to leading edge
w	upwash velocity ($= \partial \phi / \partial z$)
t	$\beta y/x$
Θ	arc cos (1/m)
Θ_1	arc cos [(1-mt)/(m-t)]
Θ_2	arc cos [(1+mt)/(m+t)]
Θ_3	arc cos h | m/t |
Θ_4	arc cos h | 1/t |
$x_{T.E.}$	value of x at trailing edge
$\Delta p/q$	lifting pressure coefficient
K, E	complete elliptic integrals of the first and second kinds, respectively, with modulus $(1-m^2)^{1/2}$
$A_i, a_i, b_i, c_i, e_i, f_i, k_i$	Functions of m, K, E defined in Table I, reference 3, with additional results tabulated in section 6.2 herein
C_n, C_ℓ, C_d	span load parameter, chord load parameter and section drag coefficients, respectively

$L, D, \bar{M}$	wing lift, drag and pitching moment, respectively
C_L, C_D, C_M	wing lift coefficient, L/qS; wing drag coefficient, D/qS; wing pitching moment, $\bar{M}/qS\bar{c}$, respectively
$E_i(t)$; $F_i(t)$; $G_i(t)$; $H_{i,j}(t)$, $g_i(t)$, $h_i(t)$	conical functions upon which the following coefficients depend, respectively: velocity potential and span loading; pressure; pitching moment; and drag
$T^*_{i,j}$	functions of m upon which the suction drags depend
q_T	a number used to indicate percentage of full leading edge suction assumed
C_{D_t}	suction drag coefficient
G_n, $G_{n,k}$, G_n^I	functions used to obtain suction drag (see section 4.3)
X_{ik}	orthogonal weighting numbers
$\lambda_{i,j}$	$C_{D^*_{i,j}} + C_{D^*_{j,i}}$
a_{kn}	weighting numbers chosen to minimize the drag
ϕ_{kn}	functions of X_{ik} and a_{kn} [equation (4.42]
$\bar{a}_{kn}$, $\bar{\phi}_{kn}$	$a_{kn}/\beta C_{L_d}$ and $\phi_{kn}/\beta C_{L_d}$, respectively
C_{L_d}	design lift coefficient
$\Gamma(Y')$, Γ_i	functions required to satisfy geometric boundary conditions
$C_{M_{a\bar{c}}}$	pitching-moment coefficient about a fraction x_m of the M.A.C.
x_m	point of zero pitching moment, percent of M.A.C.

Ω_i	Lagrangian numbers
φ_i	equations describing restraints
$\left.\begin{matrix}\delta_0, \delta_1, \delta_2, \\ \delta_3, m_1, n_1\end{matrix}\right\}$	geometric quantities relating shape and position of geometric boundary conditions (see figure 1)

4.0 ANALYSIS

4.1 Background

In order to compute the shape of wings having reduced drag-due-to-lift at supersonic speeds as well as the drag of the resulting configurations it is necessary to know the pressure distribution. The pressure distribution, however, depends upon the downwash over the wing. The procedure used herein is to assume that the wing shape is expressible in terms of the power series

$$\frac{w}{V} = -\alpha(x', y') = -\sum_{r} \sum_{s} \alpha_{rs} (x')^{r} \, |y'|^{s} \qquad (4.1)$$

for $r + s \leq 3$ where the primed quantities are non-dimensionalized by c_r and $b/2$, respectively. Solutions are obtained to the linearized equation for the velocity potential.

$$\beta^{2} \phi_{xx} - \phi_{yy} - \phi_{zz} = 0 \qquad (4.2)$$

for the boundary conditions of equation (4.1).

It has been shown in reference 3 that for each term of the boundary conditions, equation (4.1), there is associated a potential, $(\phi/\alpha)^{*}_{rs}$, and its corresponding horizontal perturbation velocity, $(\phi_x/\alpha)^{*}_{rs}$. Therefore, for convenience, † one may write the total potential and total horizontal perturbation velocity in the form

---

† The change in notation from a double summation to a single one represents, at best, an abbreviation to make the following work more readable. For example, this analysis has been restricted to $r + s \leq 3$ and so equation (4.1) may be expanded to ten terms. For each of these "i" terms there is an effective potential given by ϕ_i^{*} such that the total potential is the sum of each contribution. Since all the aerodynamic quantities are related to the potential the remaining definitions are consistent.

$$\varphi^* = \sum_i \varphi_i^* \tag{4.3}$$

$$\varphi_x^* = \sum_i (\varphi_x)_i^* \tag{4.4}$$

where i is now related to rs as shown in Table I.

TABLE I

Relation Between the Single Index, i, and the Double Index, rs

i	0	1	2	3	4	5	6	7	8	9
rs	00	01	10	02	11	20	03	12	21	30

By linear theory the lifting pressure distribution is given by

$$\frac{\Delta p}{q} = \frac{4}{V} \varphi_x \tag{4.5}$$

and it follows that the total lifting pressure coefficient may be written in terms of each of the contributions corresponding to the downwash series:

$$\left(\frac{\Delta p}{q}\right)^* = \sum_i \left(\frac{\Delta p}{q\,\alpha}\right)_i^* \alpha_i \tag{4.6}$$

The details involved with the determination of the quantities $(\varphi/\alpha)_i^*$, $(\varphi_x/\alpha)_i^*$ and $(\Delta p/q\,\alpha)_i^*$ are presented both in analytical and graphical form for the first ten terms $(r + s \leq 3)$ of the downwash for subsonic, sonic and supersonic leading edges in reference 3.

4.2 Aerodynamic Characteristics

The lift, moment and drag coefficients are defined, respectively, by

$$C_L = \frac{1}{S} \iint \frac{\Delta p}{q} \, dS \qquad (4.7)$$

$$C_M = -\frac{1}{S} \iint x \frac{\Delta p}{q} \, dS \qquad (4.8)$$

$$C_D = \frac{1}{S} \iint \frac{\Delta p}{q} \frac{dz}{dx} \, dS \qquad (4.9)$$

Substituting equation (4.6) into equations (4.7) to (4.9) results in

$$C_L^* = \sum_i (C_L/\alpha)_i^* \, \alpha_i \qquad (4.10)$$

$$C_M^* = \sum_i (C_M/\alpha)_i^* \, \alpha_i \qquad (4.11)$$

$$C_D^* = \sum_i \alpha_i \sum_j \alpha_j \, C_{D_{i,j}}^* \qquad (4.12)$$

since

$$\frac{dz}{dx} = -\alpha(x, y) \qquad (4.13)$$

The form of the drag coefficient results from the substitution of two power series for the lifting pressure coefficient and the slope, respectively, into equation (4.9).

Thus $C_{D_{i,j}}{}^*$ is the contribution of the pressure coefficient $(\Delta p/q\alpha)_i^*$ induced by α_i acting upon the downwash α_j.

The functions $(C_L/\alpha)_i^*$ and $(C_M/\alpha)_i^*$ are presented in both analytical and graphical form in reference 3 for subsonic, sonic and supersonic leading-edge delta wings.

The basic drag contributions were derived as follows:

$$C_{D_{i,j}}{}^* = \int_0^1 C_{d_{i,j}}{}^* \frac{c}{c_{av}} \, dy' \tag{4.14}$$

where

$$C_{d_{i,j}}{}^* \frac{c}{c_{av}} = 2 \int_{x'_{L.E.}}^{x'_{T.E.}} \left(\frac{\Delta p}{q\alpha}\right)_i \left(\frac{dz'}{dx'}\right)_j dx' \tag{4.15}$$

with $\frac{dz'}{dx'}$ now considered to be equal to $(x')^{r'} (y')^{s'}$ for $y' \geq 0$, where the primes on r and s signify that the loading (rs) may interfere with the downwash (r's').

Equation (4.15) reduces to

$$C_{d_{i,j}}{}^* \frac{c}{c_{av}} = \frac{2}{\pi} \left(\frac{2 c_r}{\beta b}\right)^{s+s'} (x')^{\kappa} H_{i,j}(t) \tag{4.16}$$

where

$$\left.\begin{aligned} \kappa &= 1 + n + n' + s + s' \\ x' &= m_o/(m_o - t) \\ \frac{\beta b}{2 c_r} &= \left(\frac{m_o - m}{m\, m_o}\right)^{-1} \end{aligned}\right\} \tag{4.17}$$

Equation (4.16) is valid for all triangular wings. The functions $H_{i,j}(t)$ are presented in closed form in the Appendix, section 8.1, Tables A, B and C for subsonic, sonic and supersonic leading edges, respectively.

Substituting equation (4.16) into equation (4.15) there follows

$$C_{D_{i,j}}^{*} = \frac{8}{\pi}\left(\frac{m_o - m}{m\, m_o}\right)^{1+s+s'} m_o^{2+\kappa} \int_o^m (m_o - t)^{-2\kappa} H_{i,j}(t)\, dt \qquad (4.18)$$

which, for delta wings ($m_o = \infty$) reduces to

$$C_{D_{i,j}}^{*} = \frac{8}{\pi}\left(\frac{1}{m}\right)^{1+s+s'} \int_o^m H_{i,j}(t)\, dt \qquad (4.19)$$

The functions $C_{D_{i,j}}^{*}$ are presented in the Appendix, section 8.3, Tables A, B, C and D, for subsonic, sonic and supersonic leading edges, and the limiting case, $m = o$, respectively.

For wings with swept trailing edges equation (4.18) may be readily evaluated with the aid of high-speed computing equipment, a procedure currently being programmed at Convair-San Diego.

4.3 Suction Drag Coefficients

The suction drag coefficient is defined[22] by

$$C_{D_t} = -\frac{2\pi}{S} \int_o^{b/2} \frac{G_n^2}{\beta n}\, dy \qquad (4.20)$$

where

$$\frac{G_n}{\beta_n} = \lim_{x_n \to 0} \left(\sqrt{x_n} \; \frac{v_n}{V} \right) \tag{4.21}$$

$$\beta_n = \sqrt{1 - m^2 \cos \epsilon} \tag{4.22}$$

and v_n is the velocity normal to the leading edge. x_n and y_n are the components of x, y normal to and parallel to the leading edge, respectively.

$$v_n = \frac{\partial}{\partial x_n} \phi (x_n, y_n) \tag{4.23}$$

From equation (4.4) it follows that

$$G_n^i = \sum_k^i G_{n,k} \tag{4.24}$$

where $G_{n,k}$ is the contribution of the k^{th} term of the downwash to G_n and G_n^i is the value of G_n corresponding to i terms of the downwash.

The suction drag coefficients which are presented in the Appendix, section 8.4, for various terms of the downwash equation may be expressed by

$$\frac{C_{D_{t,i}}^{(n)}}{\pi C_{L_d}^2} = \sum_{i=0}^{j} \Psi_{in} \sum_{j=0}^{n} \Xi_{jn} T^*_{i,j} \tag{4.25}$$

where the superscript (n) refers to the highest number of terms of the power series for the downwash and $T^*_{i,j}$ are functions of $m = \beta \tan \epsilon$. Uncited references indicate the amount of leading-edge suction likely to develop depends upon m and the nose shape. The parameter $0 \leq q_T \leq 1.0$ may be used empirically in this regard.

4.4 Drag Reduction

4.4.1 Orthogonal Loading

The minimization of the drag is greatly facilitated by eliminating the interference drag[15]. A set of orthogonal loadings, $(\Delta p/q)^{(k)}$, $\alpha^{(k)}$, are constructed from the basic loadings, $(\Delta p/q)_i$, α_i, by

$$\alpha^{(k)} = \sum_{i=0}^{n} X_{ik}\, \alpha_i \tag{4.26}$$

$$\left(\frac{\Delta p}{q}\right)^{(k)} = \sum_{i=0}^{n} X_{ik} \left(\frac{\Delta p}{q}\right)_i \tag{4.27}$$

where n is the number of terms (0, 1, 2 . . . 9) of the downwash power series used and

$$\alpha_i = (x')^r (y')^s \quad , \quad y' \geq 0 \tag{4.28}$$

$$\left(\frac{\Delta p}{q}\right)_i = \left(\frac{\Delta p}{\alpha}\right)_{rs} \quad , \quad \text{(reference 3)} \tag{4.29}$$

X_{ik} are weighting numbers chosen to satisfy the orthogonality requirement that the inner drag product disappears

$$\int_S \left[\left(\frac{\Delta p}{q}\right)^i \alpha_j + \left(\frac{\Delta p}{q}\right)_j \alpha^i \right] dS = 0 \tag{4.30}$$

The X_{ik} are obtained from

$$\sum_{i=0}^{k} X_{ik} \lambda_{i,j} = 0 , \quad j = 0, 1, 2 \ldots k-1 \tag{4.31}$$

$$\lambda_{i,j} = \lambda_{j,i} \equiv C_{D_{i,j}}^{*} + C_{D_{j,i}}^{*} \tag{4.32}$$

A new loading ($\Delta p/q$, α) is constructed from the orthogonal set with the aid of the weighting numbers a_{kn} where

$$\alpha = \sum_{k=0}^{n} a_{kn} \alpha^{(k)} \tag{4.33}$$

$$\frac{\Delta p}{q} = \sum_{k=0}^{n} a_{kn} \left(\frac{\Delta p}{q}\right)^{(k)} \tag{4.34}$$

Substituting equations (4.33) and (4.34) into equation (4.9) results in

$$C_D^* = \sum_{k=0}^{n} a_{kn}^{\;2} (C_D^*)^{(k)} \tag{4.35}$$

where the orthogonal drag coefficients are found by

$$\left(C_D^*\right)^{(k)} = \frac{X_{kk}}{2} \sum_{i=0}^{k} X_{ik} \lambda_{i,k} \tag{4.36}$$

4.4.2 Drag Minimization for Specified Lift

Following the results of Graham[15], one may write for the minimum drag coefficient

$$\frac{C_D}{\beta C_{L_d}^2} = \sum_{k=0}^{n} \bar{a}_{kn}^2 \left(C_D^*\right)^{(k)} \tag{4.37}$$

where

$$\bar{a}_{kn} = \left(\frac{a_{kn}}{\beta C_{L_d}}\right) \frac{\left(C_L^*\right)^{(k)} / \left(C_D^*\right)^{(k)}}{\sum_{k=0}^{n} \left[\left(C_L^*\right)^{(k)}\right]^2 / \left(C_D^*\right)^{(k)}} \tag{4.38}$$

From equations (4.7) and (4.27) it follows that

$$\left(C_L^*\right)^{(k)} = \sum_{i=0}^{k} X_{ik} C_{L_i}^* \tag{4.39}$$

The mean chord line may be determined from

$$-\frac{1}{\beta C_{L_d}} \frac{dz'}{dx'} = \frac{\alpha(x', y')}{\beta C_{L_d}} = \sum_{k=0}^{n} \bar{a}_{kn} \, \alpha^{(k)} \qquad (4.40)$$

where z and x are non-dimensionalized by c_r and y is non-dimensionalized by b/2.

Integrating equation (4.39) there results

$$-\frac{z'}{\beta C_{L_d}} = \int \left(\sum_{k=0}^{n} \bar{a}_{kn} \, \alpha^{(k)} \right) dx' + \Gamma(y') \qquad (4.41)$$

where (y') is used to satisfy geometric boundary conditions. Since $\alpha^{(k)}$ can be represented by a series in terms of the basic downwashes, α_i, equation (4.41) can be made more tractable by means of the substitution

$$\bar{\tau}_{kn} = \sum_{i=k}^{n} X_{ki} \, \bar{a}_{in} \qquad (4.42)$$

which results in

$$-\frac{z'}{\beta C_{L_d}} = \int \left(\sum_{k=0}^{n} \bar{\tau}_{kn} \, \alpha_k \right) dx' + \Gamma(y') \qquad (4.43)$$

$$-\frac{z'}{\beta C_{L_d}} = \Big[(\phi_{0n} + \phi_{1n} y' + \phi_{3n} y'^2 + \phi_{6n} y'^3) x'$$

$$+ \frac{1}{2} (\phi_{2n} + \phi_{4n} y' + \phi_{7n} y'^2) x'^2$$

$$+ \frac{1}{3} (\phi_{5n} + \phi_{8n} y') x'^3 + \frac{1}{4} \phi_{9n} x'^4 \Big] + \Gamma(y') \qquad (4.44)$$

4.4.3 Drag Reduction with Specified Static Margin at Design Lift

This problem is readily treated[23] with the aid of Lagrange's constant multipliers. The static margin is specified in terms of the pitching-moment about the leading edge apex by means of the transfer formula

$$C_{M_{x_m \bar{c}}} = C_{M_{x=0}} + \left(\frac{1+2\,x_m}{2}\right) C_L \qquad (4.45)$$

where x_m is the point at which zero moment is desired as a given fraction of the mean aerodynamic chord. From equations (4.7), (4.8) and (4.34) there results

$$\frac{C_L}{C_{L_d}} = \sum_{k=0}^{n} \bar{a}_{kn} \, (C_L^*)^{(k)} \qquad (4.46)$$

$$\frac{C_{M_{x=0}}}{C_{L_d}} = \sum_{k=0}^{n} \bar{a}_{kn} \, (C_M^*)^{(k)} \qquad (4.47)$$

where

$$(C_M^*)^{(k)} = \sum_{i=0}^{n} X_{ik} \; C_{M_i}^* \tag{4.48}$$

Define

$$\overline{D} = \frac{C_D}{\beta \, C_{L_d}^{\;2}} + \sum_{i=1}^{\ell} \Omega_i \; \varphi_i \tag{4.49}$$

(where $\ell = 2$)

$$\varphi_1 \equiv \sum_{k=0}^{n} \bar{a}_{kn} \; (C_L^*)^{(k)} - 1 = 0 \tag{4.50}$$

$$\varphi_2 \equiv \sum_{k=0}^{n} \bar{a}_{kn} \; (C_M^*)^{(k)} + \frac{1+2\,x_m}{2} = 0 \tag{4.51}$$

The condition for the drag to be a minimum for the specified lift and static margin is satisfied when

$$\frac{\partial \left(C_D / \beta \, C_{L_d}^{\;2} \right)}{\partial \, \bar{a}_{kn}} + \sum_{i=1}^{\ell} \Omega_i \; \frac{\partial \varphi_i}{\partial \, \bar{a}_{kn}} = 0 \tag{4.52}$$

The n + 3 unknowns ($\bar{a}_{kn}$, Ω_i) can be determined by matrix methods using the n + 3 equations (4.50), (4.51) and (4.52). For the simple case under consideration where ℓ = 2, an alternate approach is to relate $\bar{a}_{kn}$ to Ω_i, determine Ω_i from the two boundary equations and then compute $\bar{a}_{kn}$. Thus, from equations (4.52) and (4.35) there results

$$\bar{a}_{kn} = - \frac{\sum_{i=1}^{2} \Omega_i \frac{\partial \varphi_i}{\partial \bar{a}_{kn}}}{2\,(C_D^*)^{(k)}} \tag{4.53}$$

which is substituted into equations (4.50) and (4.51):

$$\Omega_1 \sum_{k=0}^{n} \frac{\left[(C_L^*)^{(k)}\right]^2}{(C_D^*)^{(k)}} + \Omega_2 \sum_{k=0}^{n} \frac{(C_L^*)^{(k)}\,(C_M^*)^{(k)}}{(C_D^*)^{(k)}} = -2.0 \tag{4.54}$$

$$\Omega_1 \sum_{k=0}^{n} \frac{(C_L^*)^{(k)}\,(C_M^*)^{(k)}}{(C_D^*)^{(k)}} + \Omega_2 \sum_{k=0}^{n} \frac{\left[(C_M^*)^{(k)}\right]^2}{(C_D^*)^{(k)}} = 1 + 2\,x_m \tag{4.55}$$

The summations in equations (4.54) and (4.55) are determined from the previously computed quantities $(C_L^*)^{(k)}$, $(C_M^*)^{(k)}$, $(C_D^*)^{(k)}$.

The total drag at the design condition may be determined with little effort from equation (4.35) or by the procedure indicated by Stancil[8]. Omitting the details involved in deriving the results on the basis of the current analysis using orthogonal loads,

$$\frac{C_D}{\beta\, C_{L_d}^{\,2}} = -\frac{1}{2}\sum_{i=1}^{\ell} \Omega_i\, R_i \tag{4.56}$$

$$= -\frac{1}{2}\left[\Omega_1 - \frac{1+2\,x_m}{2}\,\Omega_2\right] \tag{4.57}$$

since

$$R_1 = \sum_{k=0}^{n} \bar{a}_{kn}\,(C_L^*)^{(k)} = 1 \tag{4.58}$$

$$R_2 = \sum_{k=0}^{n} \bar{a}_{kn}\,(C_M^*)^{(k)} = -\frac{1+2\,x_m}{2} \tag{4.59}$$

The mean chord line is determined from equation (4.44) when a new set of $\bar{v}_{kn}$ are computed for the values of $\bar{a}_{kn}$ obtained in this section. The weighting numbers X_{ik} obtained in section 4.4.2 are the same for the present section.

4.4.4 Drag Reduction with Specified Static Margin and Two Straight Hinge-Lines

This problem follows directly from the previous problem when additional relations between a_{kn} are obtained which describe the desired boundary conditions. This results in additional functions φ_i ($i \geq 3$) for equation (4.52).

The solution for this problem first involves the determination of n + i + 1 constants (a_{kn} , Ω_i) for which there are a like number of equations. The values for ψ_{kn} are determined from equation (4.42) using the proper a_{kn}.

If the two straight hinge-lines are described by (see Figure 4.1)

$$-\frac{Z'}{\beta C_{L_d}} = \delta_1 + \delta_0 y' \qquad (\text{at } x' = n_1 y') \tag{4.60}$$

$$= \delta_3 + \delta_2 y' \qquad (\text{at } x' = m_1) \tag{4.61}$$

then the arbitrary function $\Gamma(y')$ consistent with the assumed conditions is

$$\Gamma(y') = \Gamma_0 + \Gamma_1 y' + \Gamma_2 y'^2 + \Gamma_3 y'^3 + \Gamma_4 y'^4 \tag{4.62}$$

where

$$\left.\begin{aligned}
\Gamma_0 &= 0 = \delta_3 - m_1 \left(\psi_{0n} + \frac{1}{2} m_1 \psi_{2n} + \frac{1}{3} m_1^2 \psi_{5n} + \frac{1}{4} m_1^3 \psi_{9n}\right) \\
\Gamma_1 &= \delta_0 - n_1 \psi_{0n} = \delta_2 - m_1 \left(\psi_{1n} + \frac{1}{2} m_1 \psi_{4n} + \frac{1}{3} m_1^2 \psi_{8n}\right) \\
\Gamma_2 &= -n_1 \left(\psi_{1n} + \frac{1}{2} n_1 \psi_{2n}\right) = -m_1 \left(\psi_{3n} + \frac{1}{2} m_1 \psi_{7n}\right) \\
\Gamma_3 &= -m_1 \psi_{6n} = -n_1 \left(\psi_{3n} + \frac{1}{2} n_1 \psi_{4n} + \frac{1}{3} n_1^2 \psi_{5n}\right) \\
\Gamma_4 &= 0 = n_1 \left(\psi_{6n} + \frac{1}{2} n_1 \psi_{7n} + \frac{1}{3} n_1^2 \psi_{8n} + \frac{1}{4} n_1^3 \psi_{9n}\right)
\end{aligned}\right\} \tag{4.63}$$

Figure 4.1

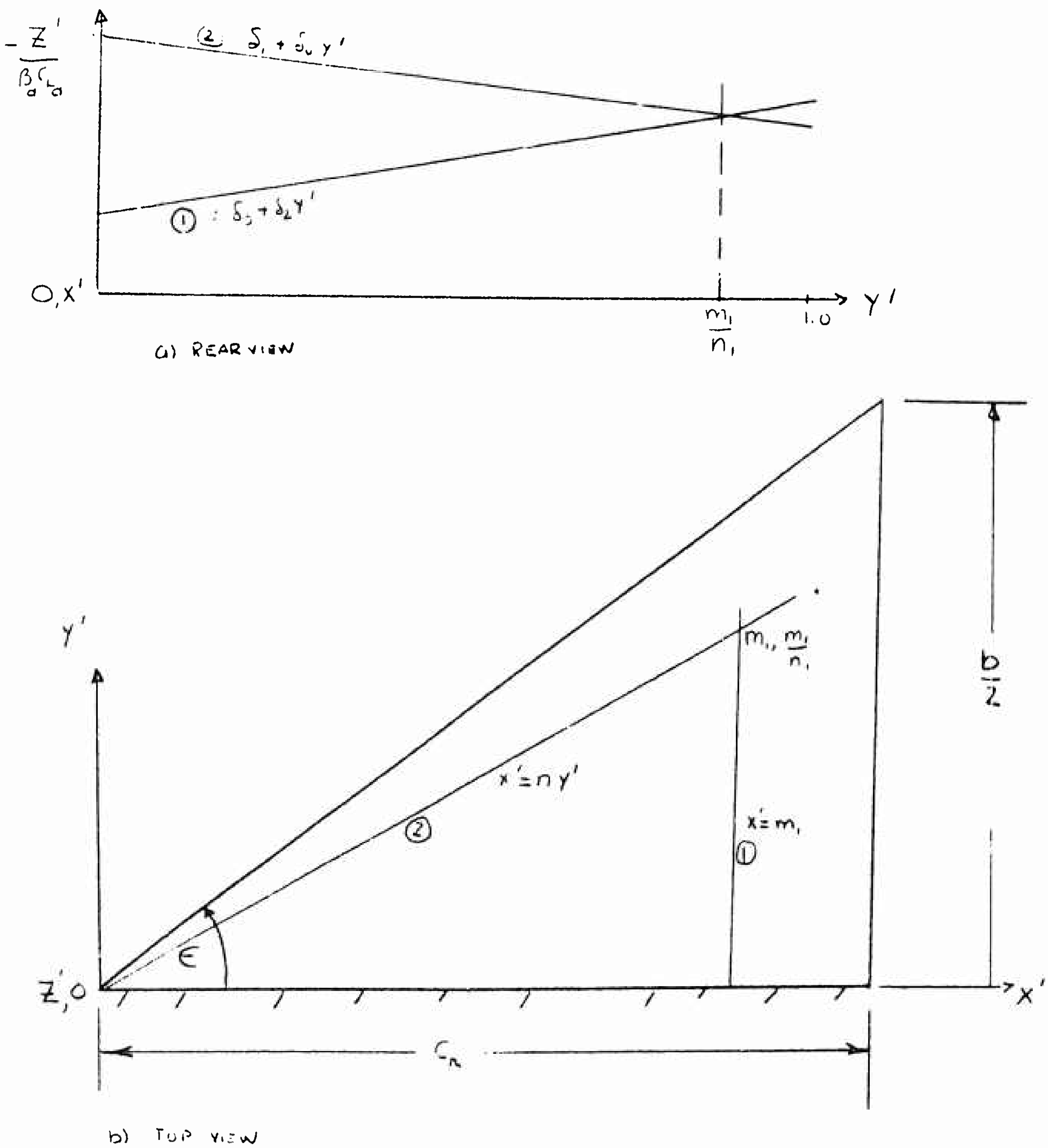
$-\frac{Z'}{\beta_a C_{L_a}}$
(2) $\delta_1 + \delta_0 y'$
(1) : $\delta_3 + \delta_2 y'$
O, X'
$\frac{m_1}{n_1}$
1.0
Y'
a) REAR VIEW
Y'
$m_1, \frac{m_1}{n_1}$
$\frac{b}{2}$
$x' = n y'$
(2)
$x' = m_1$
(1)
ϵ
Z', O
X'
c_r
b) TOP VIEW

The equations for the intersection of the two hinge-lines is

$$(\delta_2 - \delta_0) = -\frac{n_1}{m_1}(\delta_3 - \delta_1) \tag{4.64}$$

From equations (4.63) and (4.64) one can eliminate Γ_1, $(\delta_3 - \delta_1)$ and $(\delta_2 - \delta_0)$ thereby resulting in four relations for a_{kn} which are consistent with equations (4.60) and (4.61). These relations were written in the form

$$\varphi_3 \equiv \sum_{k=0}^{n} C_k \bar{a}_{kn} = 0 \tag{4.65}$$

$$\varphi_4 \equiv \sum_{k=0}^{n} D_k \bar{a}_{kn} = 0 \tag{4.66}$$

$$\varphi_5 \equiv \sum_{k=0}^{n} F_k \bar{a}_{kn} = 0 \tag{4.67}$$

$$\varphi_6 \equiv \sum_{k=0}^{n} E_k \bar{a}_{kn} = 0 \tag{4.68}$$

where C_k, D_k, E_k, F_k are known functions of m_1, n_1, X_{ik} given in section 8.5 of the Appendix. Thus, the n + i + 1 unknowns, $\bar{a}_{kn}$, Ω_i are found from the n + i + 1 equations

$$2\,\bar{a}_{kn}\,(C_D^*)^{(k)} + \sum_{L=1}^{6} \Omega_i \frac{\partial \varphi_i}{\partial \bar{a}_{kn}} = 0\,, \quad k = 0,\ 1,\ 2 \ldots 9 \tag{4.69}$$

$$\varphi_i = 0\,, \quad i = 1,\ 2 \ldots .\ 6 \tag{4.70}$$

The total drag is computed from equation (4.35) or (4.56) where $R_i = 0$ for $i \geq 3$. The mean chord line is found from equations (4.44) and (4.63).

4.4.5 Drag Reduction for Wings Having Subsonic Leading Edges

When leading edge suction is neglected the previous techniques are applicable. When complete leading edge suction is included [Equation (4.25)] the drag relation becomes

$$\frac{C_D}{\beta\, C_{L_d}^{\,2}} = \sum_{k=0}^{n} \bar{a}_{kn}^{\,2}\,(C_D^*)^{(k)}$$

$$+\ q_T \sum_{i=0}^{j} \bar{a}_{in} \sum_{j=0}^{n} \bar{a}_{jn}\, T^*_{i,\,j} \tag{4.71}$$

where q_T represents the percentage of full leading edge suction one may expect. Substituting Equation (4.71) into (4.52) results in the system of n + 1 equations

$$2\,(C_D^*)^{(k)}\,\bar{a}_{kn} + q_T\,X_{kk}\left\{\sum_{p=0}^{i} X_{pi}\,T^*_{p,k}\sum_{i=0}^{k}\bar{a}_{in}\right.$$

$$\left.+\left[\sum_{p=0}^{i} X_{pi}\,T^*_{p,k} + \sum_{p=k+1}^{i} X_{pi}\,T^*_{k,p}\right]\sum_{i=k+1}^{n}\bar{a}_{in}\right\}$$

$$+\sum_{i=1}^{\ell}\Omega_i\,\frac{\partial\varphi_i}{\partial\bar{a}_{kn}} = 0 \qquad (4.72)$$

in the $n + 1 + i$ unknowns $\bar{a}_{kn}$ and Ω_i which may be solved by the previously established method compatible with the additional φ_i equations.

The mean chord line is determined from equation (4.44) from the $\bar{\zeta}_{kn}$ which were computed in terms of the $\bar{a}_{kn}$ which resulted from the solution of equations (4.72) and the equations for φ_i.

The drag polars are computed from equation (4.71) which includes leading edge suction.

4.5 Span-Loading

When the shape of the wing has been determined the span-loading for any leading edge condition may be obtained from

$$\frac{c_n\,c}{C_{L_d}\,c_{av}} = \frac{8}{\pi}\,\frac{\beta_d}{\beta}\sum_{i=0}^{n}\left(\frac{m - m}{m\,m_o}\right)^{s}(x')^{1+n+s}_{T.E.}\,\bar{\zeta}_{in}\,E_i(t) \qquad (4.73)$$

where $(x')_{T.E.} = 1$ for the delta wing and for the wing with swept trailing edge

$$(x')_{T.E.} = \left(\frac{m\, m_o}{m_o - m}\right) \frac{y'}{m_o} + 1 \qquad (4,74)$$

The $\bar{\psi}_{in}$ were obtained from the minimization process and the $E_i(t)$ may be obtained from reference 3 (Tables II A), B), C) for subsonic, sonic and supersonic leading edges, respectively, or from Figures 5.1 to 5.20).

4.6 Chord-Loading

Consistent with the total load induced by the various basic loadings, $(\Delta p/q)_i$, the chord-loading is defined as

$$\frac{C_\ell\, y}{C_{L_d}\, b/2} = 2\, \frac{\beta d}{\beta} \sum_{i=0}^{n} \bar{\psi}_{in} \left\{ \left(\frac{m_o - m}{m\, m_o}\right) m\, x' \int_0^1 \left(\frac{\Delta p}{q}\right)_i^* dy' \right.$$

$$\left. + \left(\frac{m_o - m}{m\, m_o}\right) \left[(m - m_o)\, x' + m_o \right] \int_1^{\frac{m_o}{m_o - m}} \left(\frac{\Delta p}{q}\right)_i^* dy' \right\} \qquad (4.75)$$

which reduces to

$$\frac{C_\ell\, y}{C_{L_d}\, b/2} = 2\, \frac{\beta d}{\beta}\, x' \sum_{i=0}^{n} \bar{\psi}_{in} \int_0^1 \left(\frac{\Delta p}{q}\right)_i^* dy'$$

$$= 2\, x' \int_0^1 \left(\frac{\Delta p}{q}\right)^* dy' \qquad (4.76)$$

for delta wings.

In reference 5 it was shown that

$$\left(\frac{\Delta p}{q}\right)_i^* = \frac{4}{\pi}\left(\frac{m_o - m}{m\, m_o}\right)(x')^{r+s} F_i(t) \qquad (4.77)$$

where the $F_i(t)$ are given therein (see Tables III A), B), C) for subsonic, sonic, and supersonic leading edges, respectively, or Figures 5.21 to 5.40).

Since $(\Delta p/q)_i$ have integrable singularities at the leading edge for subsonic and sonic leading edges the results of equations (4.76) and (4.77) are presented analytically:

$$\frac{C_\ell\, y}{C_{L_d}\, b/2} = \sum_{i=0}^{n} \mp_{in}\left(\frac{C_\ell\, y}{b/2}\right)_i^* \qquad (4.78)$$

where $\left(\frac{C_\ell\, y}{b/2}\right)_i^*$ are given in Table II for $m \leq 1$.

For the supersonic leading edge case one can plot the pressure distributions [equation (4.77)] for any given chordwise position and graphically integrate equations (4.75) or (4.76) since there are no singularities.

TABLE II

Chord Loading Functions for Subsonic and Sonic Leading Edges

i	0	1	2	3	4
$\left(\frac{C_\ell y}{b/2}\right)_i^*$ m = 1	$4x'$	$2x'^2$	$4x'^2$	$(4/3)\, x'^3$	$2x'^3$
$\left(\frac{C_\ell y}{b/2}\right)_i^*$ m < 1	$\frac{2\pi m}{E} x'$	$\frac{-2mA_4}{A_1} x'^2$	$\frac{3\pi\, ma_6}{A_1} x'^2$	$\frac{2\pi m A_5}{A_2} x'^3$	$\frac{-2\ mA_8}{3A_2} x'^3$

i	5	6	7	8	9
$\left(\frac{C_\ell y}{b/2}\right)_i^*$ m = 1	$4x'^3$	x'^4	$(4/3)\, x'^4$	$2x'^4$	$4x'^4$
$\left(\frac{C_\ell y}{b/2}\right)_i^*$ m < 1	$\frac{2\pi m A_7}{A_2} x'^3$	$\frac{-mA_6}{A_3} x'^4$	$\frac{5m\pi a_6 C_{32}}{2A_3} x'^4$	$\frac{mA_9}{2A_3} x'^4$	$\frac{-15m\pi a_6 C_{42}}{2A_3} x'^4$

5.0 DISCUSSION

The analytic means and procedure for minimizing the drag-due-to-lift of triangular wings has been outlined in the previous section. To aid the engineer in carrying out similar investigations some illustrative examples for sonic ($M = 2.0$) and supersonic ($M = 2.5$) leading-edge delta wings are presented in section 9.0. The procedure is spelled out for the sonic leading-edge delta and the results are tabulated for the supersonic leading-edge design conditions.

Since there are six wings to be discussed the following designations are used:

Wing Warp "δa" : $C_{L_d} = .087$, $M_d = 2.5$ $(m = 1.323)$

"βa" : $C_{L_d} = .087$, $M_d = 2.5$, $C_{M.36\bar{c}} = 0$

"αa" : $C_{L_d} = .087$, $M_d = 2.5$, $C_{M.36\bar{c}} = 0$,

two straight hinge lines (Figure 4.1)

"δ" : $C_{L_d} = .136$, $M_d = 2.0$ $(m = 1.0)$

"β" : $C_{L_d} = .136$, $M_d = 2.0$, $C_{M.36\bar{c}} = 0$

"α" : $C_{L_d} = .136$, $M_d = 2.0$, $C_{M.36\bar{c}} = 0$,

two straight hinge lines

These lift coefficients permit the configurations to maintain level flight at the assumed design Mach numbers. The boundary conditions for the two straight hinge lines are defined in Figure 4.1.

A comparison of the drag polars with the trimmed and untrimmed flat plate is presented in Figure 5.1 These curves are trimmed only at the design lift for the "α" and "β" types. Figures 5.1 (a) and (b) present the results for configurations designed for the supersonic and sonic leading edges, respectively. As expected, less drag reduction is realized as the number of restraints are increased in all cases. The effect of Mach number on the drag polars is illustrated in Figures 5.2 to 5.3 for the supersonic and sonic leading edge design conditions, respectively.

The pitching moment curves are presented in Figure 5.4 at each design Mach number. The effect of Mach number for the various wing designs is indicated in Figures 5.5 and 5.6.

The effect of twist and camber on the span loadings at the design condition are shown in Figure 5.7 with the flat plate span loading for the supersonic and sonic leading edges. It is observed that all the warped wings deviate from the elliptic span-loading of the flat plate.* (An elliptic span-loading is a sufficient but not a necessary condition and the drag reduction results mainly from the marked improvement in the chord loading.) The requirement for two straight hinge-lines (α-type wing) is accompanied by a penalty in both drag and bending moment as indicated. Figures 5.8 and 5.9 show the effect of Mach number on the span loading for each wing at M = 2.0 and 2.5.

The chord loadings resulting at the design condition are compared to the flat plate loading in Figure 5.10. It is observed that the effect of warp generally tends to modify the undesirable triangular flat plate loadings in some manner toward the desired elliptic shape. The effect of Mach number on the chord loadings is illustrated in Figures 5.11 and 5.12 for each wing.

The shapes of the wings designed for each restraint are shown in Figure 5.13 for each of the leading-edge conditions.

* This is substantiated by Fenain and Vallée[21] who presented the span-loading for a Germain[9]-type sonic leading-edge delta wing. The results herein are in perfect agreement with the Fenain-Vallée computation.

The effect on drag reduction of each additional term in the power-series expansion for the downwash, equation (4.1), is shown in Figure 5.14 for the sonic leading-edge delta wing and the supersonic leading-edge delta wing.

Figure 5.1(a). Comparison of Drag Polars for Supersonic Leading Edge Deltas for Various Design Restrictions

($\delta_e = 0$ for warped wings)

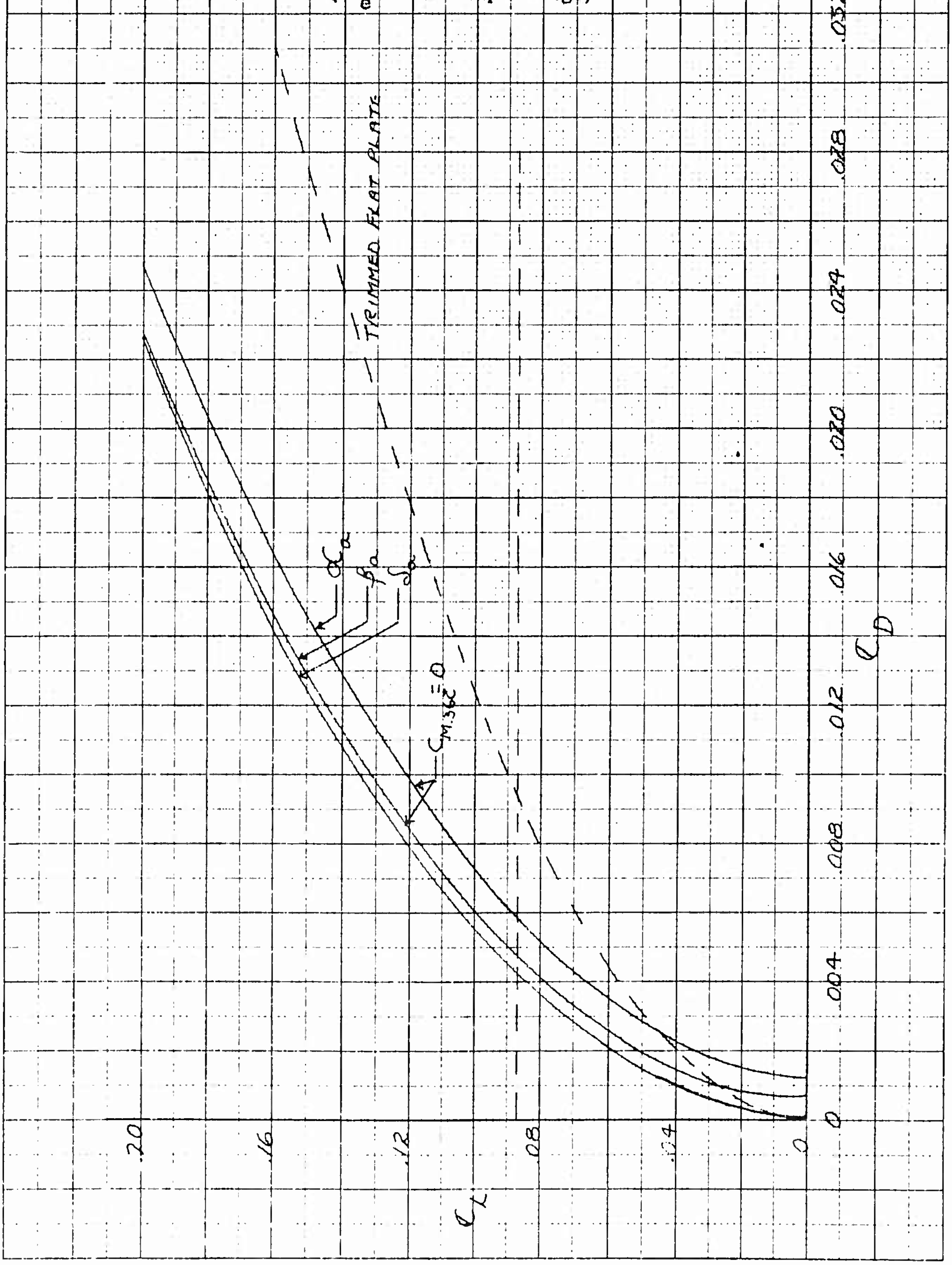

Figure 5.1(b). Comparison of Drag Polars for Sonic Leading Edge Deltas for Various Design Restrictions
($\delta_e = 0$ for warped wings)

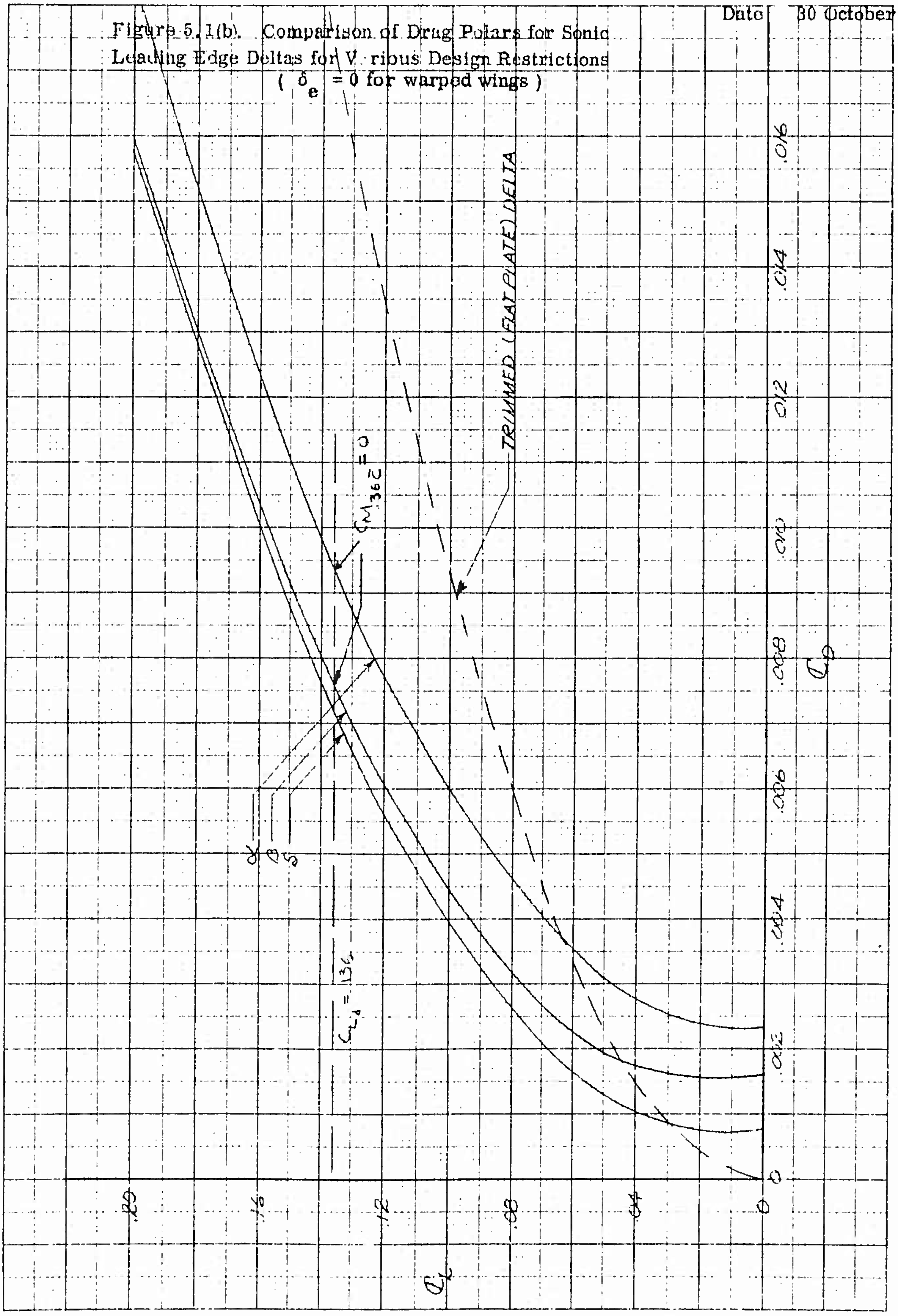

Figure 5.2(a). Effect of Mach Number on Drag Polars for Supersonic Leading Edge Delta Wing "δ_a"

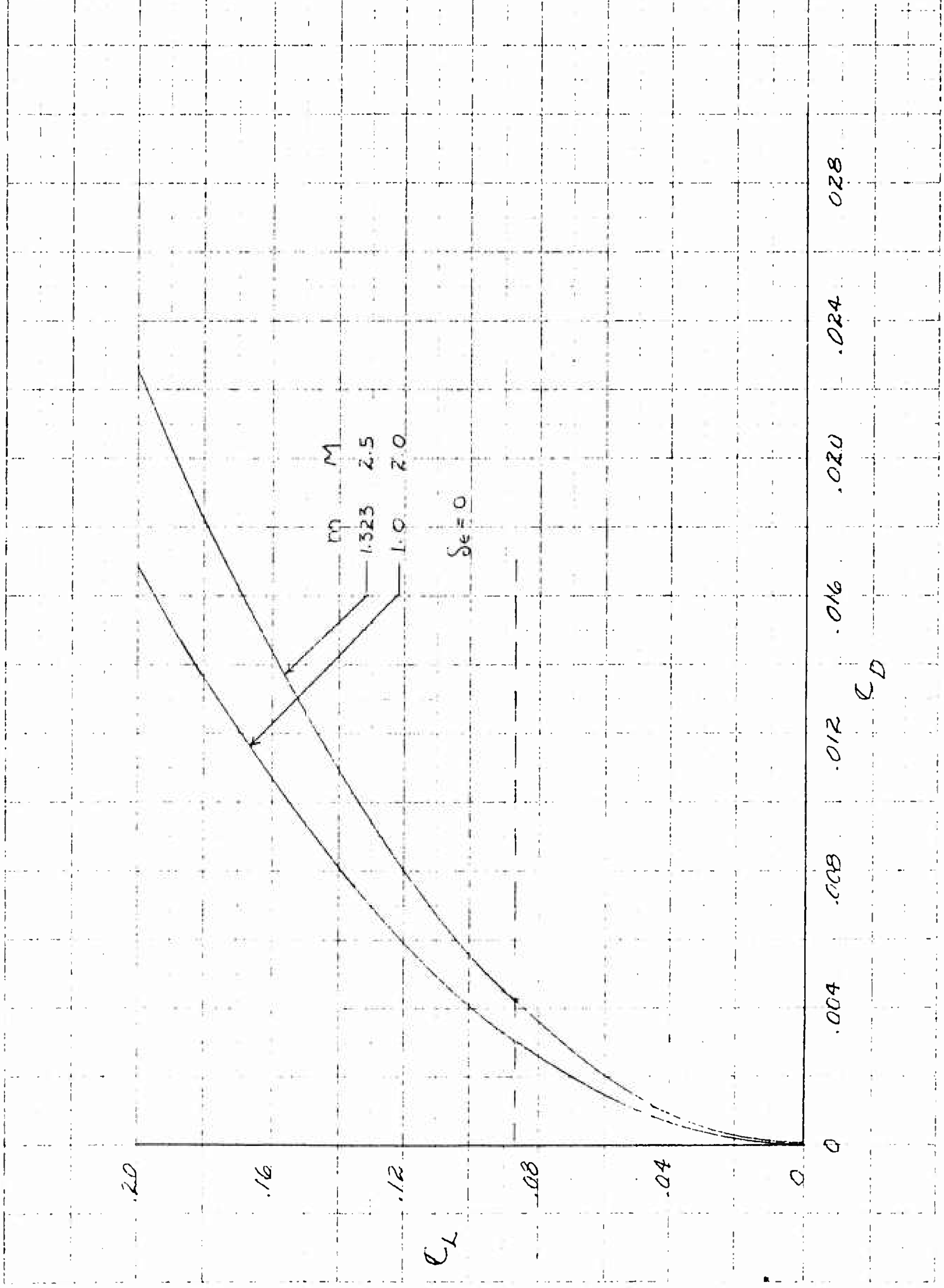

Figure 5.2(b) Effect of Mach Number on Drag Polars for Supersonic Leading Edge Delta Wing "β_a"

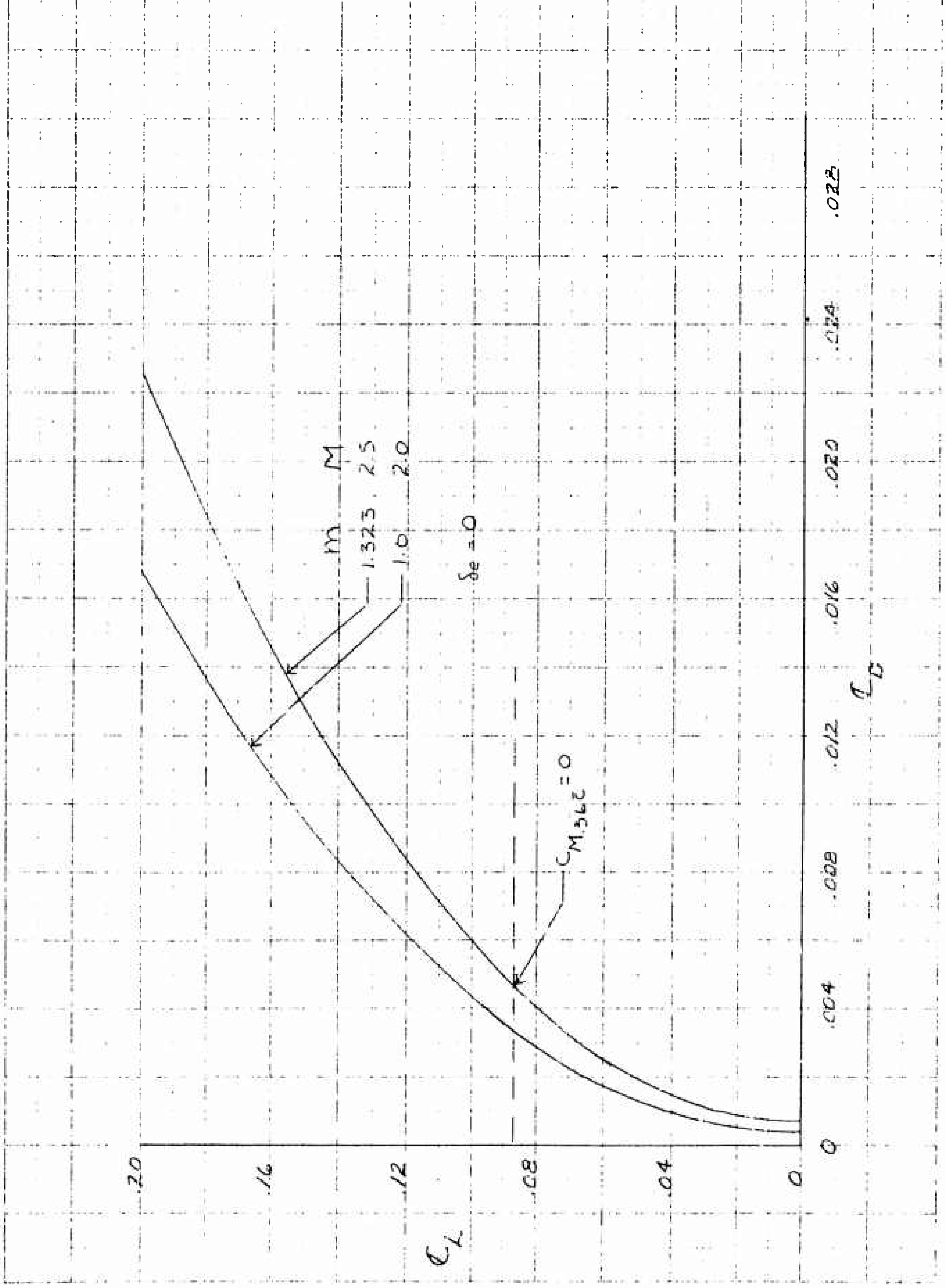

Figure 5.2(c). Effect of Mach Number on Drag Polars for Supersonic Leading Edge Delta Wing "b_a"

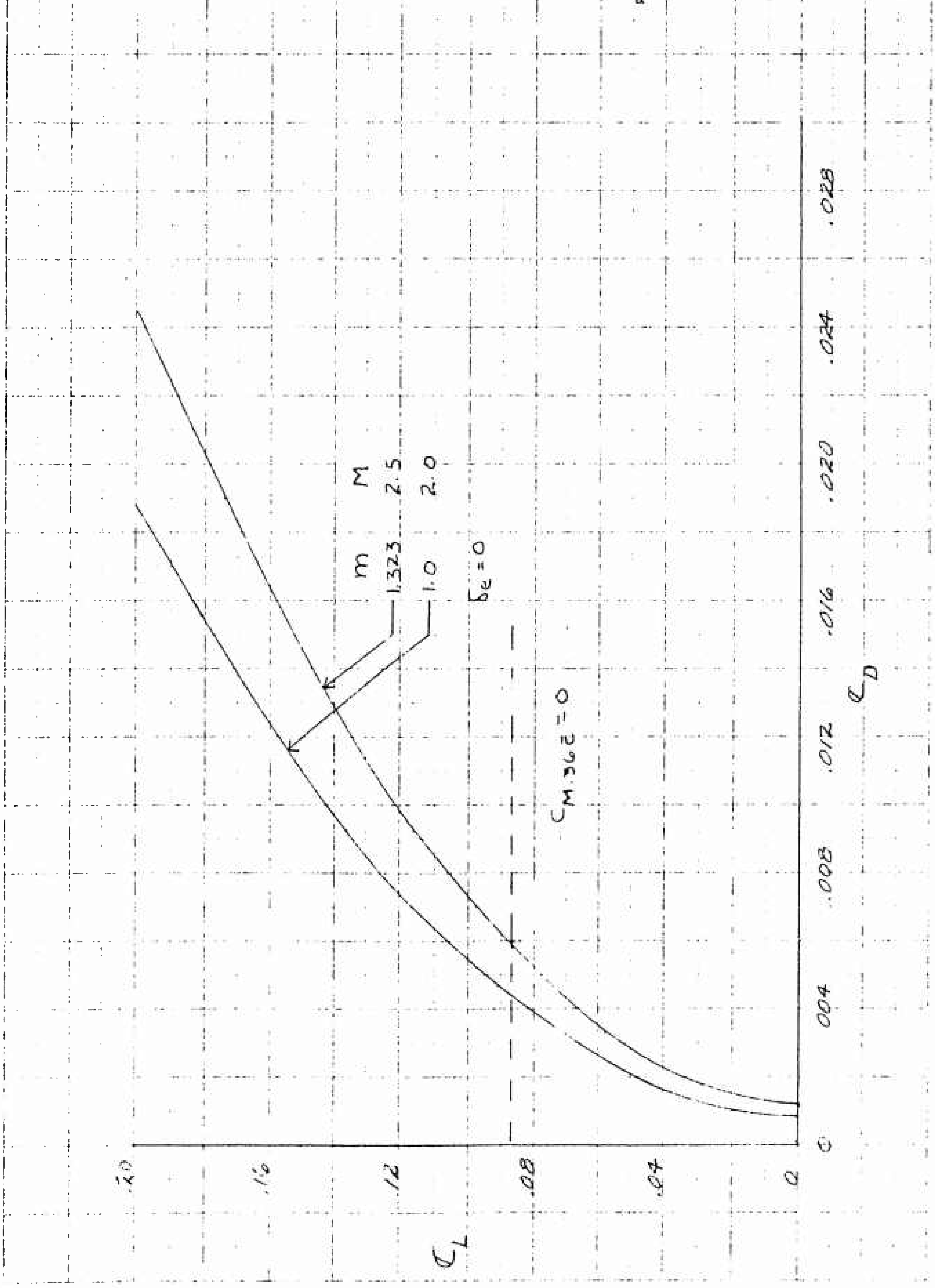

Figure 5.3(a). Effect of Mach Number on Drag Polars for Sonic Leading Edge Delta Wing "δ".

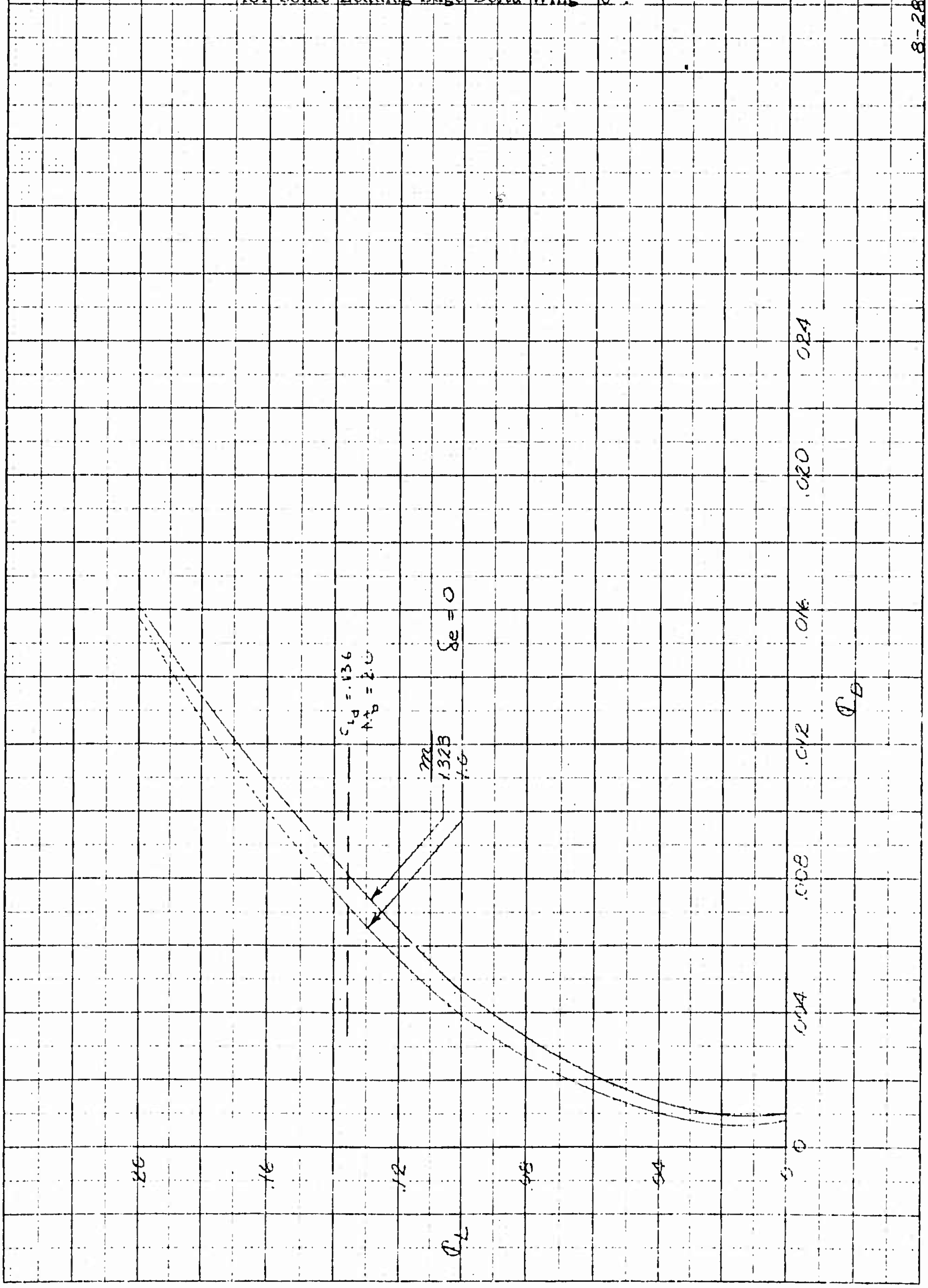

8-28-57

Figure 5.3(b). Effect of Mach Number on Drag Polars for Conic Leading Edge Delta Wing "B".

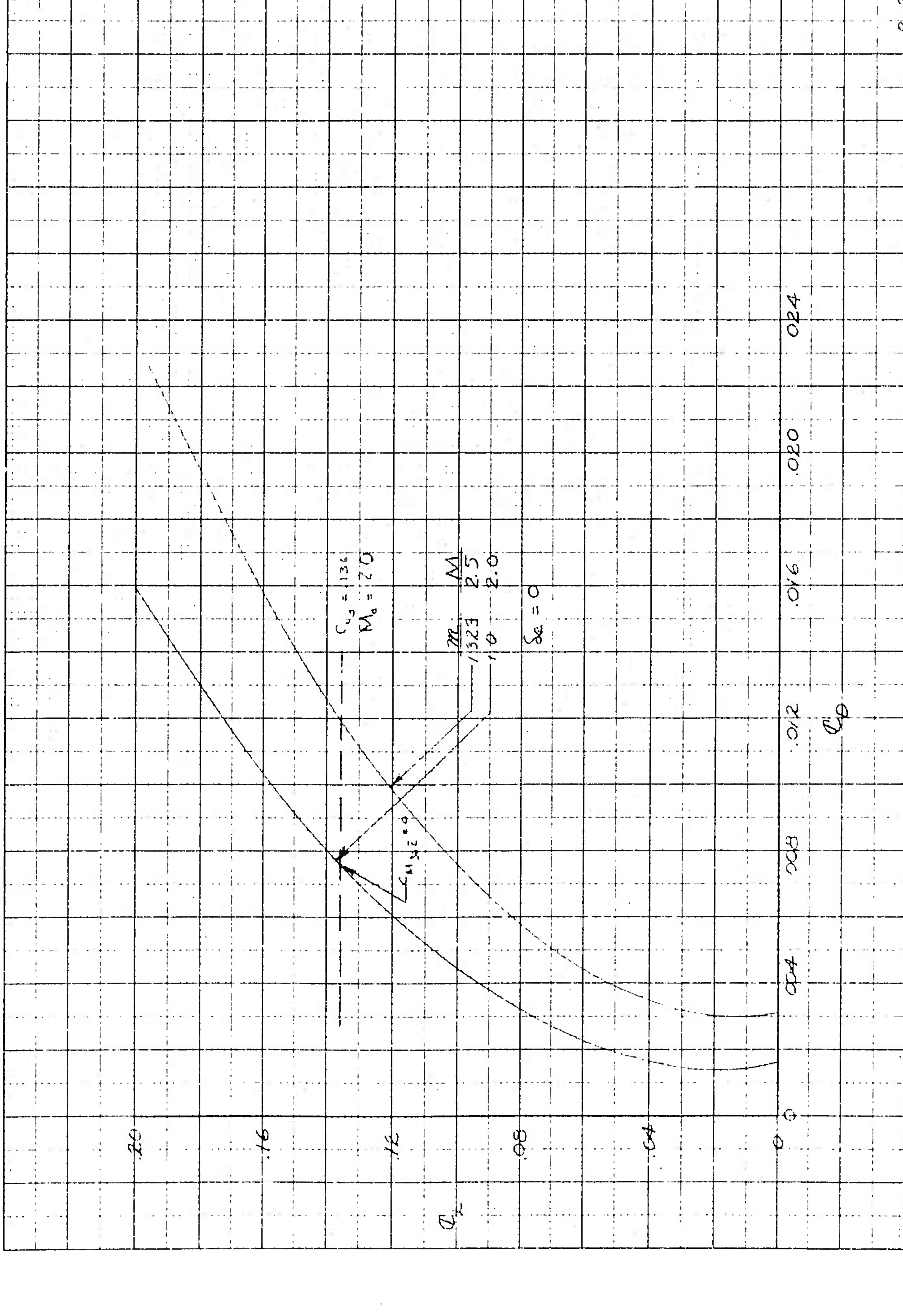

Figure 5.3(c). Effect of Mach Number on Drag Polars
for Sonic Leading Edge Delta Wing "α".

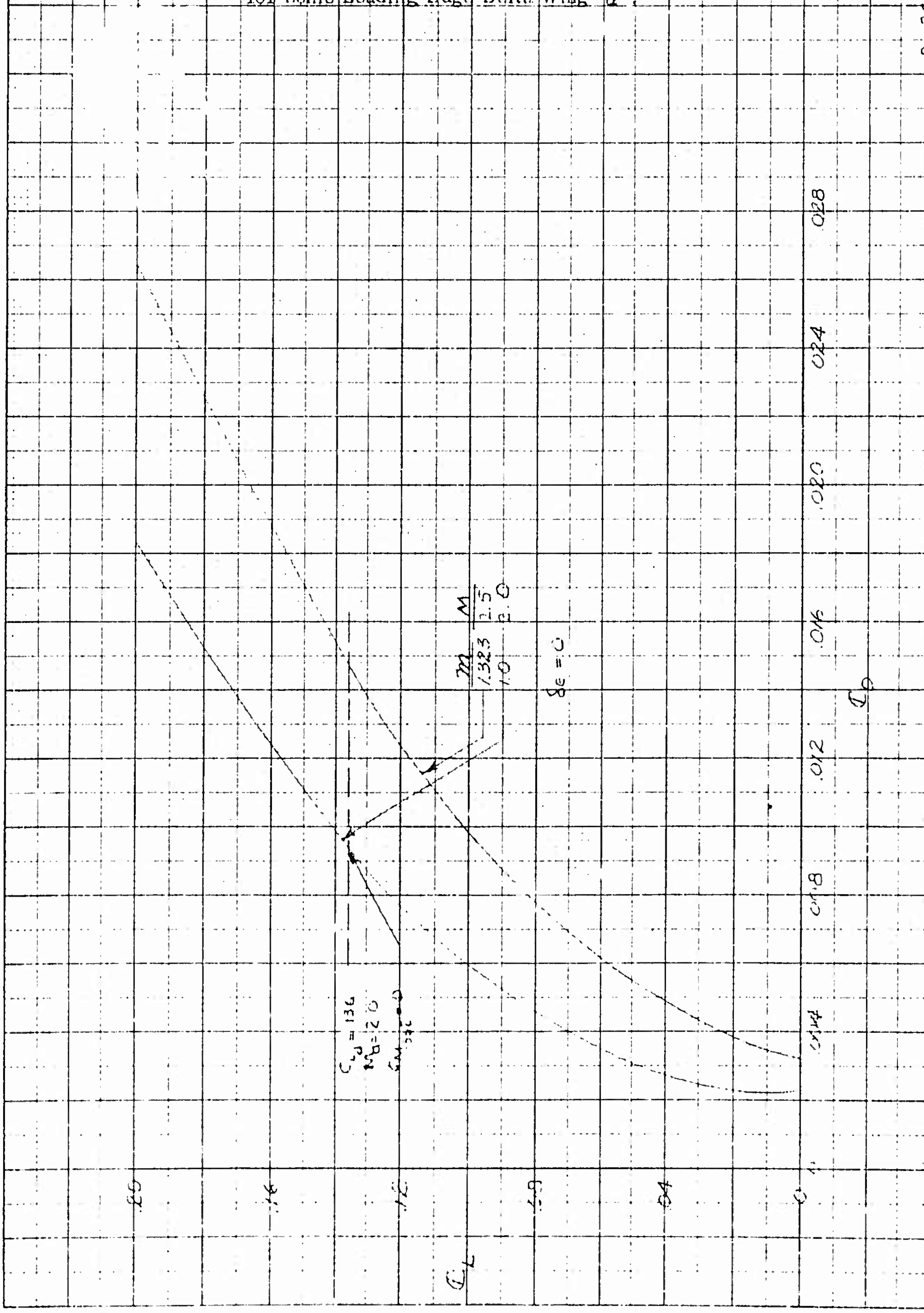

Figure 5.4(a). Pitching Moment Coefficient Comparisons for Supersonic Leading Edge Delta Wings for Various Design Restrictions

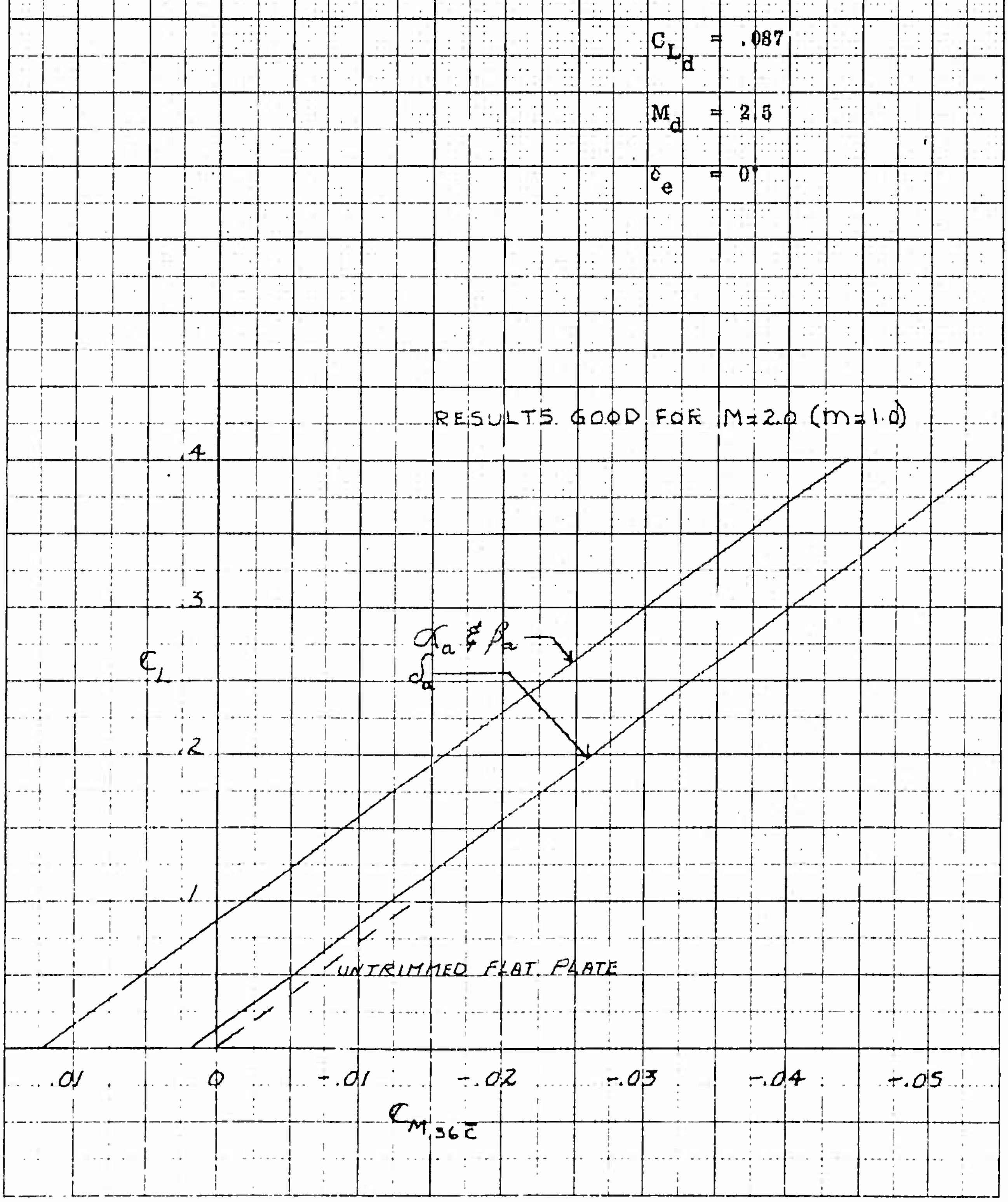

Figure 5.4(b). Pitching Moment Coefficient Comparisons for Sonic Leading Edge Delta Wings for Various Design Restrictions

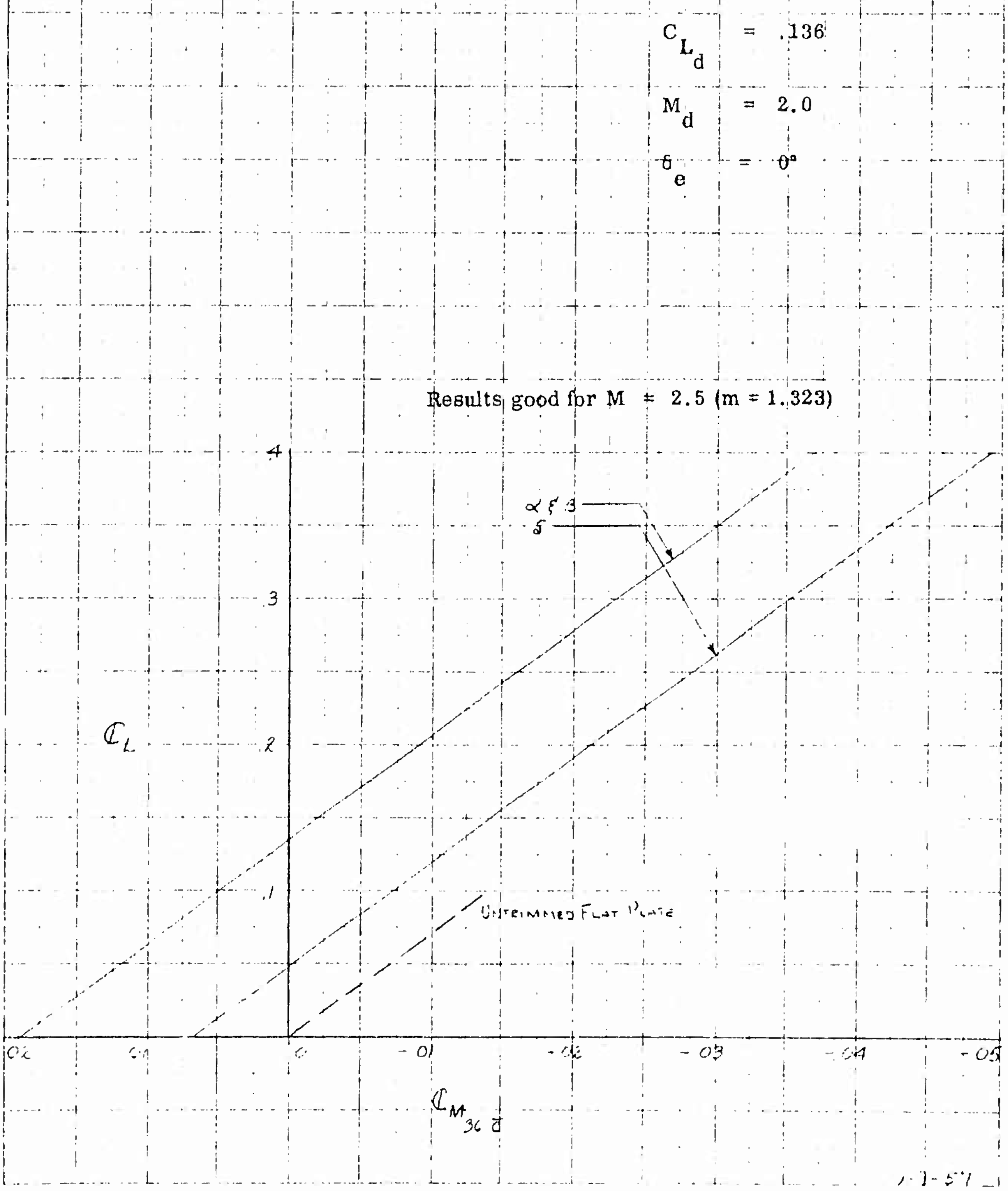

Figure 5.5(a). Effect of Mach Number on Pitching Moment Coefficient for Supersonic Leading Edge Delta Wing "δ_a"

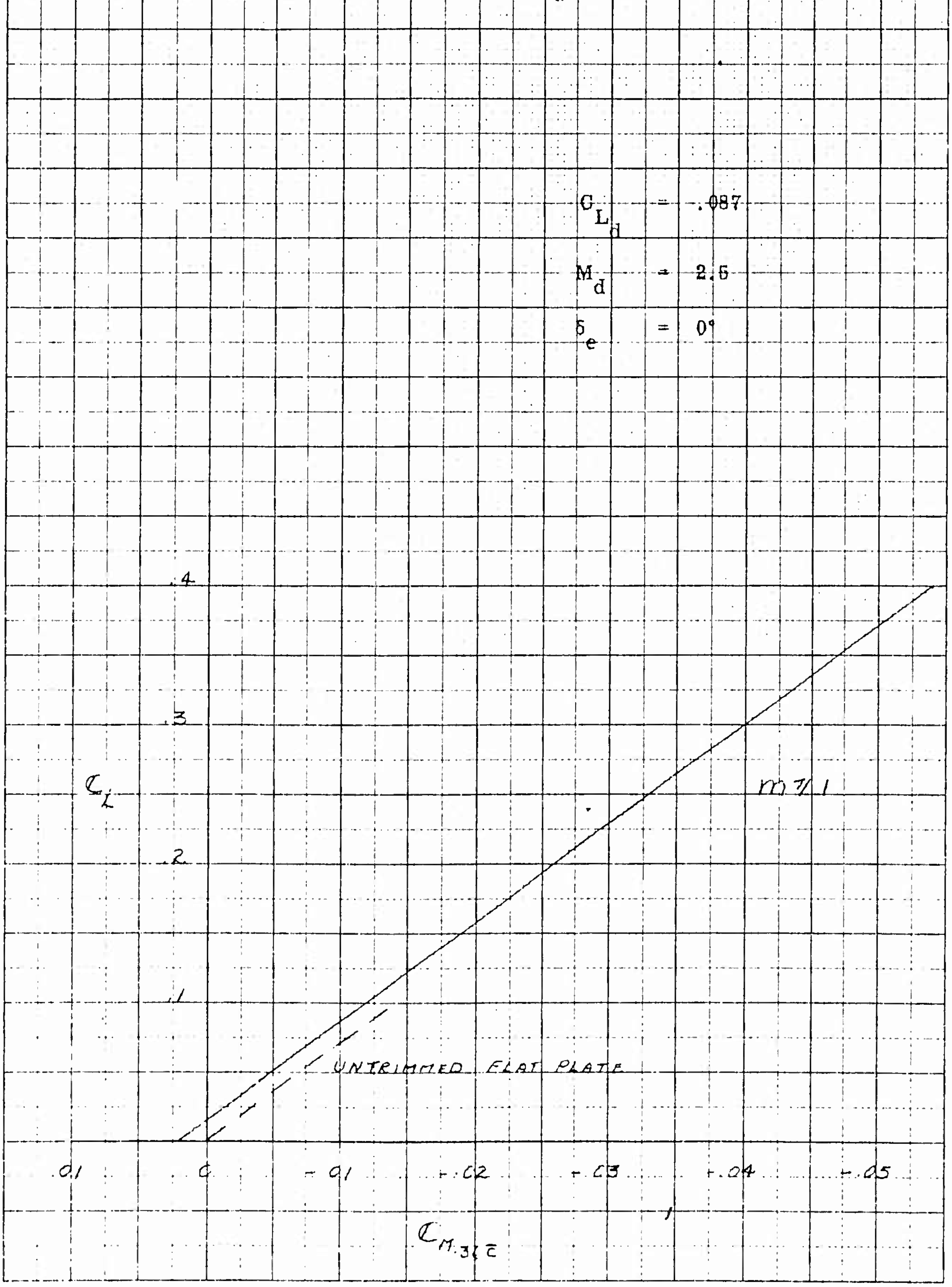

Figure 5.5(b). Effect of Mach Number on Pitching Moment Coefficients for Supersonic Leading Edge Wing "β_a".

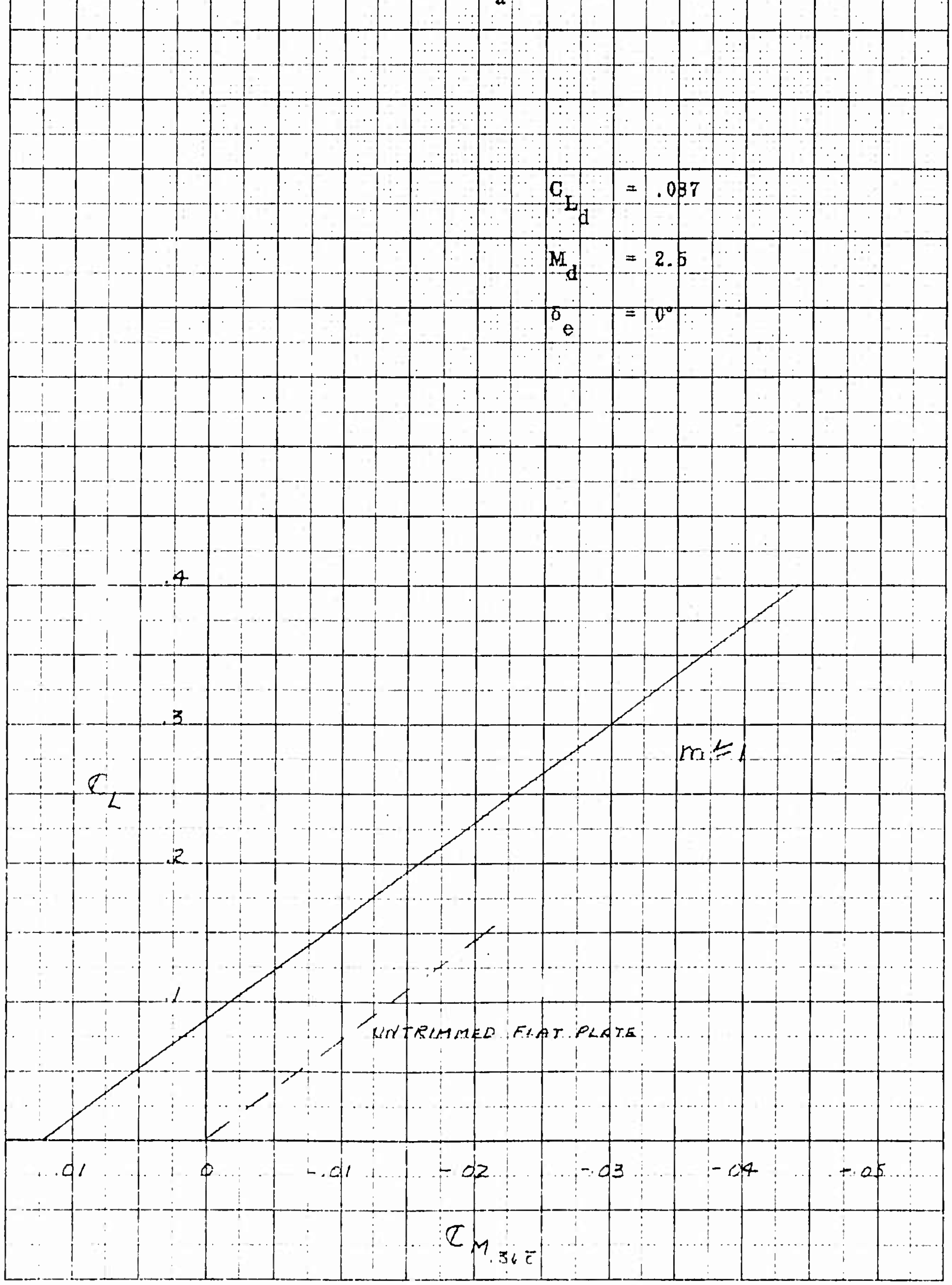

Figure 5.5(c). Effect of Mach Number on Pitching Moment Coefficient for Supersonic Leading Edge Delta Wing "α_a".

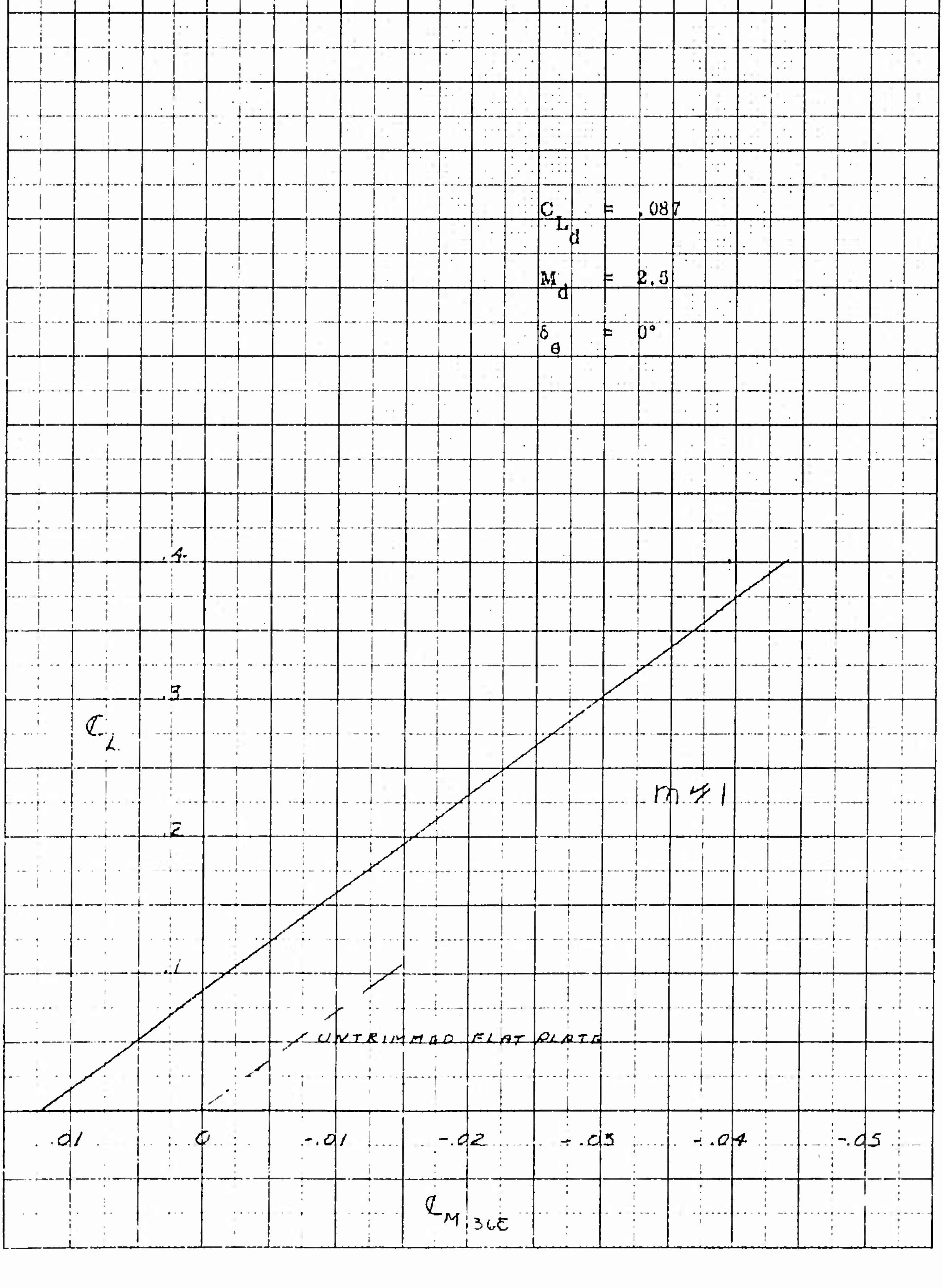

Figure 5.6(a). Effect of Mach Number on Pitching Moment Coefficient for Sonic Leading Edge Delta Wing "δ"

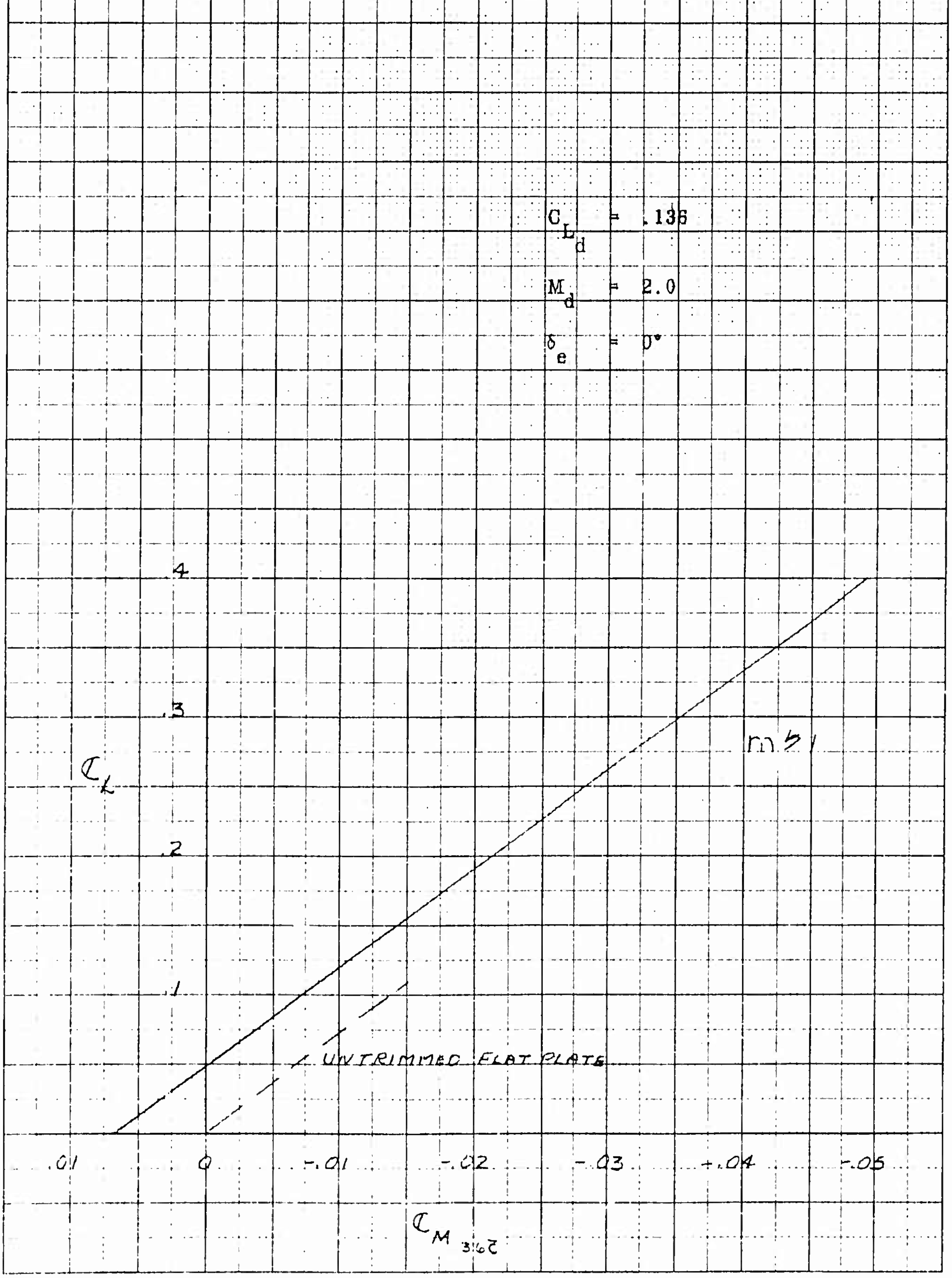

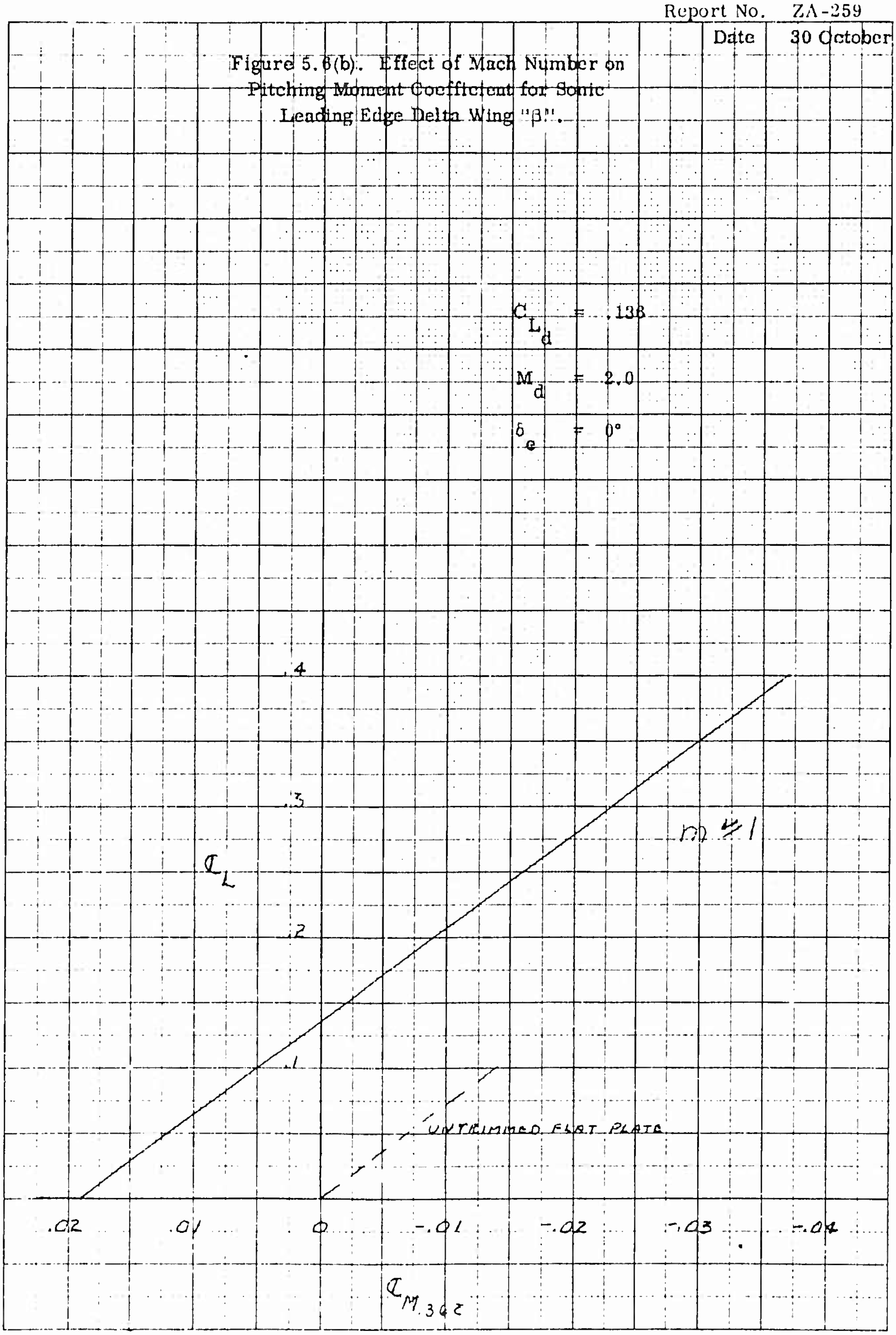

Figure 5.6(b). Effect of Mach Number on Pitching Moment Coefficient for Sonic Leading Edge Delta Wing "β".

Figure 5.5(c). Effect of Mach Number on Pitching Moment Coefficient for Sonic Leading Edge Delta Wing "a".

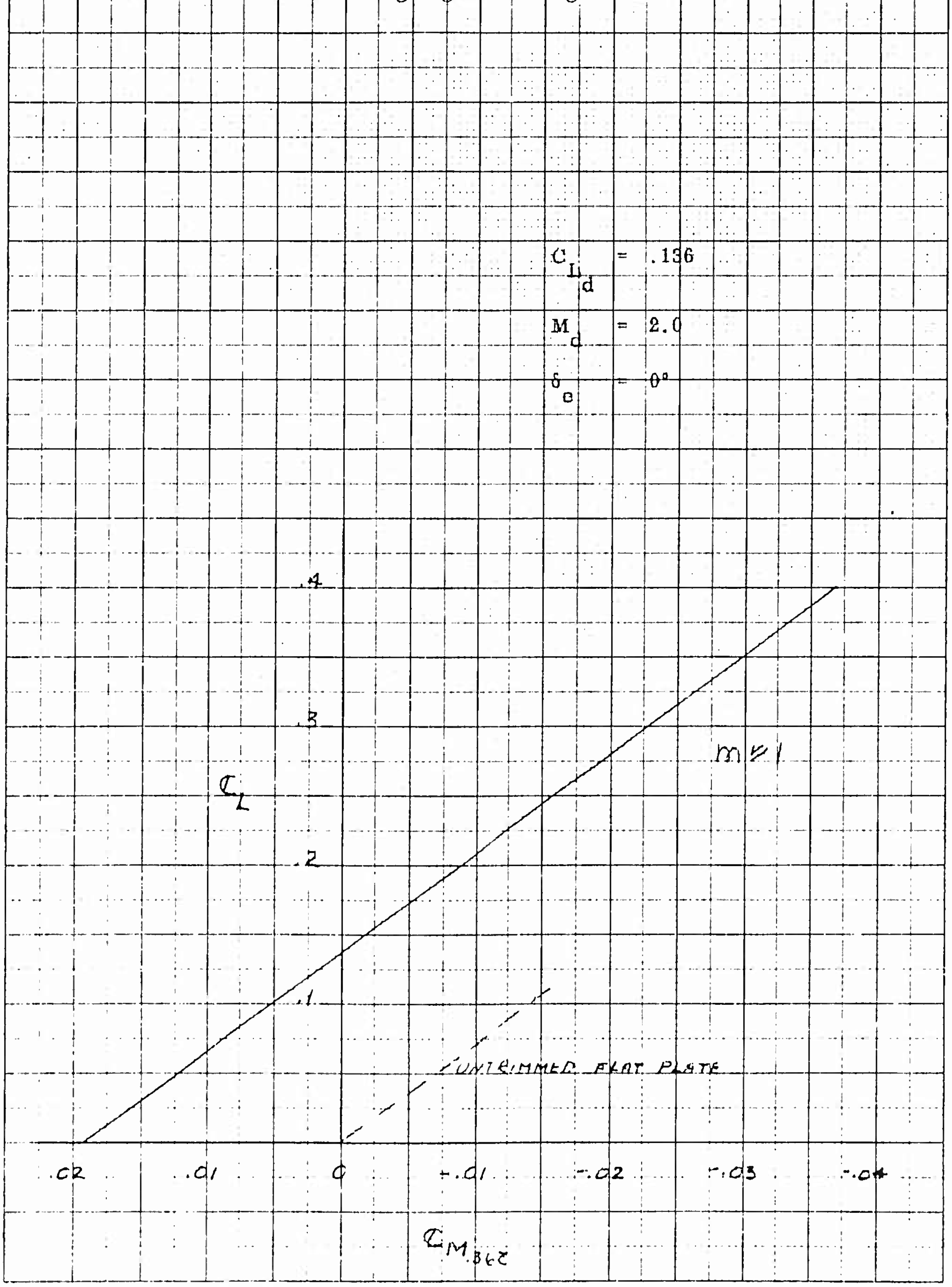

Figure 5.7(a). Comparison with Flat Plate of Span Loading at Design Lift for Supersonic Leading Edge Deltas with Various Design Restrictions.

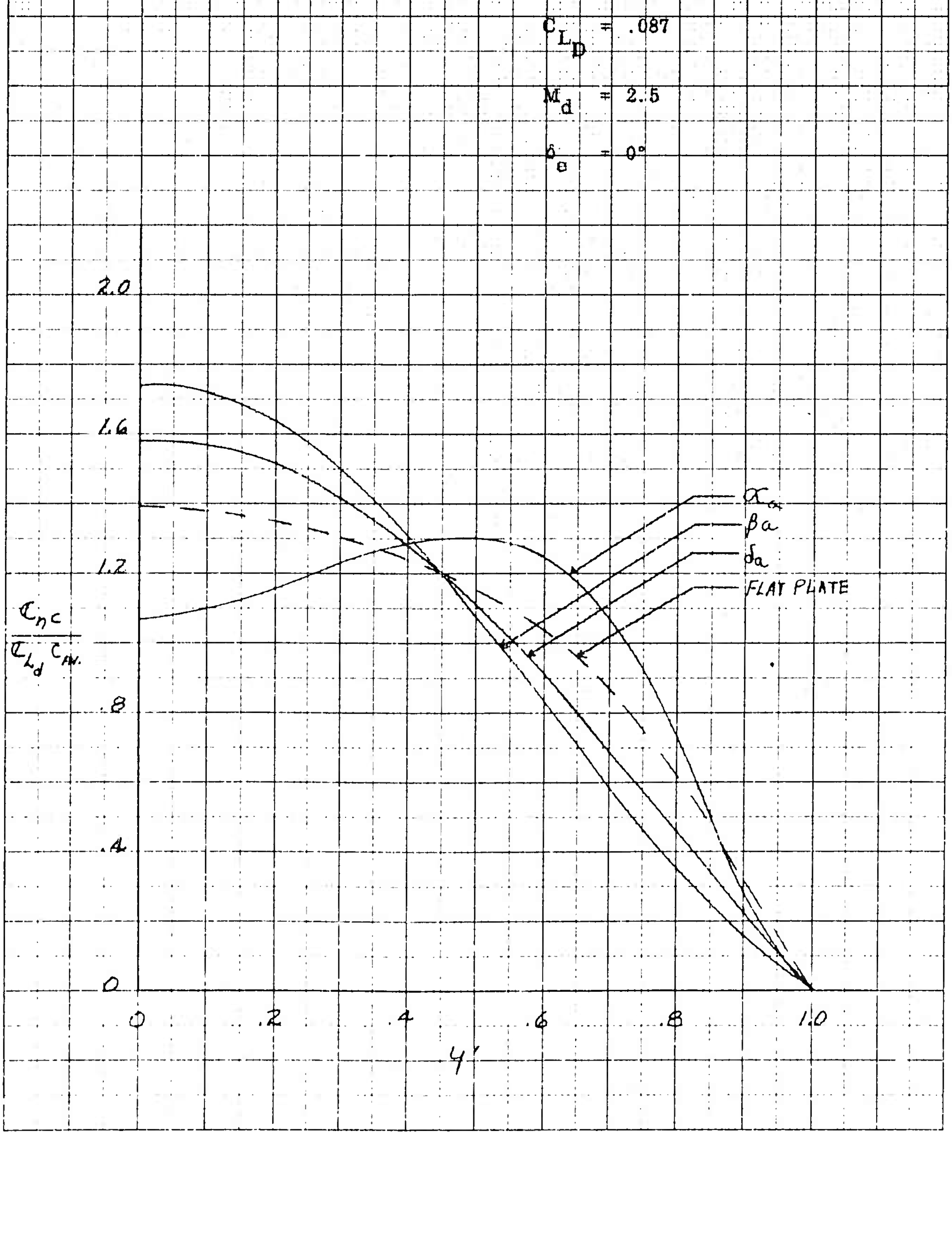

Figure 5.7(b). Comparison with Flat Plate of Span Loading at Design Lift for Sonic Leading Edge Delta Wings with Various Design Restrictions

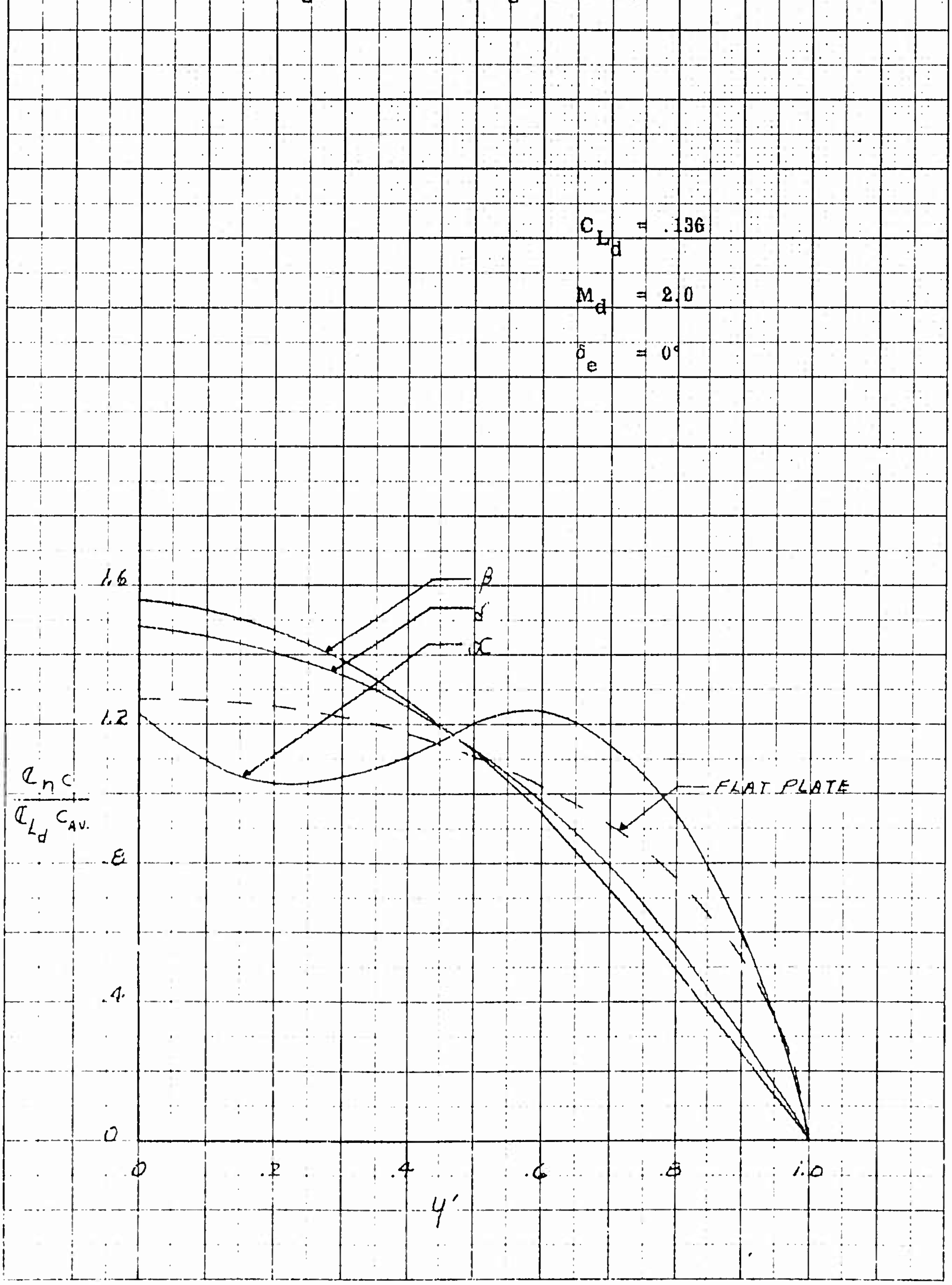

Figure 5.7(b). Comparison with Flat Plate of Span Loading at Design Lift for Sonic Leading Edge Delta Wings with Various Conditions.

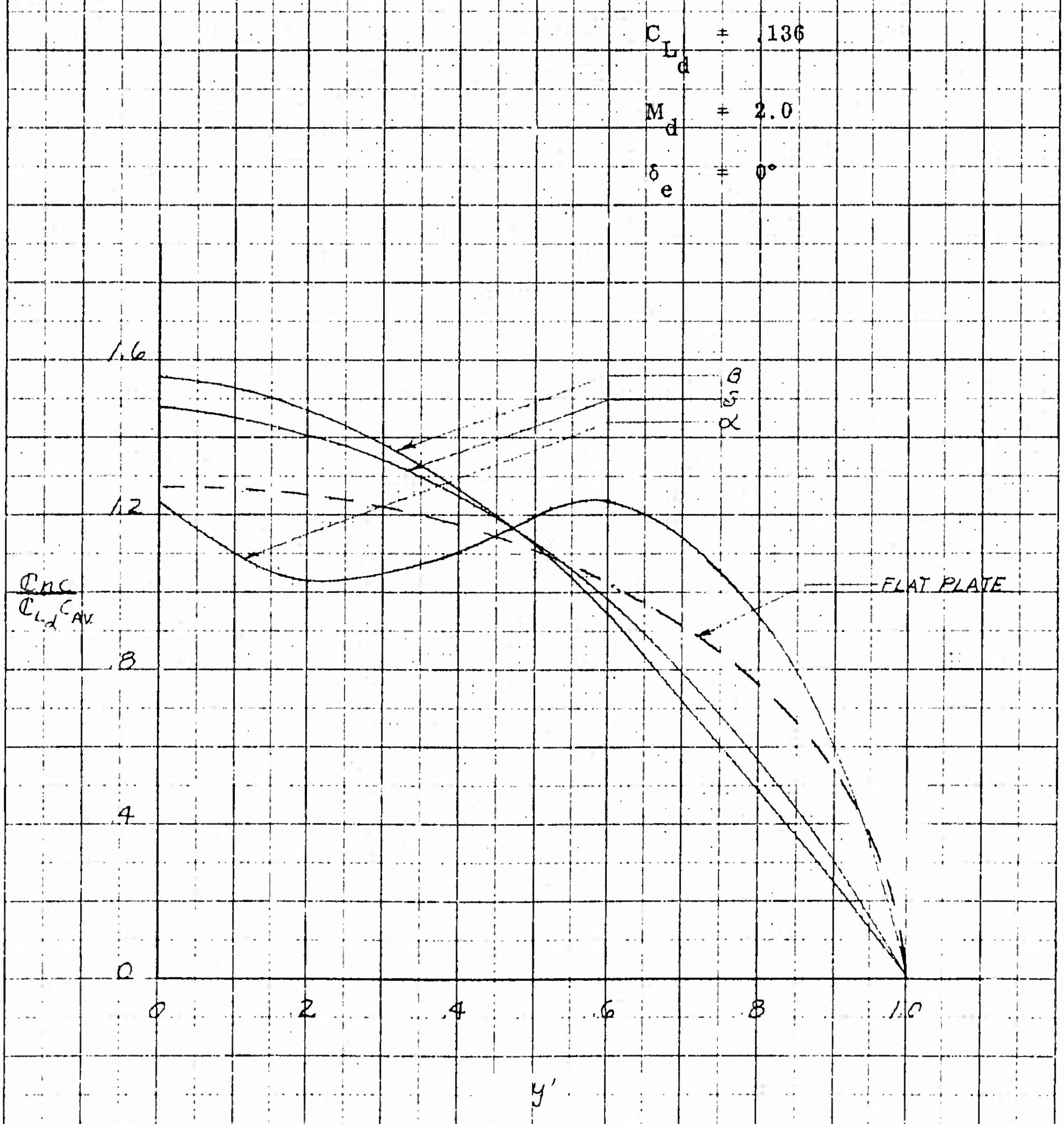

Figure 5.8(a). Effect of Mach Number on Span Loading of Supersonic Leading Edge Delta Wing "δ_a"

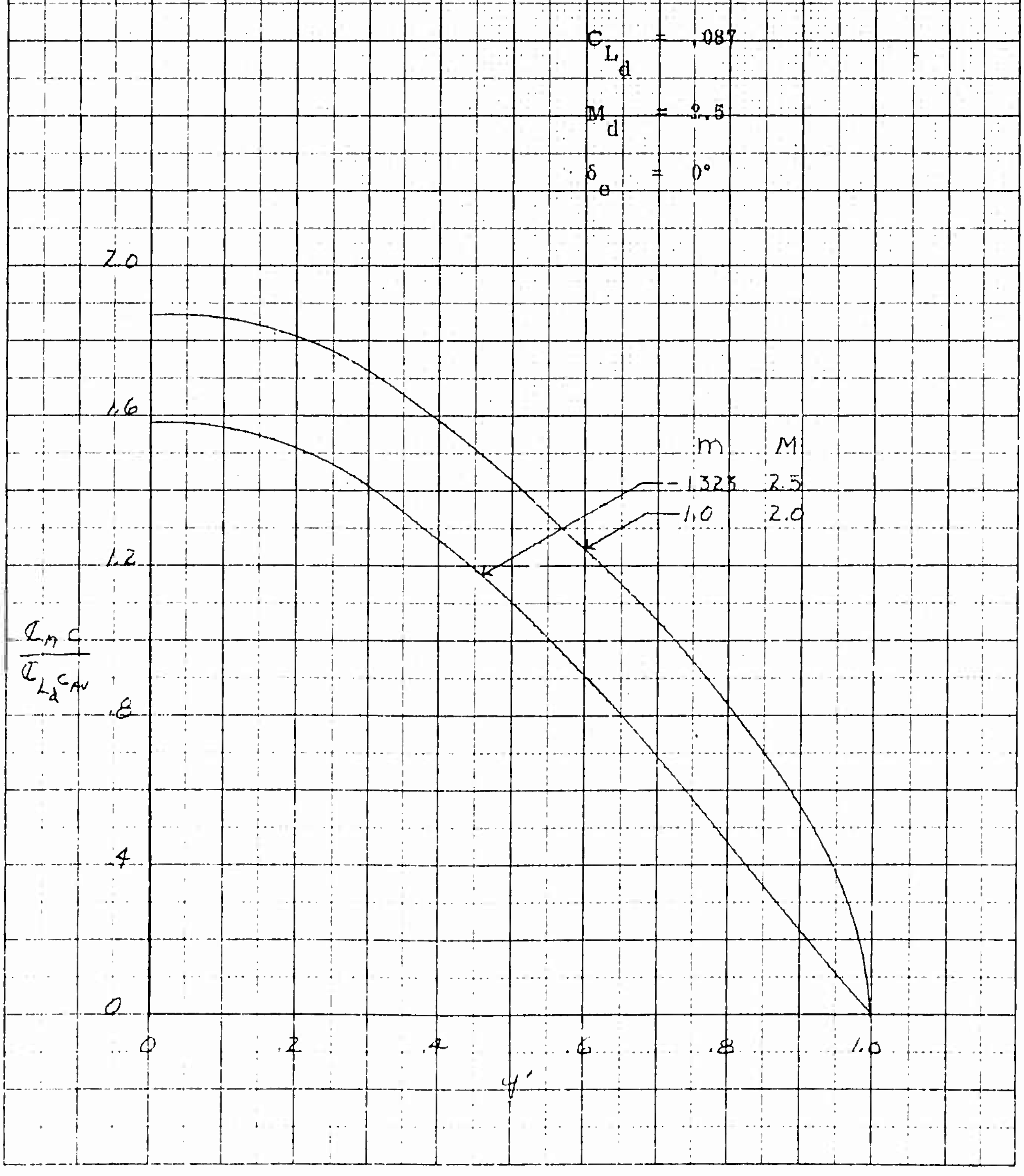

Figure 5.8(b). Effect of Mach Number on Span Loading of Supersonic Leading Edge Delta Wing "β_a".

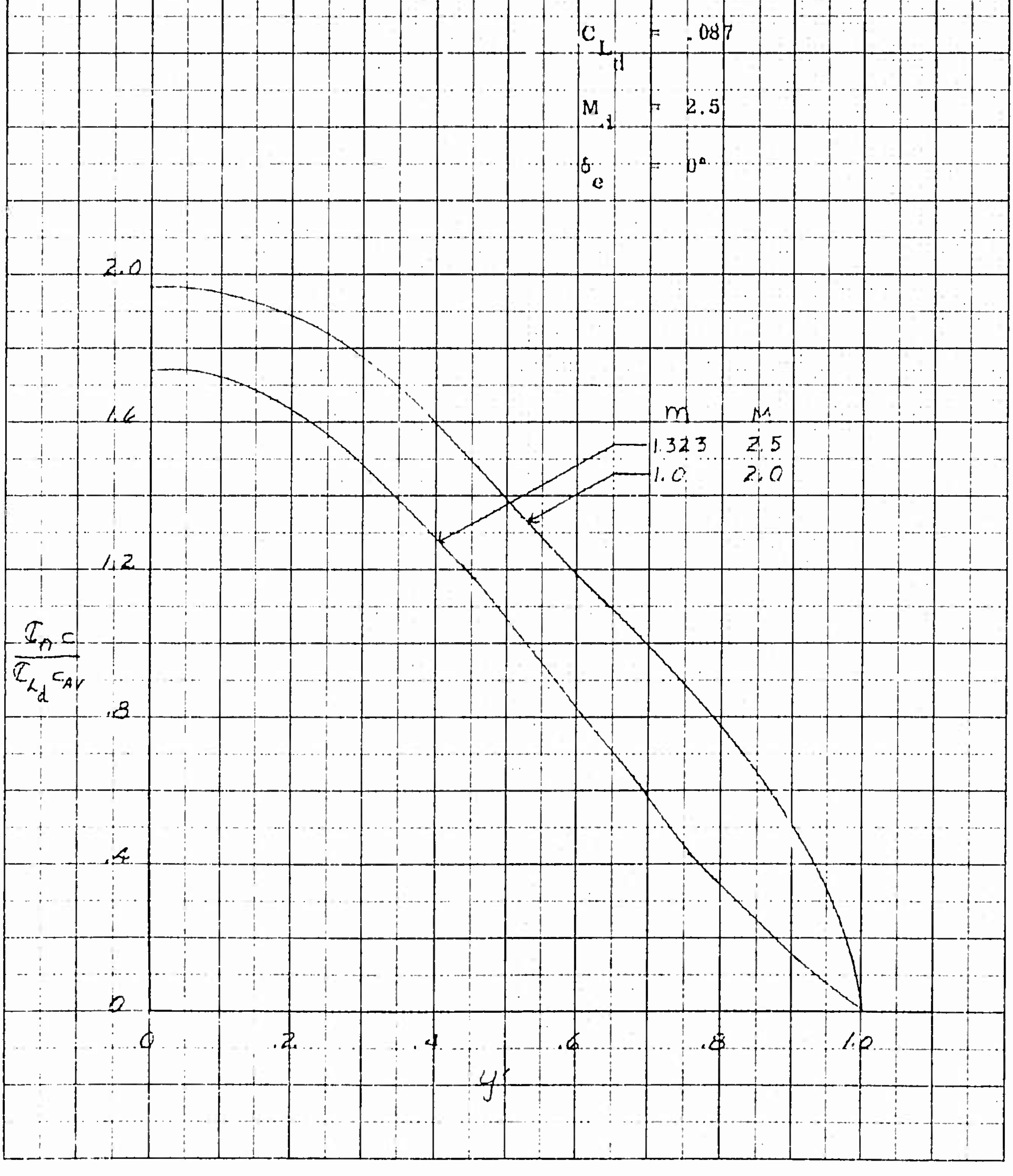

Figure 5.8(c). Effect of Mach Number on Span Loading of Supersonic Leading Edge Delta Wing "α_a"

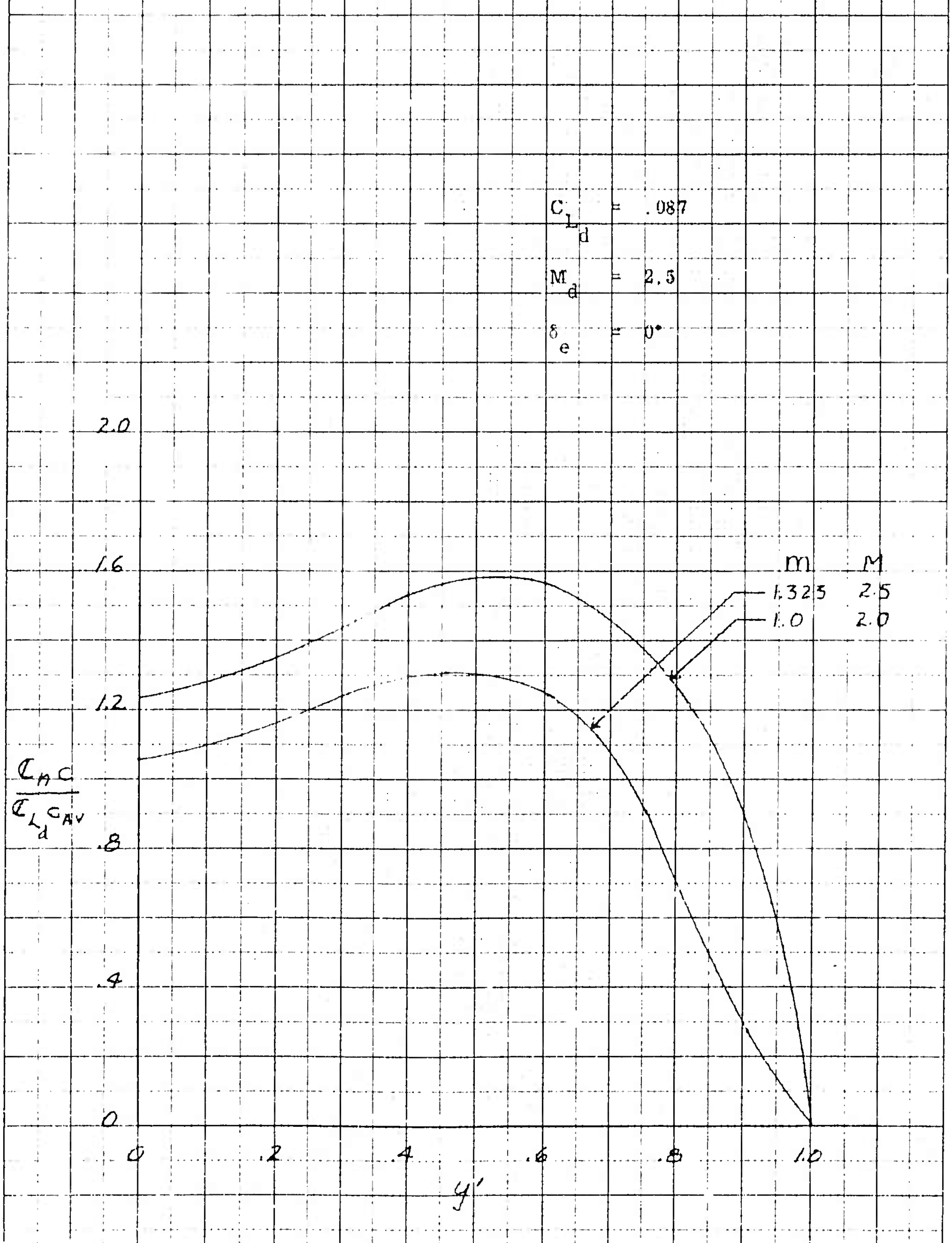

Figure 5. 9(h). Effect of Mach Number on Span Loading of Sonic Leading Edge Delta Wing "δ".

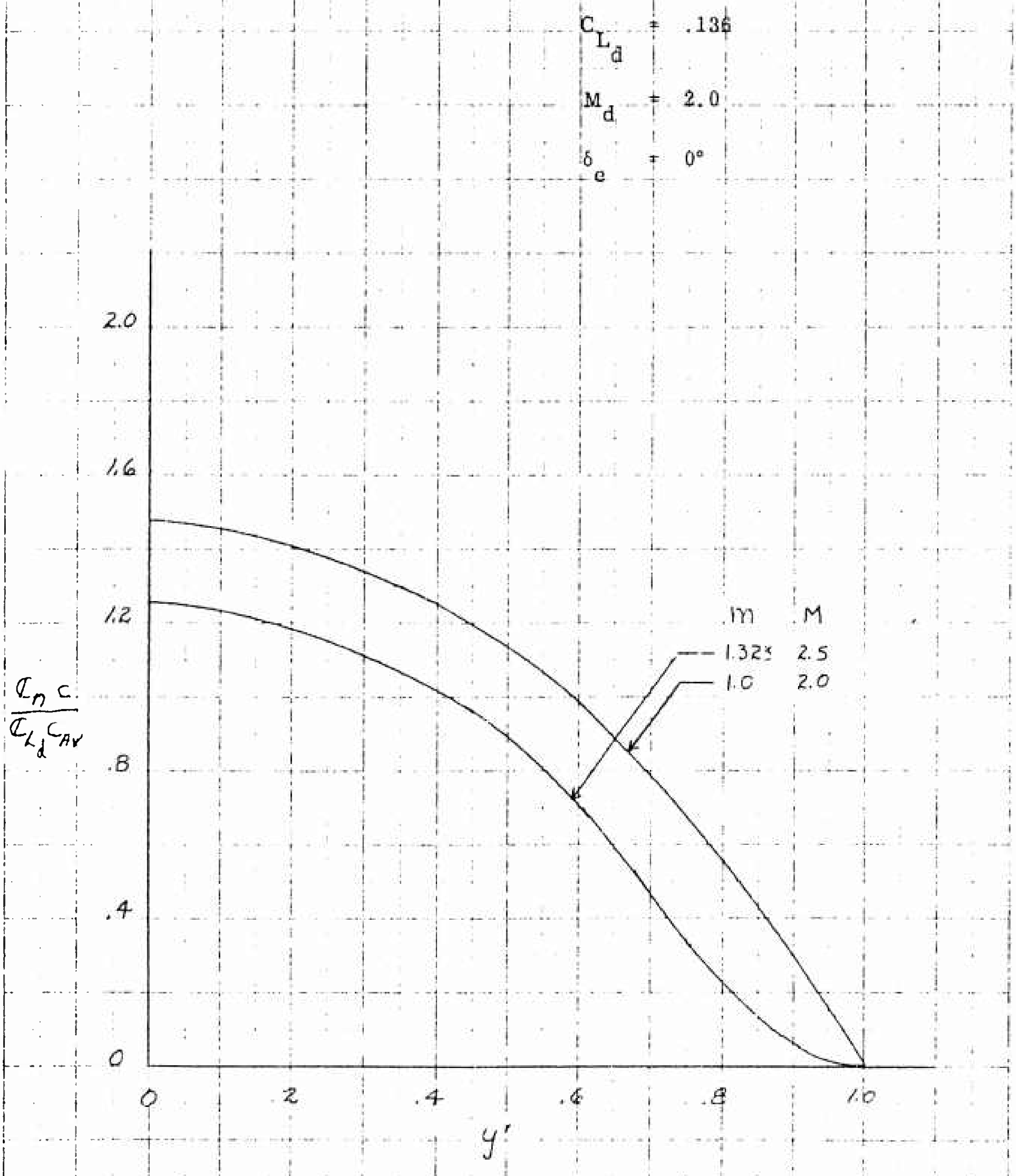

Figure 5.9(b). Effect of Mach Number on Span Loading of Sonic Leading Edge Delta Wing "β".

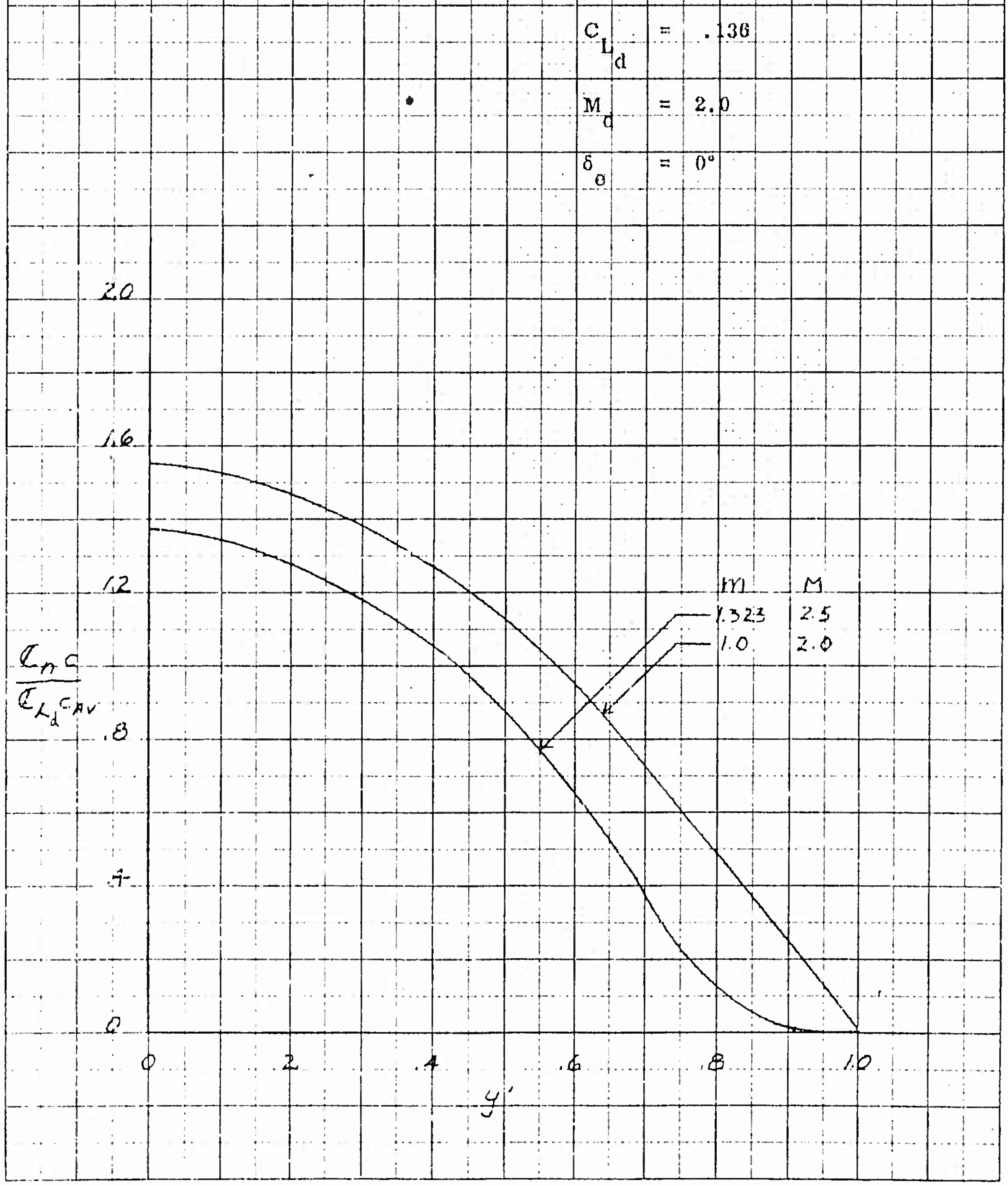

Figure 5.9(d). Effect of Mach Number on Span Loading for Sonic Leading Edge Delta Wing "d".

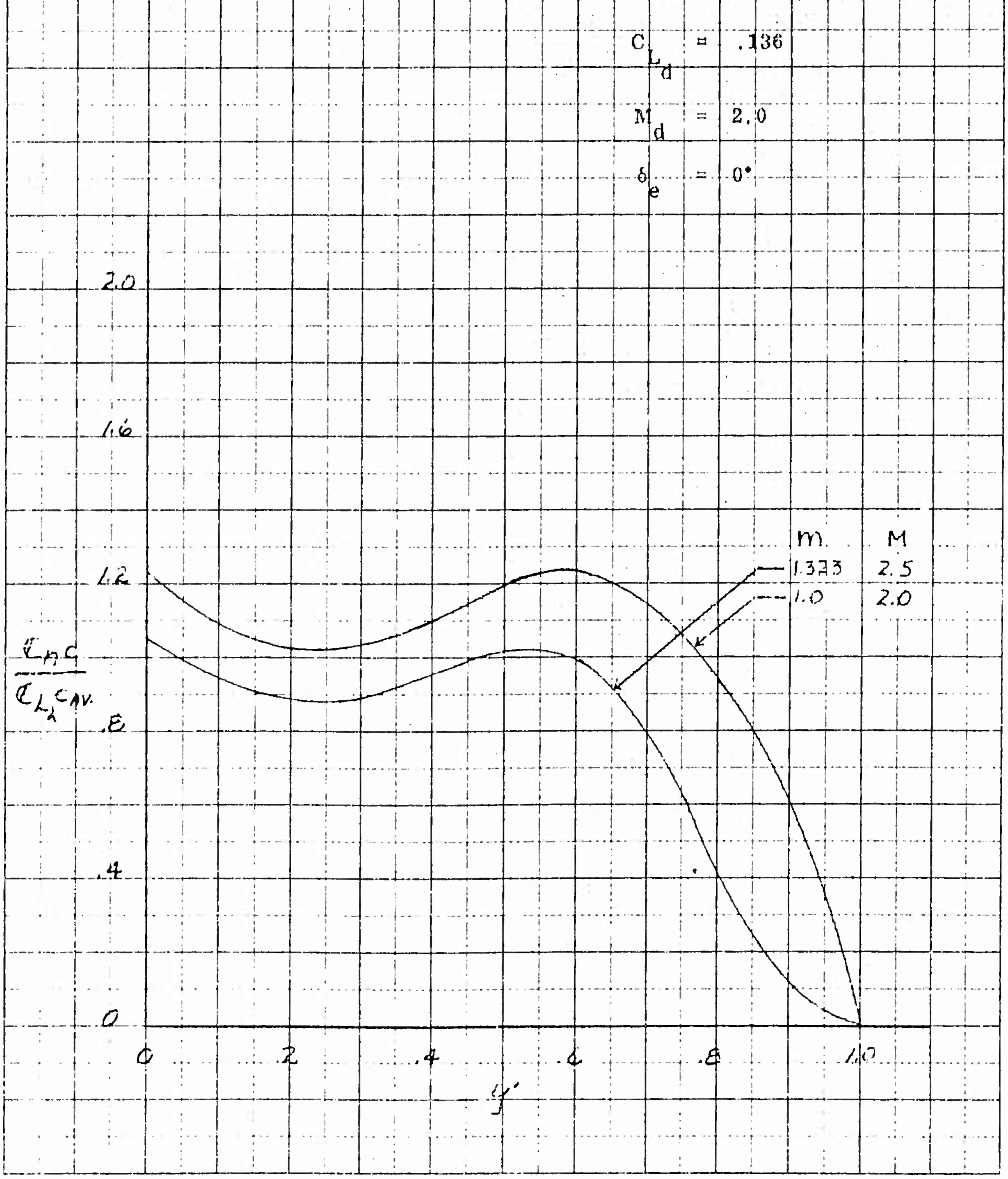

Figure 5.10(a). Comparison with Flat Plate of Chord Loadings at Design Lift for Supersonic Leading Edge Delta Wings with Various Design Restrictions.

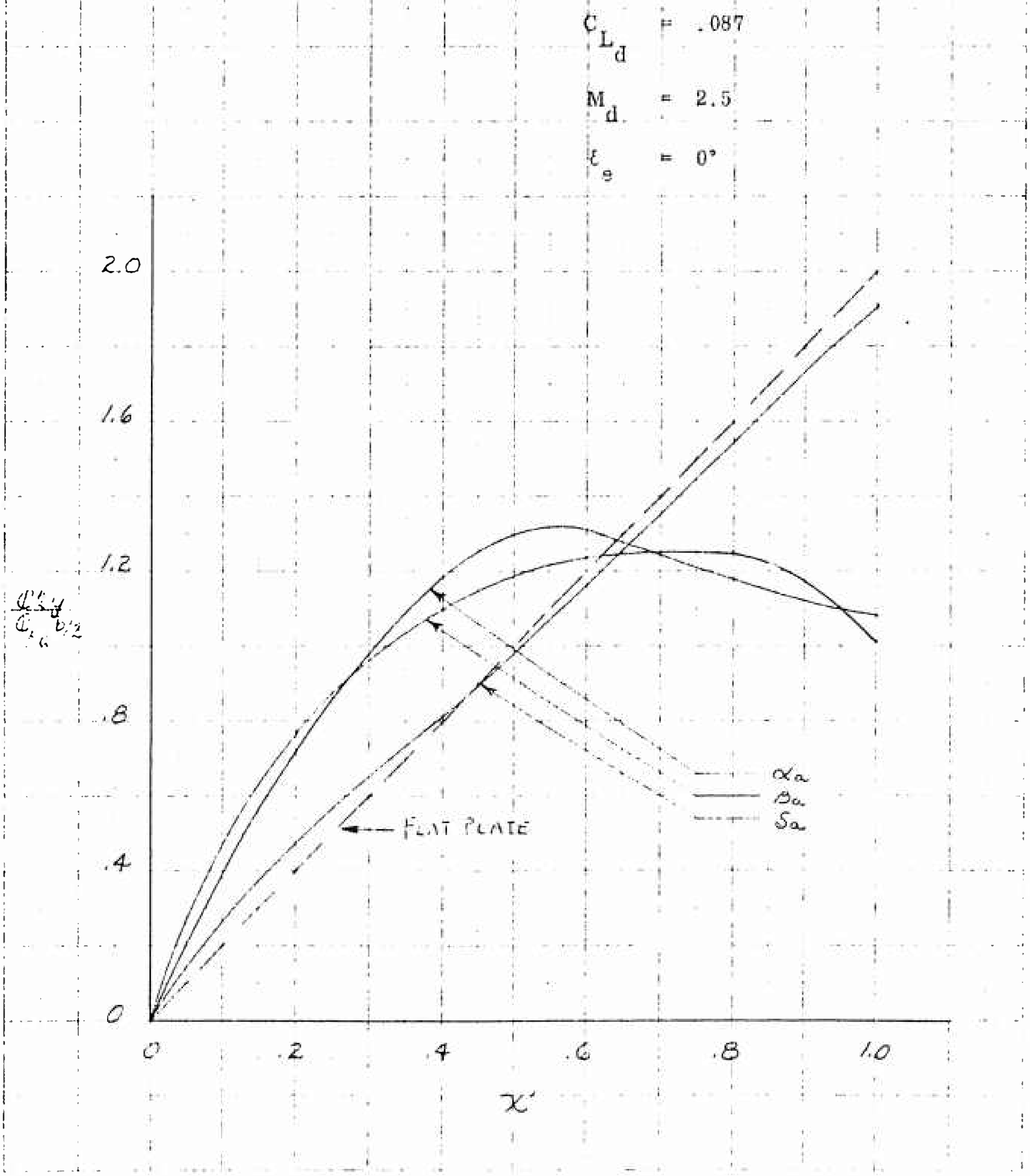

Figure 5.10(b). Comparison with Flat Plate of Chord Loading at Design Lift for Sonic Leading Edge Delta Wings with Various Design Restrictions.

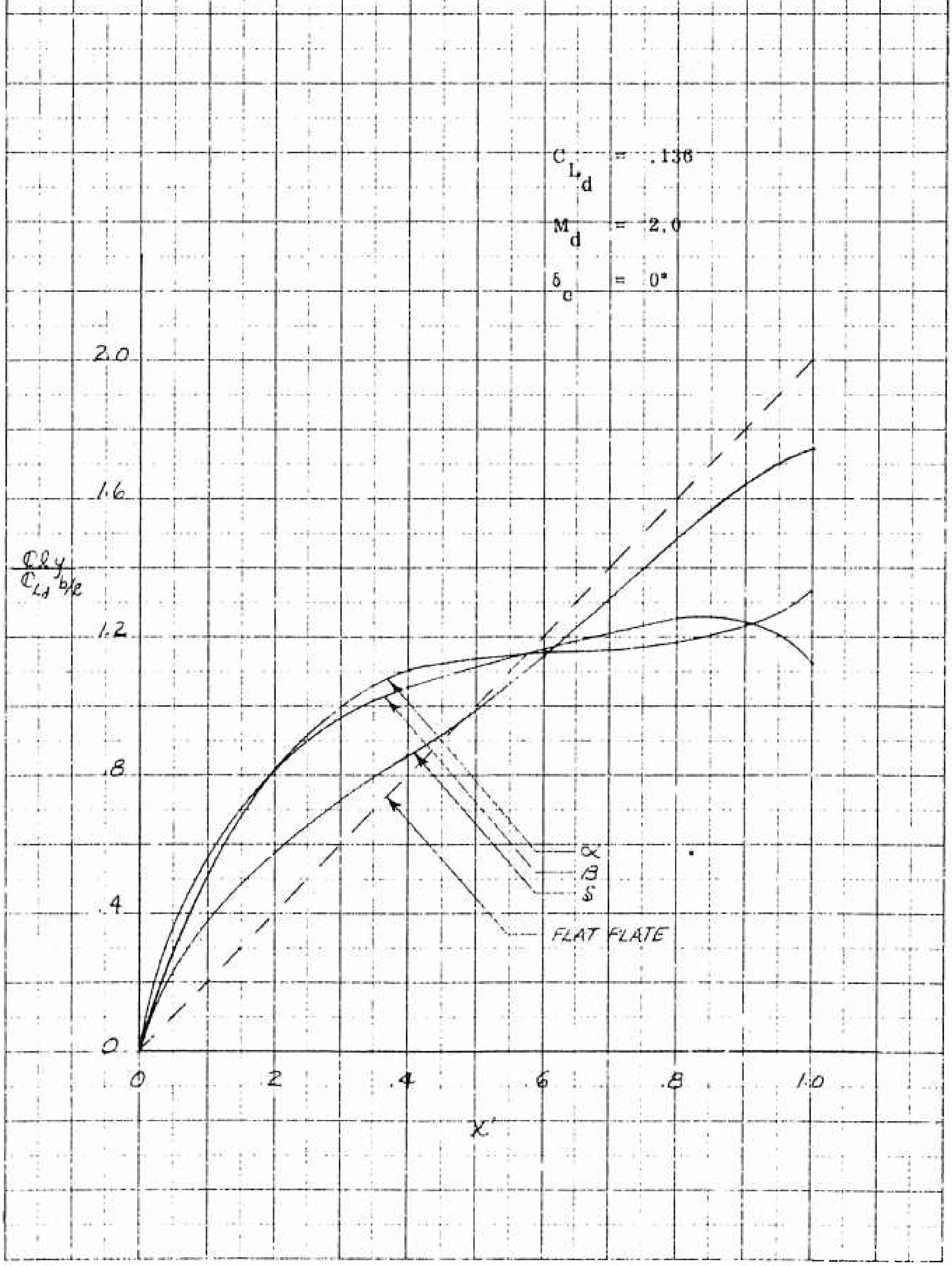

Figure 5.11(a). Effect of Mach Number on Chord Loading of Supersonic Leading Edge Delta Wing "δ_a"

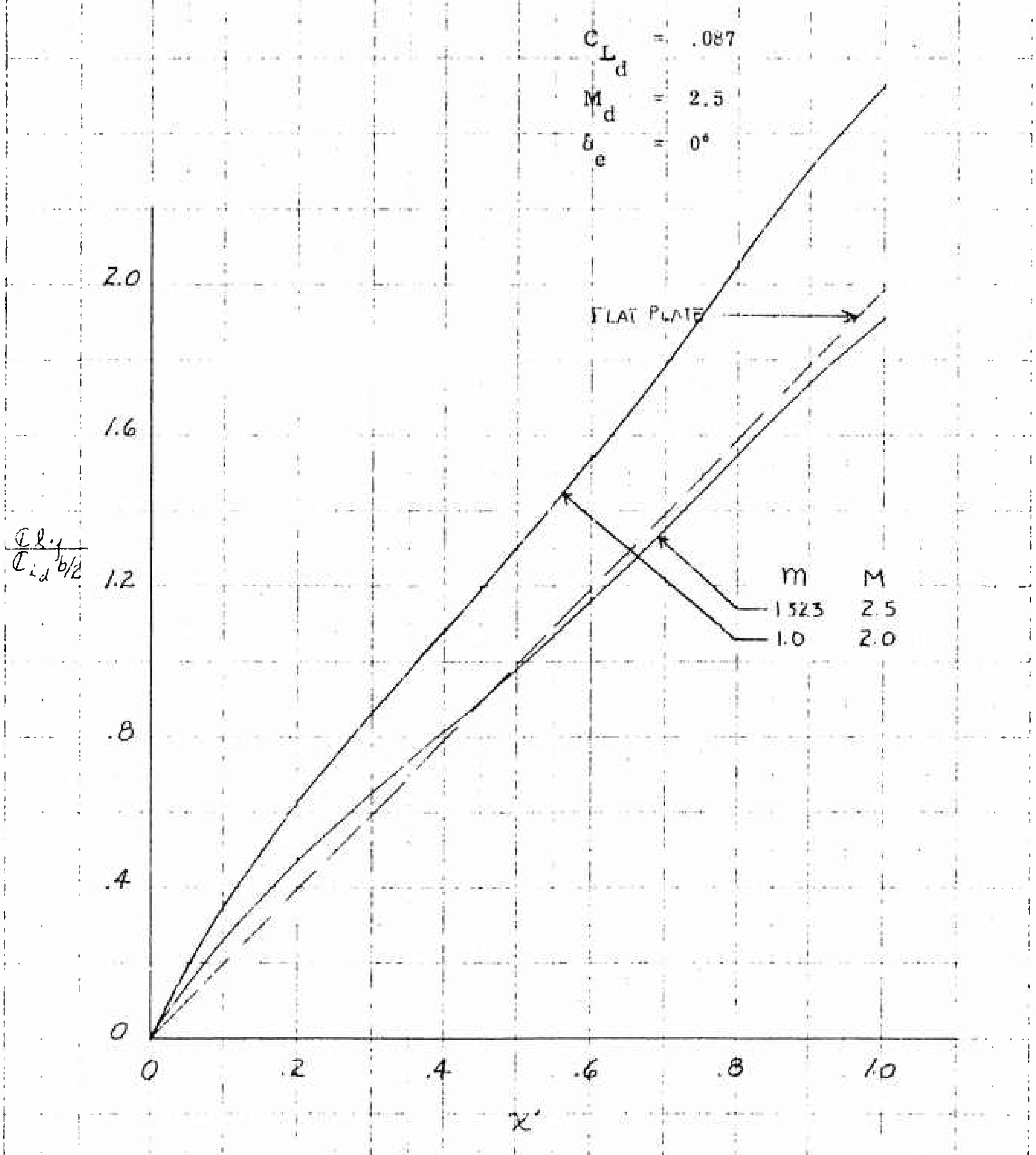

Figure 5.11(b). - Effect of Mach Number on Chord Loading of Supersonic Leading Edge Delta Wing "β_a"

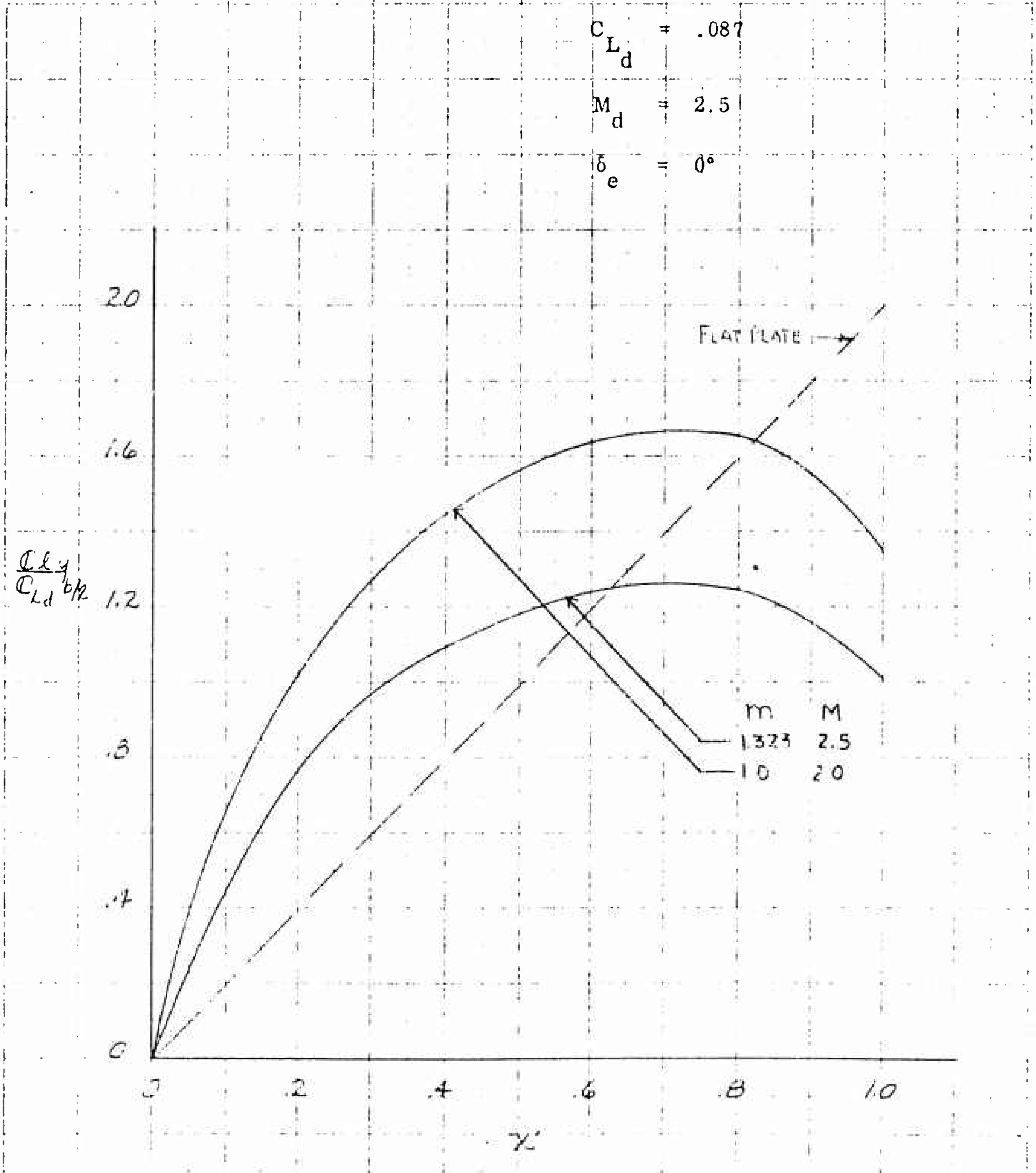

Figure 5.11(c). Effect of Mach Number on Chord Loading of Supersonic Leading Edge Delta Wing "α_a".

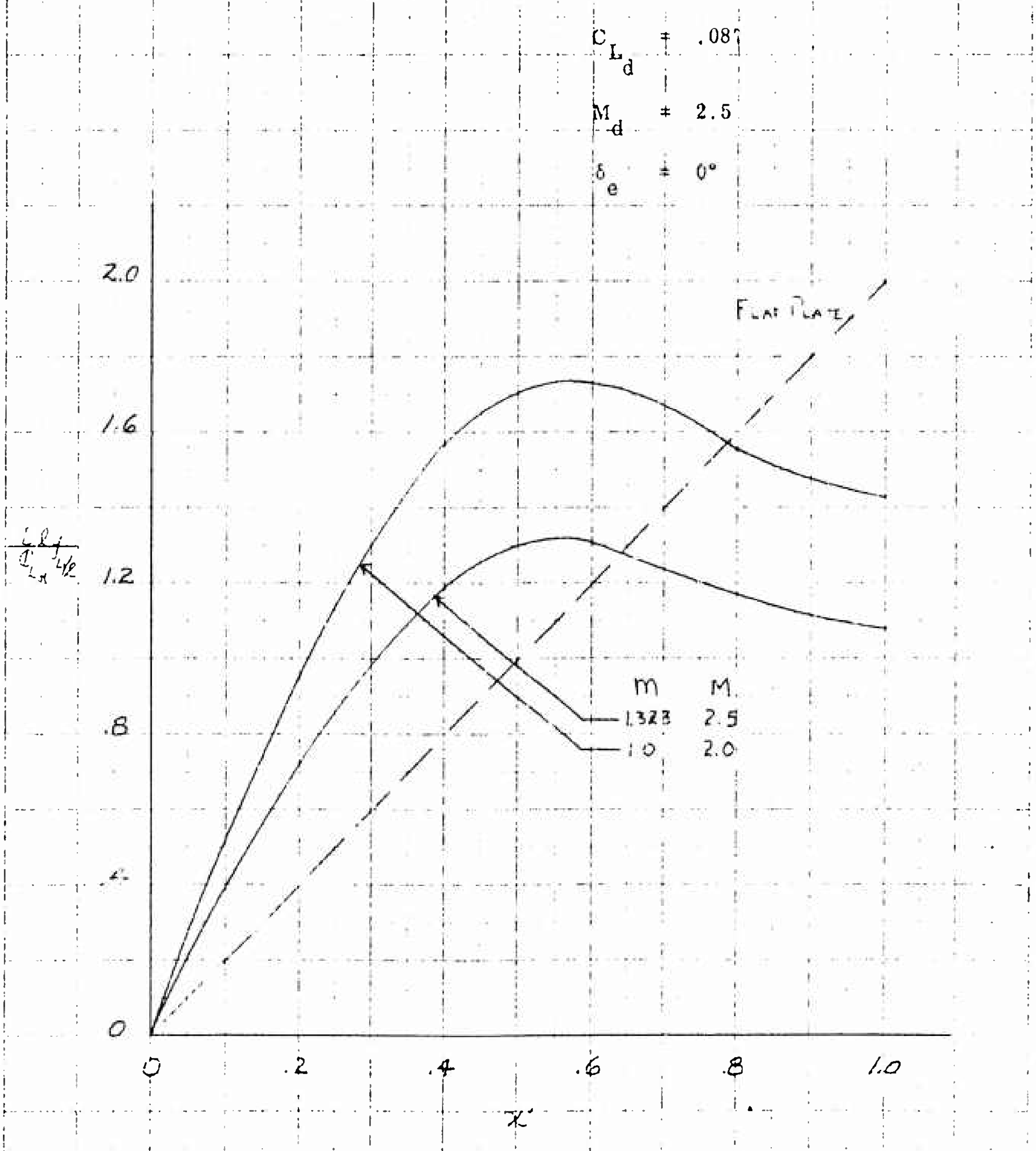

Figure 5.12(a). Effect of Mach Number on Chord Loading of Sonic Leading Edge Wing "8".

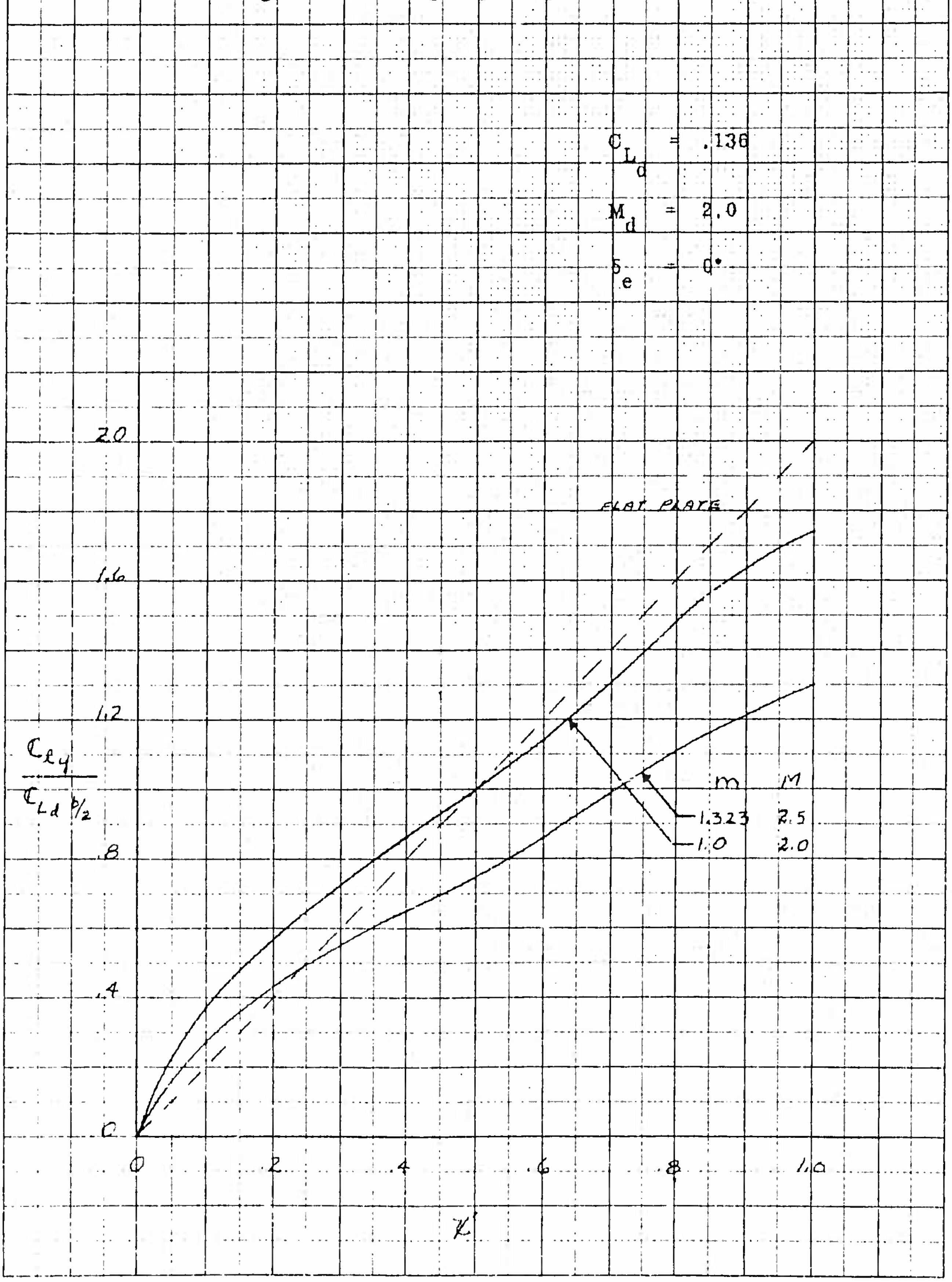

Figure 5.12(b). Effect of Mach Number on Chord Loading of Sonic Leading Edge Delta Wing "β".

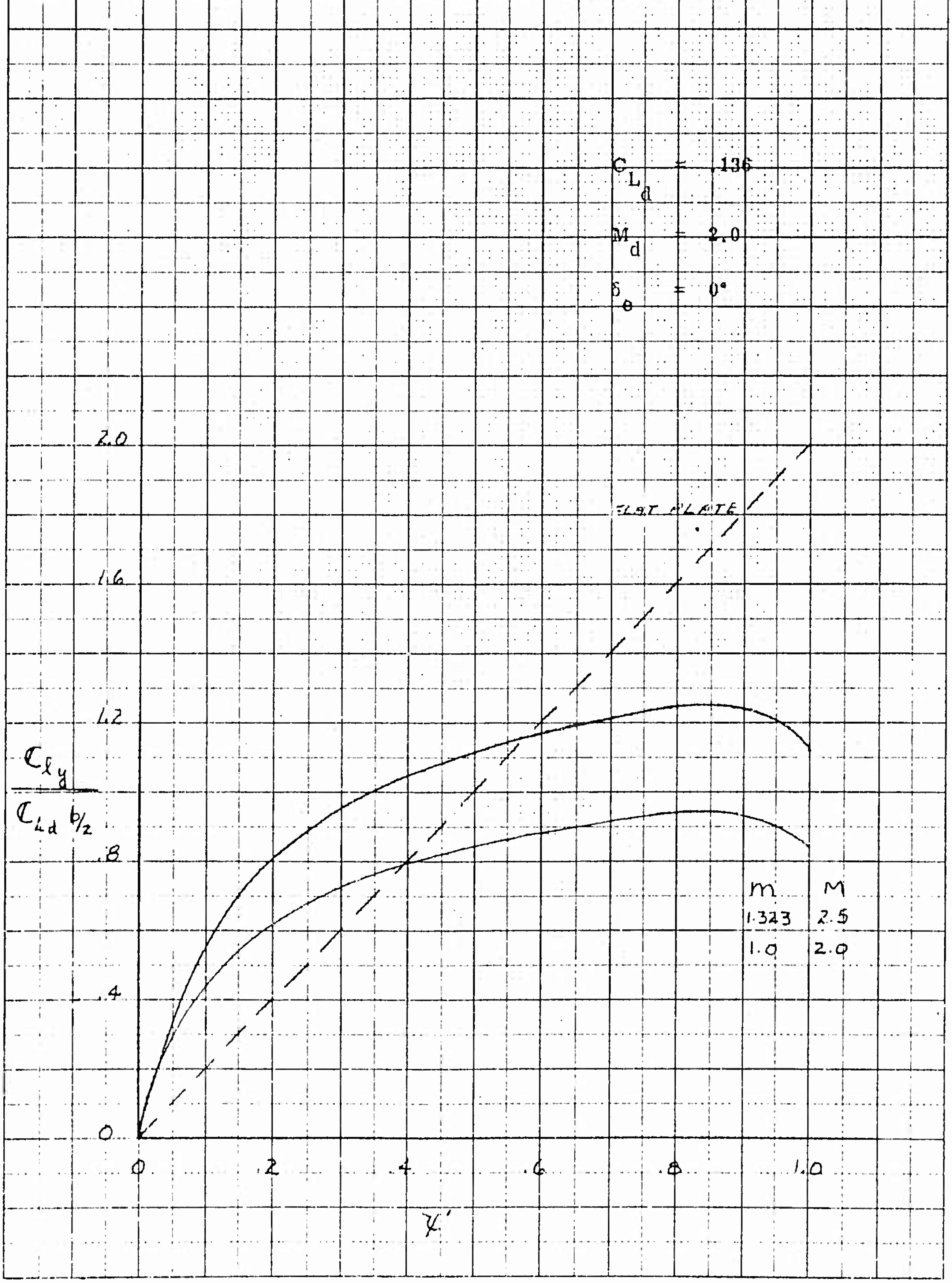

Figure 5.12(c). Effect of Mach Number on Chord Loading of Sonic Leading Edge Delta Wing "α".

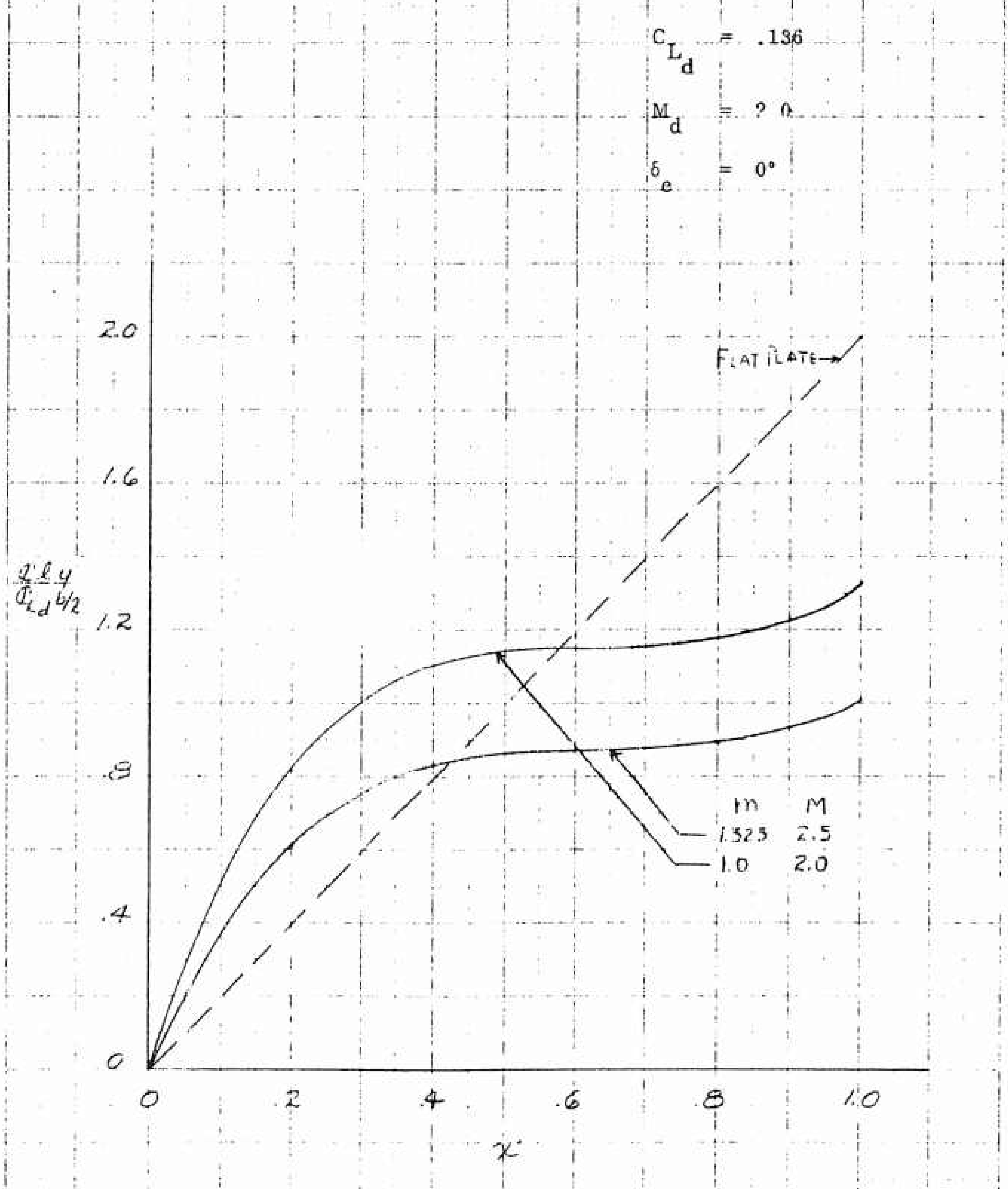

Figure 5.13(a). Comparison of Mean Chord Lines for Supersonic Leading Edge Designs for Various Design Restrictions.

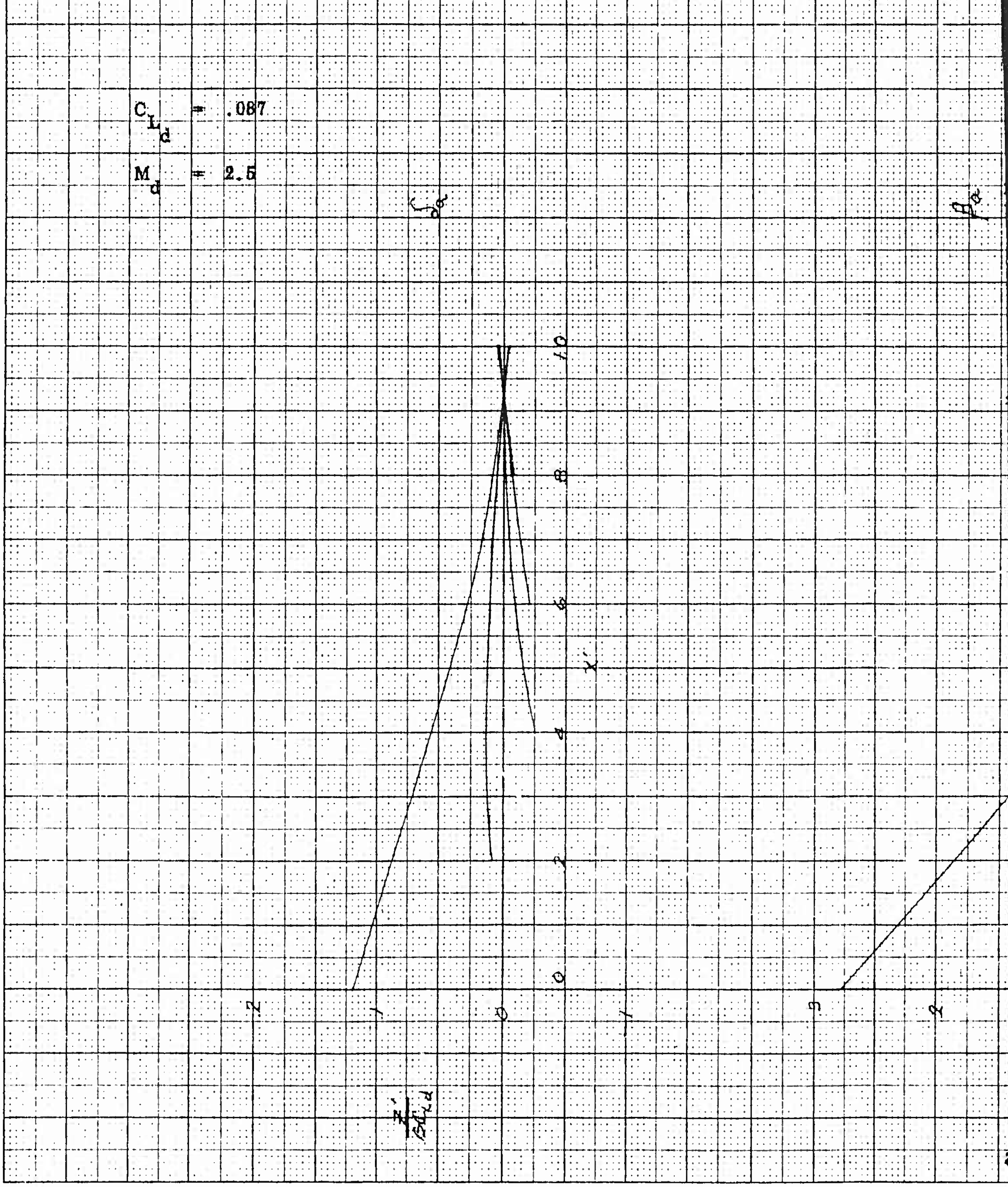

A

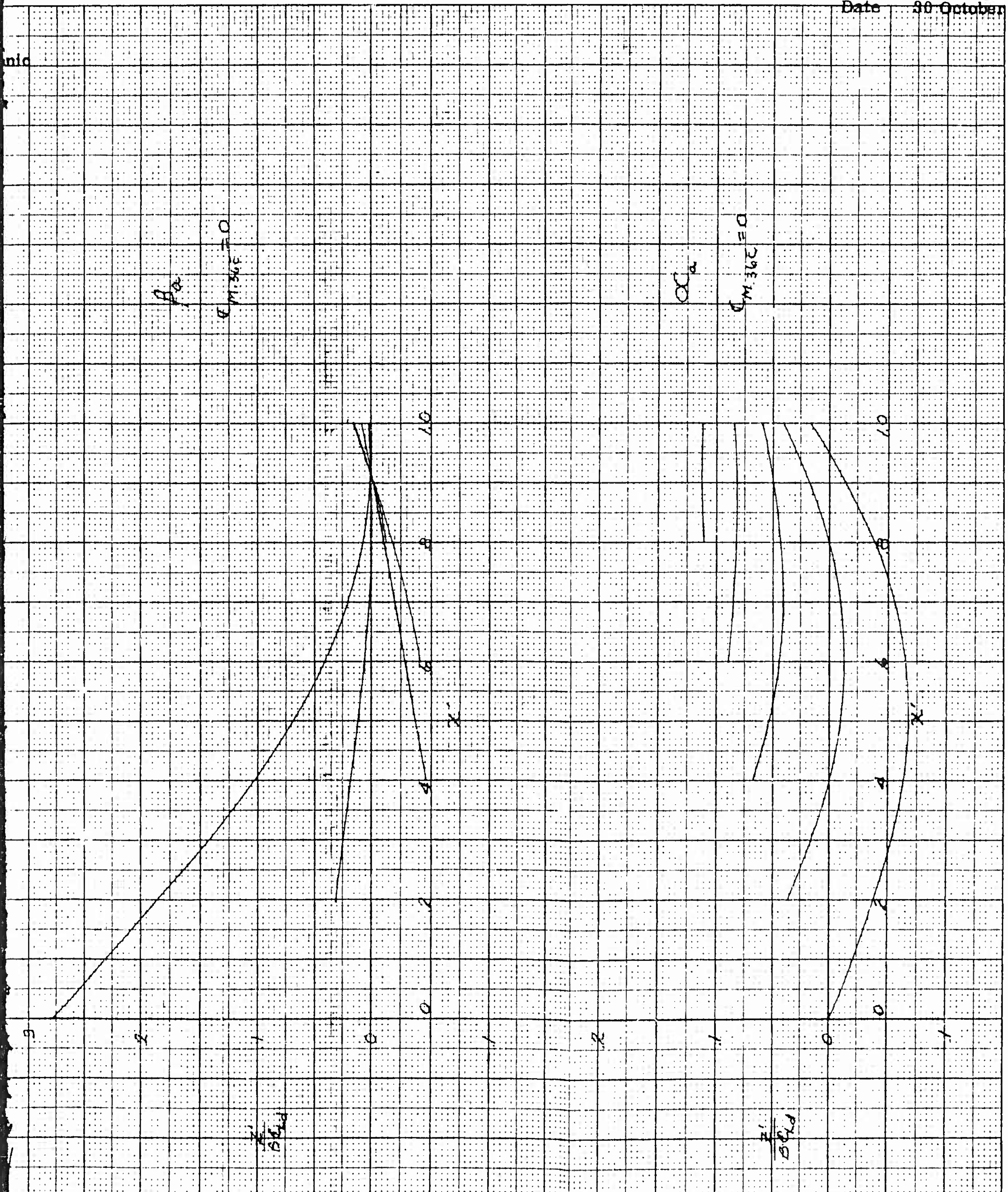

B

Figure 5.13(b). Comparison of Mean Chord Lines for Sonic Leading Edge Designs for Various Design Restrictions.

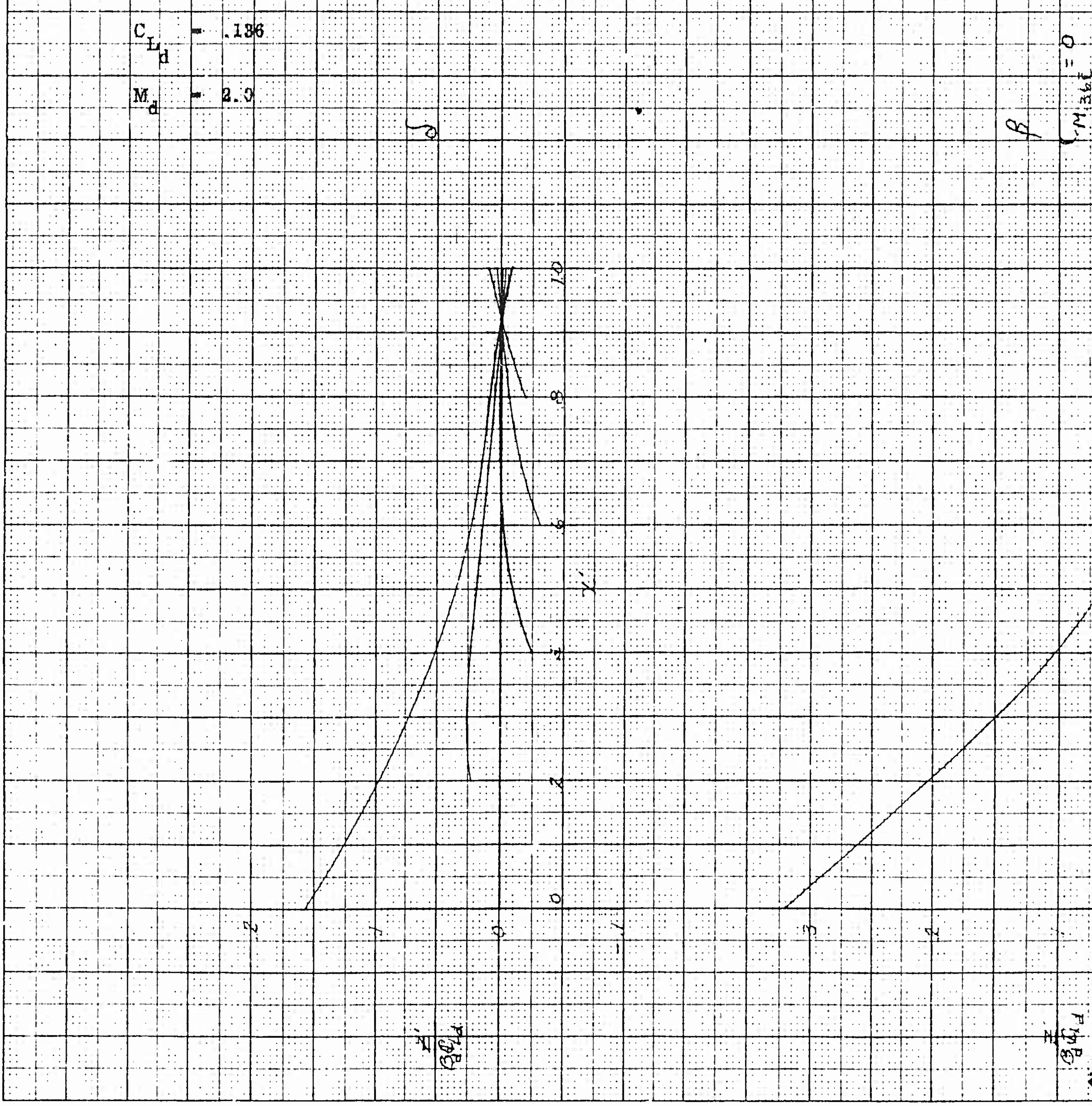

A

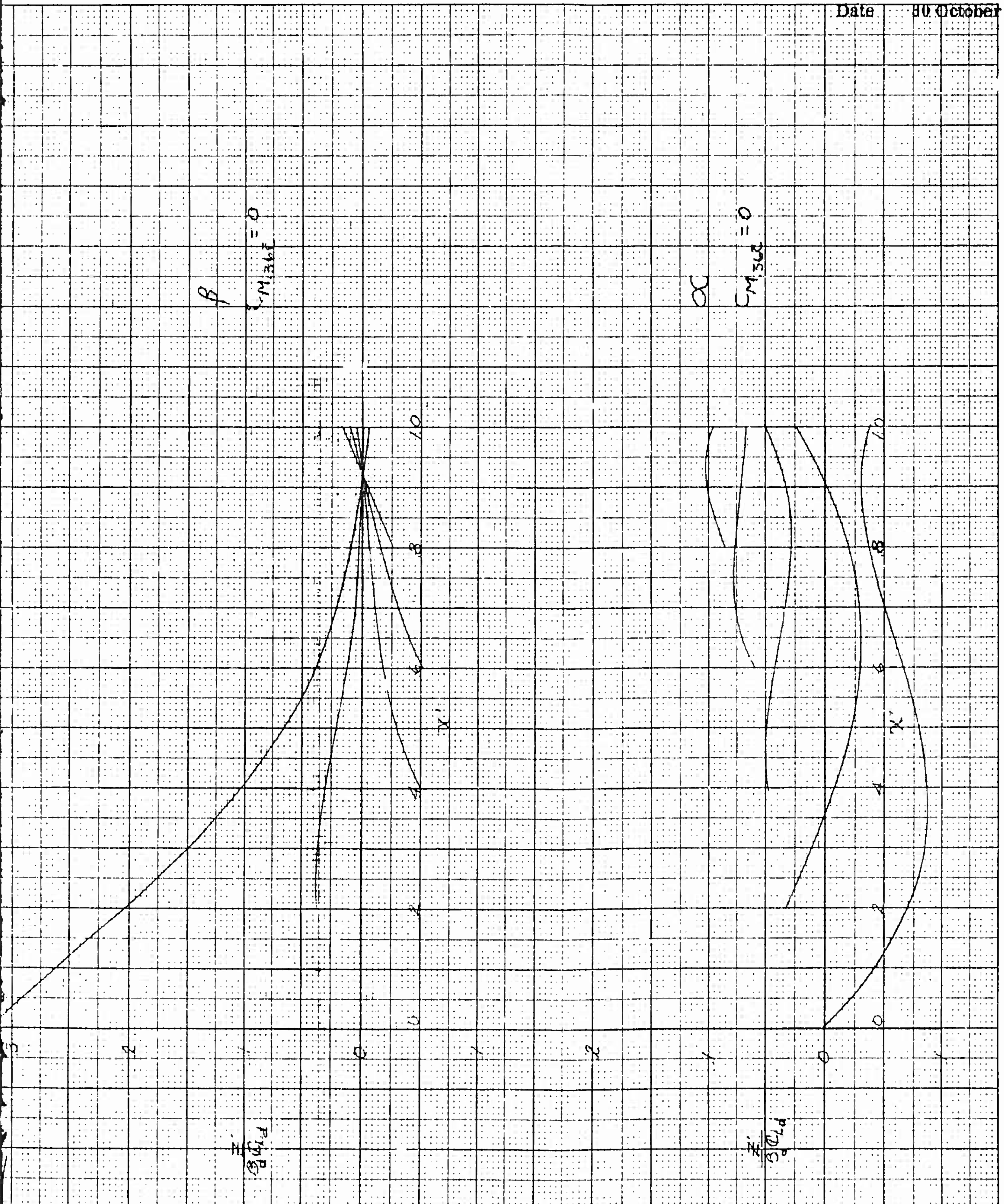
β
$C_{M_{3b\xi}} = 0$
α
$C_{M_{3c\xi}} = 0$
x'
10
8
6
4
2
0
x'
10
8
6
4
2
0
3
2
1
0
1
2
1
0
1
$\frac{z'}{\beta_d C_{L_d}}$
$\frac{z'}{\beta_d C_{L_d}}$

B

Figure 5.14. Relative Effect on Drag Reduction of Increasing Number of Terms of Power Series Expansion for Downwash.

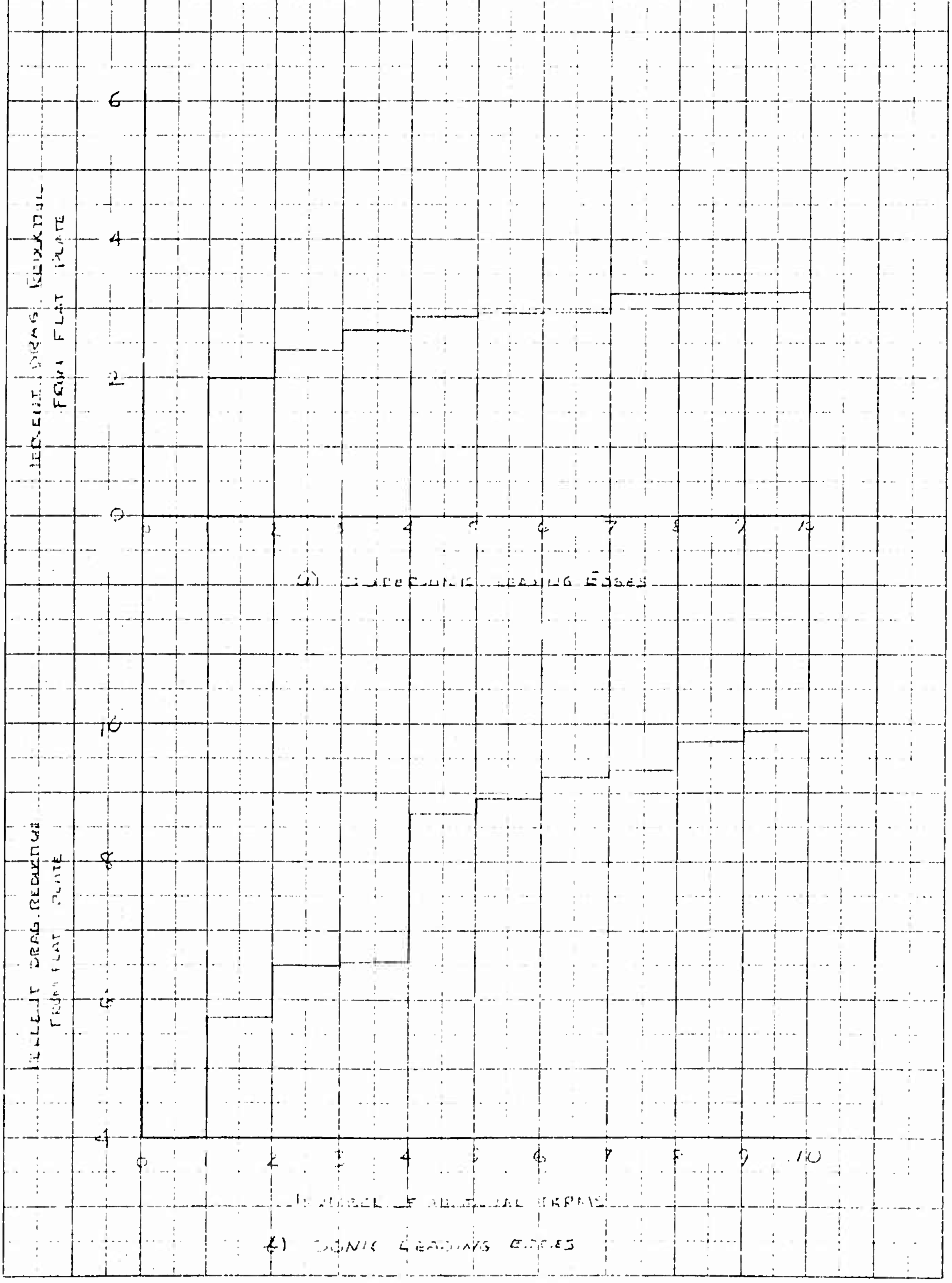

6.0 CONCLUSIONS

(1) Maximum drag reductions of the order of 10% are possible depending upon the leading edge condition for untrimmed warped delta wings at supersonic speeds. Delta wings, however, commonly use elevons as trimming devices although they are inefficient. For trimmed delta wings, however, very significant reduction in drag-due-to-lift is realized by proper warping for both sonic and supersonic leading edges. (No investigation was made for subsonic leading edge designs.) The drag reductions were 46% and 33% for the trimmed sonic leading wings with one (β wing) and two straight hinge lines (α wing) respectively, and 51% and 39% for the corresponding supersonic leading edge designs (β_a and α_a, respectively).

(2) The drag reduction procedures lead to marked forward shift in chord loading from the triangular flat plate loading for the trimmed wings (α, β). Very little change is observed for the untrimmed (δ)cases. However,

(3) the span loading does not retain the elliptic shape indicated by flat plates having sonic or subsonic leading edges. The trimmed wings appear to be affected more adversely than the untrimmed type wings. The trimmed wings with one straight hinge line (β-type) indicate greater inboard shift of load than the untrimmed wings (δ-type) for sonic and supersonic leading edge designs whereas a significant outward shift in load is observed for trimmed wing types having two straight hinge lines (α). (It is pointed out, however, that the current approximation agrees excellently with the loading for the absolute minimum drag wing computed by Fenain and Vallée[21].

(4) Without trim as an aerodynamic restraint the shapes resulting from the current procedure for sonic and supersonic leading edge designs results in the desirable bending of the leading edge into the free stream. The imposed condition

of trim counteracts this feature and requires large positive angles of attack in the immediate vicinity of the root chord.

(5) Preliminary results (not shown) indicate that the trimmed drag increases significantly below and above the design condition.

(6) The Dynamics Group has programmed a procedure to determine the shape required to deflect to the design shape under aeroelastic load. This IBM 704 program has been arranged to provide the input required for the design of sweptback wings having streamwise tips.

(7) The Theoretical Aerodynamics Group has had programmed the procedure to obtain the input required to design pointed tip wings with swept supersonic trailing edges.

7.0 REFERENCES

1- Kainer, J. H.: Equations for the Loading on Triangular Wings Having Supersonic Leading and Trailing Edges Due to Various Basic Twist Distributions. JAS. Vol. 20, No. 7, p. 469, July 1953.

2- Kainer, J. H.: Equations for the Loading, Section Pitching-Moment Coefficient, and Center-of-Pressure Distributions on Triangular Wings Having Supersonic Leading and Trailing Edges for Various Basic Camber Distributions. JAS, Vol. 23, No. 2, p. 127, February 1956.

3- Kainer, J. H., and Grijalva, Helen M.: Unified Analysis of Aerodynamic Loads at Supersonic Speeds on Triangular Wings Having Arbitrary Camber and Twist. Convair report ZA-251, Vol. I and II, 1956.

4- Lance, G. N.: The Delta Wing in a Non-Uniform Supersonic Stream. The Aeronautical Quarterly, Vol. V, May 1954.

5- Lance, G. N.: The Lift of Twisted and Cambered Wings in Supersonic Flow. The Aeronautical Quarterly, Vol. VI, May 1955.

6- Zienkiewicz, H. K.: A Note on Generalized Conical Fields with Application to Lift of Some Twisted and Cambered Delta Wings with Subsonic Leading Edges. English Electric Co., Rep L.A.T. 0.50, September 1953.

7- Zienkiewicz, H. K.: Load Distributions on Some Twisted and Cambered Delta Wings with Supersonic Leading and Trailing Edges. JAS, Vol. 21, No. 6, Readers Forum, June 1954.

8- Stancil, Robert T.: Comments on the Lagrangian Multiplier in Drag Minimization. JAS, Vol. 24, No. 5, p. 388, 1957, Readers Forum.

9- Germain, M. Paul: Sur le Minimum De Traînée d'une Aile Forme En Plan Donnée (On the Minimum Drag of Wings of Given Planform), Compte Rendus, February 25, 1957.

10- Roper, G. M.: Calculation of the Effect of Camber and Twist on the Pressure Distribution and Drag on Some Curved Plates at Supersonic Speeds. Royal Aircraft Establishment Report No. Aero. 2356, September 1950.

11- Baldwin, Barrett S., Jr.: Triangular Wings Cambered and Twisted to Support Specified Distributions of Lift at Supersonic Speeds. NACA TN 1816, February 1949.

12- Tucker, Warren A.: A Method for the Design of Sweptback Wings Warped to Produce Specified Flight Characteristics at Supersonic Speeds. NACA RM L51F08, September 1951.

13- Tsien, S. H.: The Supersonic Conical Wing of Minimum Drag. JAS, Vol. 22, No. 12, p. 805, December 1955.

14- Rodriguez, A. M.; Lagerstrom, P.A.; and Graham, E. W.: Theorems Concerning the Drag Reduction of Wings of Fixed Plan Form. JAS, Vol. 21, No. 1, p. 1, January 1954.

15- Graham, E. W.: A Drag Reduction Method for Wings of Fixed Plan Form. JAS, Vol. 19, No. 12, p. 823, December 1952.

16- Strand, Torstein: Minimum Drag Due to Lift for a Delta Wing with Sonic Leading Edges. Thesis, California Institute of Technology, 1954.

17- Grant, Frederick C.: The Proper Combination of Lift Loadings for Least Drag on a Supersonic Wing. NACA TN 3533, October 1955.

18- Jones, R. T.: The Minimum Drag of Thin Wings in Frictionless Flow, JAS, Vol.18, No. 2, p. 75, February 1951.

19- Jones, R. T.: Theoretical Determination of the Minimum Drag of Airfoils at Supersonic Speeds. JAS, Vol. 19, No. 12, p. 813, December 1952.

20- Cohen, Doris: The Warping of Triangular Wings for Minimum Drag at Supersonic Speeds. JAS, Vol. 24, No. 1, Readers Forum, p. 67, February 1957.

21- Fenain, M. Maurice, and Vallée, Denise: Effets De Portance, En Regime Supersonique, Pour Certaines Ailes En Fleche Effilées. Calcul De Traînée Minimum. (Effects of Lift in Supersonic Flow for Some Thin Warped Wings. Calculation of Minimum Drag.) Compte Rendus, February 25, 1957.

22- Boyd, John W.; Migotsky, Eugene; and Wetzel, Benton E.: A Study of Conical Camber for Triangular and Swept Back Wings, NACA RM A55 G19, 1955.

23- Falk, Theodore, J.: Leading Edge Shapes for Twisted and Cambered Delta Wings. Convair report No. ZA-268.

8.0 APPENDIX OF FUNCTIONS

8.1 Tabulated Functions $H_{i,j}(t)$

In general

$$H_{i,0}(t) = E_i(t) \tag{8.1}$$

$$H_{i,1}(t) = t\,E_i(t) \tag{8.2}$$

$$H_{i,2}(t) = G_i(t) \tag{8.3}$$

$$H_{i,3}(t) = t^2\,E_i(t) \tag{8.4}$$

$$H_{i,4}(t) = t\,G_i(t) \tag{8.5}$$

$$H_{i,5}(t) = g_i(t) \tag{8.6}$$

$$H_{i,6}(t) = t^3\,E_i(t) \tag{8.7}$$

$$H_{i,7}(t) = t^2\,G_i(t) \tag{8.8}$$

$$H_{i,8}(t) = t\,g_i(t) \tag{8.9}$$

$$H_{i,9}(t) = h_i(t) \tag{8.10}$$

$E_i(t)$, $G_i(t)$ for $0 \leq i \leq 9$ are given in Tables II, A, B, C, and III, A, B, C, of reference 3, respectively, for subsonic, sonic and supersonic leading edges. The functions $g_i(t)$ and $h_i(t)$ are given below:

ANALYSIS
PREPARED BY
CHECKED BY
REVISED BY

CONVAIR
A DIVISION OF GENERAL DYNAMICS CORPORATION
SAN DIEGO

PAGE 77
REPORT NO. ZA-259
MODEL
DATE 30 October 1957

A. Subsonic Leading Edges, $m < 1$

$$g_0(t) = \frac{\pi}{3m^2 E} (m^2 + 2t^2) \sqrt{m^2 - t^2} \tag{8.11}$$

$$g_1(t) = \frac{1}{4m^2 A_1} [m (2m a_1 + A_{35} t^2) + A_{33} t^4 \Theta_3] \tag{8.12}$$

$$g_2(t) = \frac{\pi a_5}{4m^3 A_1} [m (2m^2 + t^2) \sqrt{m^2 - t^2} + t^4 \Theta_3] \tag{8.13}$$

$$g_3(t) = \frac{\pi}{30m^2 A_2} [12m^4 a_2 + m^2 (a_2 - 5c_3) t^2$$

$$+ 2 (a_2 - 5c_3) t^4] \sqrt{m^2 - t^2} \tag{8.14}$$

$$g_4(t) = \frac{1}{180m^4 A_2} \Big\{ [108m^4 a_{11} + m^2 (9 a_{11} - 15m c_9 + 10m A_2) t^2$$

$$+ 2 (9 a_{11} + 10m A_2 - 15m c_9) t^4] \sqrt{m^2 - t^2}$$

$$+ 60m^4 A_2 t^2 \Theta_3 \Big\} \tag{8.15}$$

$$g_5(t) = \frac{\pi}{15m^4 A_2} (6m^4 a_7 + m^2 c_{30} t^2 - 2 c_{30} t^4) \sqrt{m^2 - t^2} \tag{8.16}$$

$$g_6(t) = \frac{1}{120m^5 A_3} \Big\{ m \left[40m^4 a_4 + 2m^2 (a_4 + 6me_1)\, t^2 \right.$$

$$\left. + (3a_4 + 2me_1 - 2m^3 c_5)\, t^4 \right] \sqrt{m^2 - t^2}$$

$$+ (3a_4 + 2me_1 - 2m^3 c_5)\, t^6\, \Theta_3 \Big\} \tag{8.17}$$

$$g_7(t) = \frac{\pi a_6}{180m^5 A_3} \Big\{ m \left[80m^4 a_{13} + 2m^2 (2a_{13} - 9m^2 e_3)\, t^2 \right.$$

$$\left. + (6a_{13} - 3m^2 e_3 - 4m^2 c_{11})\, t^4 \right] \sqrt{m^2 - t^2}$$

$$+ (6a_{13} - 3m^2 e_3 - 4m^2 c_{11})\, t^6\, \Theta_3 \Big\} \tag{8.18}$$

$$g_8(t) = \frac{1}{144m^4 A_3} \left[m (8m^3 a_{15} + m^2 f_3 t^2 + f_4 t^4) \sqrt{m^2 - t^2} \right.$$

$$\left. + (72m^4 A_3 + f_4 t^4)\, t^2\, \Theta_3 \right] \tag{8.19}$$

$$g_9(t) = \frac{\pi a_6}{60m^5 A_3} \Big\{ m \left[80m^4 a_9 + 2m^2 (2a_9 + 9e_2)\, t^2 \right.$$

$$\left. + 3 (2a_9 + e_2 + 4a_{49})\, t^4 \right] \sqrt{m^2 - t^2}$$

$$+ 3 (2a_9 + e_2 + 4a_{49})\, t^6\, \Theta_3 \Big\} \tag{8.20}$$

$$h_0(t) = \frac{\pi}{8m^3 E} \left[m\,(2m^2 + 3t^2)\sqrt{m^2 - t^2} + 3t^4\,\Theta_3 \right] \tag{8.21}$$

$$h_1(t) = \frac{1}{30m^4 A_1} \left[12m^4 a_1 + m^2 (a_1 + 5m\,A_{35})\, t^2 \right.$$

$$\left. + 2\,(a_1 + 5m\,A_{35})\, t^4 \right] \sqrt{m^2 - t^2} \tag{8.22}$$

$$h_2(t) = \frac{\pi\, a_6}{5m^4 A_1} \,(2m^4 + m^2 t^2 + 2\,t^4) \sqrt{m^2 - t^2} \tag{8.23}$$

$$h_3(t) = \frac{\pi}{120m^3 A_2} \left\{ m \left[40m^4 a_2 + 2m^2 (a_2 - 6A_{36})\, t^2 \right. \right.$$

$$\left. + 3\,(a_2 - 6\,A_{36})\, t^4 \right] \sqrt{m^2 - t^2}$$

$$\left. + 3\,(a_2 - 6\,A_{36})\, t^6\, \Theta_3 \right\} \tag{8.24}$$

$$h_4(t) = \frac{1}{32m^5 A_2} \left\{ m \left[16m^4 a_{11} + 2m^2 (a_{11} - m\,c_9 + mA_2)\, t^2 \right. \right.$$

$$\left. + 3\,(a_{11} - m\,c_9 + m\,A_2)\, t^4 \right] \sqrt{m^2 - t^2}$$

$$\left. + \left[8m^5 A_2 + 3\,(a_{11} - m\,c_9 + m\,A_2)\, t^4 \right] t^2\, \Theta_3 \right\} \tag{8.25}$$

$$h_5(t) = \frac{\pi}{120m^5 A_2} \Big\{ m \left[40m^4 a_7 + 2m^2 (a_7 - 3c_{30}) t^2 \right.$$

$$\left. + 3 (a_7 - 3c_{30}) t^4 \right] \sqrt{m^2 - t^2} + 3 (a_7 - 3c_{30}) t^6 \Theta_3 \Big\} \tag{8.26}$$

$$h_6(t) = \frac{1}{3150m^6 A_3} \left[900m^6 a_4 + 36m^4 (2a_4 + 7m e_1) t^2 \right.$$

$$+ m^2 (96a_4 + 56m e_1 - 35m^3 c_5) t^4$$

$$\left. + 2 (96a_4 + 56m e_1 - 35m^3 c_5) t^6 \right] \sqrt{m^2 - t^2} \tag{8.27}$$

$$h_7(t) = \frac{2 \pi a_6}{4725m^6 A_3} \left[900m^6 a_{13} + 9m^4 (8a_{13} - 21m^2 e_3) t^2 \right.$$

$$+ m^2 (96a_{13} - 42m^2 e_3 - 35m^2 c_{11}) t^4$$

$$\left. + 2 (96a_{13} - 42m^2 e_3 - 35m^2 c_{11}) t^6 \right] \sqrt{m^2 - t^2} \tag{8.28}$$

$$h_8(t) = \frac{1}{75{,}600m^6 A_3} \Big\{ \left[3600m^6 a_{15} + 60m^5 (2a_{15} - 7f_3) t^2 \right.$$

$$+ m^2 (160 a_{15} + 35m f_3 + 350m f_4 + 2016m A_3) t^4$$

$$+ 2\,(160\,a_{15} + 35m\,f_3 + 550m\,f_4 + 2016m\,A_3)\,t^6\,]\;\sqrt{m^2 - t^2}$$

$$+ 30,240m^6 A_3\,t^2\,\Theta_3 \Big\} \tag{8.29}$$

$$h_9(t) = \frac{2\pi a_6}{35m^6 A_3}\,(20m^6 a_9 + m^4 f_1\,t^2 + 3m^2\,f_2\,t^4$$

$$+ 6\,f_2\,t^6\,)\;\sqrt{m^2 - t^2} \tag{8.30}$$

B. Sonic Leading Edges, m = 1

$$g_0(t) = \frac{2}{3}\,(1 + 2t^2)\,\sqrt{1 - t^2} \tag{8.31}$$

$$g_1(t) = \frac{1}{12}\,[\,(2 + 7t^2)\,\sqrt{1 - t^2} + 7\,t^4\,\Theta_4\,] \tag{8.32}$$

$$g_2(t) = \frac{1}{3}\,[\,(2 + t^2)\,\sqrt{1 - t^2} + t^4\,\Theta_4\,] \tag{8.33}$$

$$g_3(t) = \frac{4}{225}\,(3 + 19\,t^2 + 38\,t^4)\,\sqrt{1 - t^2} \tag{8.34}$$

$$g_4(t) = \frac{1}{225}\,[\,(27 + 46\,t^2 + 92\,t^4)\,\sqrt{1 - t^2} + 75\,t^2\,\Theta_4\,] \tag{8.35}$$

$$g_5(t) = \frac{4}{75}\,(\,11 + 3\,t^2 + 6\,t^4)\,\sqrt{1 - t^2} \tag{8.36}$$

$$g_6(t) = \frac{1}{420}\,[\,(8 + 82\,t^2 + 147\,t^4)\,\sqrt{1 - t^2} + 147\,t^6\,\Theta_4\,] \tag{8.37}$$

$$g_7(t) = \frac{2}{945}\left[(16 + 206\, t^2 + 105\, t^4)\sqrt{1 - t^2} + 105\, t^6\, \Theta_4 \right] \tag{8.38}$$

$$g_8(t) = \frac{1}{1680}\left[(144 - 22\, t^2 + 237\, t^4)\sqrt{1 - t^2} \right.$$

$$\left. + 7\,(120 + 41\, t^4)\, t^2\, \Theta_4 \right] \tag{8.39}$$

$$g_9(t) = \frac{2}{315}\left[(80 + 22\, t^2 + 21\, t^4)\sqrt{1 - t^2} + 21\, t^6\, \Theta_4 \right] \tag{8.40}$$

$$h_0(t) = \frac{1}{4}\left[(2 + 3\, t^2)\sqrt{1 - t^2} + 3\, t^4\, \Theta_4 \right] \tag{8.41}$$

$$h_1(t) = \frac{2}{15}\,(1 + 3\, t^2 + 6\, t^4)\sqrt{1 - t^2} \tag{8.42}$$

$$h_2(t) = \frac{4}{15}\,(2 + t^2 + 2\, t^4)\sqrt{1 - t^2} \tag{8.43}$$

$$h_3(t) = \frac{1}{180}\left[(8 + 46\, t^2 + 69\, t^4)\sqrt{1 - t^2} + 69\, t^6\, \Theta_4 \right] \tag{8.44}$$

$$h_4(t) = \frac{1}{480}\left[(48 + 86\, t^2 + 129\, t^4)\sqrt{1 - t^2} \right.$$

$$\left. + \text{[illegible]}\,(40 + 43\, t^4)\, t^2\, \Theta_4 \right] \tag{8.45}$$

$$h_5(t) = \frac{1}{180}\left[(88 + 26\, t^2 + 39\, t^4)\sqrt{1 - t^2} + 39\, t^6\, \Theta_4 \right] \tag{8.46}$$

$$h_6(t) = \frac{4}{3675}\,(15 + 144\, t^2 + 227\, t^4 + 454\, t^6)\sqrt{1 - t^2} \tag{8.47}$$

$$h_7(t) = \frac{16}{11025} \left(20 + 241\, t^2 + 123\, t^4 + 246\, t^6\right) \sqrt{1 - t^2} \tag{8.48}$$

$$h_8(t) = \frac{2}{11025} \Big[\left(405 + 66\, t^2 + 788\, t^4 + 1576\, t^6\right) \sqrt{1 - t^2}$$

$$+ 2205\, t^2\, \Theta_4 \Big] \tag{8.49}$$

$$h_9(t) = \frac{16}{3675} \left(100 + 29\, t^2 + 27\, t^4 + 54\, t^6\right) \sqrt{1 - t^2} \tag{8.50}$$

C. Supersonic Leading Edges, $m > 1$

$$g_0(t) = \frac{1}{3m^2 \sqrt{m^2 - 1}} \Big[(m^3 - t^3)\, \Theta_1 + (m^3 + t^3)\, \Theta_2$$

$$+ 2m \sqrt{m^2 - 1}\; t^2 \sqrt{1 - t^2} \Big] \tag{8.51}$$

$$g_1(t) = \frac{1}{12 m^2 (m^2 - 1)^{3/2}} \Big[m^2 \sqrt{m^2 - 1}\, (6m^2 + k_{16} t^2) \sqrt{1 - t^2}$$

$$+ (m^2 - 1)^{3/2}\, k_{18}\, t^4\, \Theta_4 - (3m^4 - 4m^5\, t + k_{17}\, t^4)\, \Theta_1$$

$$- (3m^4 + 4m^5\, t + k_{17}\, t^4)\, \Theta_2 \Big] \tag{8.52}$$

$$g_2(t) = \frac{1}{12m^3 (m^2-1)^{5/2}} \Big[2m^2 \sqrt{m^2-1}\, (3m^2 - t^2) \sqrt{1-t^2}$$

$$+ (5m^4 a_{29} + 4m^3 t - c_{14} t^4)\, \Theta_1 + (3m^4 a_{29} - 4m^3 t - c_{14} t^4)\, \Theta_2$$

$$+ 4 (m^2-1)^{3/2}\, t^4\, \Theta_4 \Big] \tag{8.53}$$

$$g_3(t) = \frac{1}{60m^2 (m^2-1)^{5/2}} \Big[(6m^5 a_{18} - 45m^6 t + 10m^5 a_{19} t^2 - k_{21} t^5)\, \Theta_1$$

$$+ (6m^5 a_{18} + 45m^6 t + 10m^5 a_{19} t^2 + k_{21} t^5)\, \Theta_2$$

$$- 2m \sqrt{m^2-1}\, (15m^4 + m^2 k_{19} t^2 - k_{20} t^4) \sqrt{1-t^2} \Big] \tag{8.54}$$

$$g_4(t) = \frac{1}{180m^3 (m^2-1)^{5/2}} \Big[3(18m^5 + 15m^6 a_{35} t + 10m^3 a_{36} t^2$$

$$- k_{43} t^5)\, \Theta_1 + 3(18m^5 - 15m^6 a_{35} t + 10m^3 a_{36} t^2 + k_{43} t^5)\, \Theta_2$$

$$+ 2m \sqrt{m^2-1}\, (18m^4 a_{35} - m^2 k_{44} t^2 - k_{45} t^4) \sqrt{1-t^2}$$

$$+ 60m^3 (m^2-1)^{5/2}\, t^2\, \Theta_4 \Big] \tag{8.55}$$

$$g_5(t) = \frac{1}{60m^4 (m^2-1)^{5/2}} \Big[3(2m^5 a_{30} - 5m^4 a_{18} t + 10m^5 t^2 - c_{16} t^5)\, \Theta_1$$

$$+ \; 3\,(2m^5 a_{30} + 5m^4 a_{15}\, t + 10m^3\, t^2 + c_{16}\, t^5)\,\Theta_2$$

$$+ \; 2m\,\sqrt{m^2-1}\;\;(6m^4 a_{31} - m^2 a_{21}\, t^2 - c_{44}\, t^4)\,\sqrt{1-t^2}\;] \qquad (8.56)$$

$$g_6(t) \;=\; \frac{1}{360m^2\,(m^2-1)^{7/2}}\;\;[\;2m^2\sqrt{m^2-1}\;\;(10m^4 a_{22} + m^2 k_{22}\, t^2$$

$$+ \; 3k_{23}\, t^4)\,\sqrt{1-t^2} \;+\; 6(m^2-1)^{7/2}\, k_{25}\, t^6\, \Theta_4$$

$$-\; 3\,(10m^6 a_{24} - 36m^7 a_{25}\, t + 45m^6 a_{26}\, t^2 - 20m^7 a_{27}\, t^3 + k_{24}\, t^6)\,\Theta_1$$

$$-\; 3\,(10m^6 a_{24} + 36m^7 a_{25}\, t + 45m^6 a_{26}\, t^2 + 20m^7 a_{27}\, t^3$$

$$+\; k_{24}\, t^6)\,\Theta_2\;] \qquad (8.57)$$

$$g_7(t) \;=\; \frac{1}{360m^3\,(m^2-1)^{7/2}}\;\;[\;5\,(2m^6 a_{37} + 108m^7\, t + 9m^6 a_{38}\, t^2$$

$$+\; 4m^7 a_{39}\, t^3 - k_{27}\, t^6)\,\Theta_1 \;+\; 5\,(2m^6 a_{37} - 108m^7\, t$$

$$+\; 9m^6 a_{38}\, t^2 - 4m^7 a_{39}\, t^3 - k_{27}\, t^6)\,\Theta_2 + 10\,(m^2-1)^{7/2}\, t^6\, \Theta_4$$

$$+\; 10m^2\sqrt{m^2-1}\;\;(2m^4 a_{40} + m^2 k_{28}\, t^2 - k_{29}\, t^4)\,\sqrt{1-t^2}\;] \qquad (8.58)$$

$$g_8(t) = \frac{1}{720m^4 (m^2-1)^{7/2}} \left[3 (m^2-1)^{7/2} (120m^4 + f_{12} t^4) t^2 \Theta_4 \right.$$

$$+ m^2 \sqrt{m^2-1} \; (40m^4 a_{42} + 2m^2 f_{10} t^2 + 3 f_{11} t^4) \sqrt{1-t^2}$$

$$- 6 (10m^6 a_{25} - 12m^7 a_{44} t + 15m^4 a_{45} t^2 - 100m^7 t^3 + f_9 t^6) \Theta_1$$

$$- 6 (10m^6 a_{25} + 12m^7 a_{44} t + 15m^4 a_{45} t^2$$

$$\left. + 100m^7 t^3 + f_9 t^6) \Theta_2 \right] \qquad (8.59)$$

$$g_9(t) = \frac{1}{360m^5 (m^2-1)^{7/2}} \left[3 (10m^6 a_{32} + 36m^5 a_{24} t - 45m^6 a_{25} t^2 \right.$$

$$+ 20m^5 a_{26} t^3 - k_{40} t^6) \Theta_1 + 3 (10m^6 a_{32} - 36m^5 a_{24} t$$

$$- 45m^6 a_{25} t^2 - 20m^5 a_{26} t^3 - k_{40} t^6) \Theta_2$$

$$+ 48 (m^2-1)^{7/2} t^6 \Theta_4 + 2m^2 \sqrt{m^2-1} \; (10m^4 a_{32}$$

$$\left. + m^2 k_{41} t^2 - 3k_{42} t^4) \sqrt{1-t^2} \right] \qquad (8.60)$$

$$h_0(t) = \frac{1}{4m^3 \sqrt{m^2-1}} \left[(m^4 - t^4) (\Theta_1 + \Theta_2) \right.$$

$$\left. + m^2 \sqrt{m^2-1} \; t^2 \sqrt{1-t^2} + [illegible] \sqrt{m^2-1} \; t^4 \Theta_4 \right] \qquad (8.61)$$

$$h_1(t) = \frac{1}{60m^3 (m^2-1)^{3/2}} \Big[2m \sqrt{m^2-1} \; (12m^4 + m^2 a_{35} t^2$$

$$+ k_{31} t^4) \sqrt{1-t^2} - 3 (4m^5 - 5m^6 t + k_{30} t^5) \Theta_1$$

$$- 3 (4m^5 + 5m^6 t - k_{30} t^5) \Theta_2 \Big] \qquad (8.62)$$

$$h_2(t) = \frac{1}{20m^4 (m^2-1)^{3/2}} \Big[(4m^5 a_{29} + 5m^4 t - k_{46} t^5) \Theta_1$$

$$+ (4m^5 a_{29} - 5m^4 t + k_{46} t^5) \Theta_2$$

$$+ 2m \sqrt{m^2-1} \; (4m^4 - m^2 t^2 + a_{67} t^4) \sqrt{1-t^2} \Big] \qquad (8.63)$$

$$h_3(t) = \frac{1}{120m^3 (m^2-1)^{5/2}} \Big[(10m^6 a_{18} - 72m^7 t + 15m^6 a_{19} t^2$$

$$- k_{32} t^6) \Theta_1 + (10m^6 a_{18} + 72m^7 t + 15m^6 a_{19} t^2 - k_{32} t^6) \Theta_2$$

$$- 2m^2 \sqrt{m^2-1} \; (20m^4 + m^2 k_{33} t^2 - k_{34} t^4) \sqrt{1-t^2}$$

$$+ 2 (m^2-1)^{5/2} k_{35} t^6 \Theta_4 \Big] \qquad (8.64)$$

FORM 1512 A

$$h_4(t) = - \frac{1}{480 m^4 (m^2-1)^{5/2}} \Big[12 (10m^6 + 8m^7 a_{35} t + 5m^4 a_{36} t^2$$

$$- k_{50} t^6) \Theta_1 + 12 (10m^6 - 8m^7 a_{35} t + 5m^4 a_{36} t^2 - k_{50} t^6) \Theta_2$$

$$+ m^2 \sqrt{m^2-1} \; (30m^4 a_{35} - 2m^2 k_{51} t^2 - 3k_{52} t^4) \sqrt{1 - t^2}$$

$$+ 3 (m^2-1)^{5/2} \; (40m^4 - k_{53} t^4) t^2 \Theta_4 \Big] \qquad (8.65)$$

$$h_5(t) = \frac{1}{120 m^5 (m^2-1)^{5/2}} \Big[(10m^6 a_{30} - 24m^5 a_{18} t + 45m^6 t^2$$

$$- k_{47} t^6) \Theta_1 + (10m^6 a_{30} + 24m^5 a_{18} t + 45m^6 t^2 - k_{47} t^6) \Theta_2$$

$$+ 2m^2 \sqrt{m^2-1} \; (10m^4 a_{31} - 3m^2 a_{17} t^2 + k_{48} t^4) \sqrt{1 - t^2}$$

$$+ 2 (m^2-1)^{5/2} k_{49} t^6 \Theta_4 \Big] \qquad (8.66)$$

$$h_6(t) = \frac{1}{840 m^3 (m^2-1)^{7/2}} \Big[2m \sqrt{m^2-1} \; (20m^6 a_{22} + 2m^4 k_{37} t^2$$

$$+ m^2 k_{38} t^4 + k_{39} t^6) \sqrt{1 - t^2} - 3 \; (20m^7 a_{24} - 70m^8 a_{25} t$$

$$+ 84m^7 a_{26} t^2 - 35m^8 a_{27} t^3 + k_{36} t^7) \Theta_1$$

$$- 3 (20m^7 a_{24} + 70m^8 a_{25} t + 84m^7 a_{26} t^2 + 35m^8 a_{27} t^3$$

$$- k_{36} t^7) \Theta_2] \qquad (8.67)$$

$$h_7(t) = \frac{1}{840m^4 (m^2-1)^{7/2}} [(20m^7 a_{37} + 1050m^8 t + 84m^7 a_{38} t^2$$

$$+ 35m^4 a_{39} t^3 - 3k_{58} t^7) \Theta_1 + (20m^7 a_{37} - 1050m^8 t$$

$$+ 84m^7 a_{38} t^2 - 35m^4 a_{39} t^3 + 3k_{58} t^7) \Theta_2$$

$$+ 2m \sqrt{m^2-1} \ (20m^6 a_{40} + 2m^4 k_{59} t^2$$

$$- m^2 k_{60} t^4 + k_{61} t^6) \sqrt{1-t^2}] \qquad (8.68)$$

$$h_8(t) = \frac{1}{37800m^5 (m^2-1)^{7/2}} [- 45 (60m^7 a_{25} - 70m^8 a_{44} t$$

$$+ 84m^5 a_{45} t^2 - 525m^8 t^3 + k_{54} t^7) \Theta_1$$

$$- 45 (60m^7 a_{25} + 70m^8 a_{44} t + 84m^5 a_{45} t^2$$

$$+ 525m^8 t^3 - k_{54} t^7) \Theta_2 + 2m \sqrt{m^2-1} \ (900m^6 a_{42} - 18m^4 k_{55} t^2$$

$$+ 5m^2 k_{56} t^4 + k_{57} t^6) \sqrt{1-t^2} + 15120m^5 (m^2-1)^{7/2} t^2 \Theta_4] \qquad (8.69)$$

$$h_9(t) = \frac{1}{840m^6 (m^2-1)^{7/2}} \Big[3\,(20m^7 a_{32} + 70m^6 a_{24}\, t$$

$$- 84m^7 a_{25}\, t^2 + 35m^6 a_{26}\, t^3 - f_5\, t^7)\, \Theta_1$$

$$+ 3\,(20m^7 a_{32} - 70m^6 a_{24}\, t - 84m^7 a_{25}\, t^2 - 35m^6 a_{26}\, t^3$$

$$+ f_5\, t^7)\, \Theta_2 + 2m \sqrt{m^2-1}\ (20m^6 a_{33} + 2m^4 f_6\, t^2$$

$$+ m^2 f_7\, t^4 + f_8\, t^6)\ \sqrt{1-t^2}\ \Big] \qquad (8.70)$$

8.2 Tabulated Abbreviations

See Table I, Reference 3, for A_i, b_i, c_i, e_i, f_i not listed here.

$$A_{35} = [\ m^2 K + E\,(3 - 4m^2)\ ]$$

$$A_{36} = [\ m^2 K\,(7 - 5m^2) + 2E\,(2 - 8m^2 + 5m^4)\ ]$$

$$A_{37} = [\ m^2 K - E\,(4 - 3m^2)\ ]$$

$$A_{38} = [\ 5m^4 K^2 - 2m^2 KE\,(13 - 7m^2) + E^2\,(32 - \text{[illegible]}m^2 + 12m^4)\ ]$$

$$A_{39} = [\ 2m^2 K\,(3 - 4m^2) - E\,(12 - 19m^2 + 5m^4)\ ]$$

$$A_{40} = \left[m^4 K^2 (16 - 57m^2 + 37m^4) - 2m^2 KE (8 - 25m^2 - 19m^4 + 32m^6) \right.$$

$$\left. - E^2 (32 - 140m^2 + 265m^4 - 173m^6 + 20m^8) \right]$$

$$A_{41} = \left[m^4 K^2 (336 - 1663m^2 + 2046m^4 - 655m^6) + 2m^2 KE (168 - 145m^2 \right.$$

$$+ 650m^4 - 1417m^6 + 630m^8) - E^2 (2016 - 7652m^2 + 12383m^4 - 9742m^6$$

$$\left. + 2831m^8 + 100m^{10}) \right]$$

$$A_{42} = \left[m^2 K (6 - 9m^2 - 5m^4) - E (12 - 27m^2 + 17m^4 - 10m^6) \right]$$

$$A_{43} = \left[m^2 K - E (5 - 4m^2) \right]$$

$$A_{44} = \left[2m^2 K (1 - 2m^2) + E (5 - 11m^2 + 8m^4) \right]$$

$$A_{45} = \left[m^4 K^2 (7 - 24m^2) + 8m^2 KE (7 - 8m^2 + 6m^4) - E^2 (140 - 245m^2 \right.$$

$$\left. + 128m^4) \right]$$

$$A_{46} = \left[m^2 K (7 - 9m^2) - 2E (7 - 11m^2 + 3m^4) \right]$$

$$A_{47} = - \left[m^2 K (15 - 39m^2 + 16m^4) + E (15 - 57m^2 + 82m^4 - 32m^6) \right]$$

$$A_{48} = \left[m^4 K^2 (420 - 1657m^2 + 1673m^4 - 600m^6) + 2m^4 KE (68 + 555m^2 \right.$$

$$- 1315m^4 + 624m^6) - E^2 (168 - 6776m^2 + 11245m^4 - 3309m^6 + 2528m^8$$

$$\left. + 96m^{10}) \right]$$

$$A_{49} = [\ m^2 K (\text{[illegible]} - 9m^2 - 6m^4) - E (14 - 51m^2 + 21m^4 - 12m^6)\ ]$$

$$A_{50} = [\ m^4 K^2 - 2m^4 KE - E^2 (4 - 5m^2)\ ]$$

$$A_{51} = [\ m^4 K^2 (21 - 19m^2) - 8m^2 KE (3 + m^2 + 5m^4) - E^2 (36 - 107m^2 + 77m^4 + 4m^6)\ ]$$

$$k_1 = 4m^2 - 5$$

$$k_2 = 12m^4 - 7m^2 - 2$$

$$k_3 = 20m^4 - 47m^2 + 30$$

$$k_4 = 60m^6 - 101m^4 + 28m^2 + 4$$

$$k_5 = 5m^2 - 6$$

$$k_6 = 15m^4 - 8m^2 - 4$$

$$k_7 = 10m^4 - 23m^2 + 14$$

$$k_8 = 30m^6 - 49m^4 + 12m^2 + 4$$

$$k_9 = 70m^6 - 2\text{[illegible]}5m^4 + 272m^2 - 112$$

$$k_{10} = 210m^8 - 565m^6 + \text{[illegible]}m^4 - 72m^2 - 16$$

$$k_{11} = 24m^4 - 56m^2 + 35$$

$$k_{12} = 24m^6 - 40m^4 + 11m^2 + 2$$

$$k_{13} = 28m^6 - 95m^4 + 112m^2 - 48$$

$$k_{14} = 420m^8 - 1145m^6 + 954m^4 - 168m^2 - 16$$

$$k_{15} = 3m^2 - 4$$

$$k_{16} = m^2 - 3$$

$$k_{17} = 4m^2 - 3$$

$$k_{18} = m^2 + 6$$

$$k_{19} = 7m^2 - 4$$

$$k_{20} = 6m^4 - 21m^2 + 12$$

$$k_{21} = 20m^4 - 29m^2 + 12$$

$k_{22} = 132m^4 +$ 11[illegible]$m^2 - 15$

$$k_{23} = m^6 - 25m^4 + 27m^2 - 10$$

$$k_{24} = 40m^6 - 84m^4 + 69m^2 - 20$$

$$k_{25} = m^2 + 20$$

$$k_{26} = 0$$

$$k_{27} = 15m^6 - 35m^4 + 28m^2 - \text{[illegible]}$$

$$k_{28} = 18m^4 + 49m^2 - 10$$

$$k_{29} = 16m^4 - 11m^2 + 4$$

$$k_{30} = 5m^2 - 4$$

$$k_{31} = 2m^4 + 7m^2 - 12$$

$$k_{32} = 30m^4 - 47m^2 + 20$$

$$k_{33} = 8m^2 - 5$$

$$k_{34} = 3m^4 - 16m^2 + 10$$

$$k_{35} = 3m^2 + 20$$

$$k_{36} = 70m^6 - 161m^4 + 136m^2 - 40$$

$$k_{37} = 167m^4 + 100m^2 - 12$$

$$k_{38} = 2m^6 - 51m^4 + 104m^2 - 4\text{[illegible]}$$

$$k_{39} = 4m^8 + 45m^6 - 275m^4 + 528m^2 - 120$$

$$k_{40} = 20m^6 - 35m^4 + 28m^2 - 8$$

$$k_{41} = 20m^4 + 271m^2 - 6$$

$$k_{42} = 12m^4 - 11m^2 + 4$$

$$k_{43} = 15m^4 - 20m^2 + 8$$

$$k_{44} = m^4 + 16m^2 - 8$$

$$k_{45} = (2m^6 - 13m^4 + 44m^2 - 24)$$

$$k_{46} = 4m^2 - 3$$

$$k_{47} = 20m^4 - 29m^2 + 12$$

$$k_{48} = m^4 - 10m^2 + 6$$

$$k_{49} = m^2 + 12$$

$$k_{50} = 3m^4 - 12m^2 + 5$$

$$k_{51} = m^4 + 26m^2 - 15$$

$$k_{52} = m^6 - 6m^4 + 55m^2 - 20$$

$$k_{53} = m^4 - 4m^2 - 40$$

$$k_{54} = 140m^6 - 301m^4 + 245m^2 - 72$$

$$k_{55} = 174m^6 - 697m^4 - 758m^2 + 36$$

$$k_{56} = 8m^8 - 24m^6 - 801m^4 + 952m^2 - 360$$

$$k_{57} = 48m^{10} - 144m^8 + 1494m^6 - 7833m^4 + 9000m^2 - 3240$$

$$k_{58} = 56m^6 - 124m^4 + 103m^2 - 30$$

$$k_{59} = 84m^4 + 215m^2 - 44$$

$$k_{60} = 64m^4 - 79m^2 + 30$$

$$k_{61} = 40m^6 - 214m^4 + 249m^2 - 90$$

$$k_{62} = 165m^6 - 568m^4 + 665m^2 - 280$$

$$k_{63} = 168m^8 - 456m^6 + 377m^4 - 66m^2 - 8$$

8.3 Tabulated $C^*_{D_{i,j}}$ Functions

A. Subsonic Leading Edges

i \ j	0	1	2	3	4	5	6	7	8	9
0	$\frac{2\pi m}{E}$	$\frac{8m}{3E}$	$\frac{2}{3} C^*_{D_{0,0}}$	$\frac{m\pi}{2E}$	$\frac{3}{4} C^*_{D_{0,1}}$	$\frac{1}{2} C^*_{D_{0,0}}$	$\frac{16m}{15E}$	$\frac{4}{5} C^*_{D_{0,3}}$	$\frac{3}{5} C^*_{D_{0,1}}$	$\frac{4}{5} C^*_{D_{0,5}}$
1	$\frac{-4m\,A_1}{3A_1}$	$\frac{-4m\,A_{15}}{3\pi\,A_1}$	$\frac{3}{4} C^*_{D_{1,0}}$	$\frac{-m\,A_{37}}{5A_1}$	$\frac{4}{5} C^*_{D_{1,1}}$	$\frac{3}{5} C^*_{D_{1,0}}$	$\frac{-16m\,A_{43}}{45\pi\,A_1}$	$\frac{5}{6} C^*_{D_{1,3}}$	$\frac{2}{3} C^*_{D_{1,1}}$	$\frac{5}{6} C^*_{D_{1,5}}$
2	$\frac{2\pi m\,a_6}{A_1}$	$\frac{8m\,a_6}{3A_1}$	$\frac{3}{4} C^*_{D_{2,0}}$	$\frac{m\pi\,a_6}{2A_1}$	$\frac{4}{5} C^*_{D_{2,1}}$	$\frac{3}{5} C^*_{D_{2,0}}$	$\frac{16m\,a_6}{15A_1}$	$\frac{5}{6} C^*_{D_{2,3}}$	$\frac{2}{3} C^*_{D_{2,1}}$	$\frac{5}{6} C^*_{D_{2,5}}$
3	$\frac{m\pi\,A_5}{A_2}$	$\frac{16m\,A_{25}}{15A_2}$	$\frac{4}{5} C^*_{D_{3,0}}$	$\frac{-m\pi\,A_{16}}{3A_2}$	$\frac{5}{6} C^*_{D_{3,1}}$	$\frac{2}{3} C^*_{D_{3,0}}$	$\frac{-32m\,A_{44}}{105A_2}$	$\frac{6}{7} C^*_{D_{3,3}}$	$\frac{5}{7} C^*_{D_{3,1}}$	$\frac{6}{7} C^*_{D_{3,5}}$
4	$\frac{\pi m\,A_3}{3A_2}$	$\frac{4m\,A_{29}}{15\pi\,A_2}$	$\frac{4}{5} C^*_{D_{4,0}}$	$\frac{-m\,A_{38}}{10A_2}$	$\frac{5}{6} C^*_{D_{4,1}}$	$\frac{2}{3} C^*_{D_{4,0}}$	$\frac{16m\,A_{45}}{315\pi\,A_2}$	$\frac{6}{7} C^*_{D_{4,3}}$	$\frac{5}{7} C^*_{D_{4,1}}$	$\frac{6}{7} C^*_{D_{4,5}}$
5	$\frac{\pi m\,A_7}{A_2}$	$\frac{16m\,A_{21}}{15A_2}$	$\frac{4}{5} C^*_{D_{5,0}}$	$\frac{\pi m\,A_{39}}{5A_2}$	$\frac{5}{6} C^*_{D_{5,1}}$	$\frac{2}{3} C^*_{D_{5,0}}$	$\frac{32m\,A_{46}}{105A_2}$	$\frac{6}{7} C^*_{D_{5,3}}$	$\frac{5}{7} C^*_{D_{5,1}}$	$\frac{5}{7} C^*_{D_{5,5}}$
6	$-2\pi m\,A_{[illegible]} / 5A_3$	$16m\,A_{2[illegible]} / 15\pi\,A_3$	$\frac{5}{6} C^*_{D_{6,0}}$	$\frac{m\,A_{40}}{7A_3}$	$\frac{6}{7} C^*_{D_{6,1}}$	$\frac{5}{7} C^*_{D_{6,0}}$	$\frac{8m\,A_{17}}{105\pi\,A_3}$	$\frac{7}{8} C^*_{D_{6,3}}$	$\frac{3}{4} C^*_{D_{6,1}}$	$\frac{7}{8} C^*_{D_{6,5}}$
7	$\frac{\pi m\,a_6\,c_{32}}{A_3}$	$\frac{16m\,a_6\,A_{30}}{15A_3}$	$\frac{5}{6} C^*_{D_{7,0}}$	$\frac{\pi m\,a_6\,A_{19}}{42A_3}$	$\frac{6}{7} C^*_{D_{7,1}}$	$\frac{5}{7} C^*_{D_{7,0}}$	$\frac{32m\,a_6\,A_{47}}{105A_3}$	$\frac{7}{8} C^*_{D_{7,3}}$	$\frac{3}{4} C^*_{D_{7,1}}$	$\frac{7}{8} C^*_{D_{7,5}}$
8	$\frac{m\,A_9}{5A_3}$	$\frac{4m\,A_{20}}{135\pi\,A_3}$	$\frac{5}{6} C^*_{D_{8,0}}$	$\frac{m\,A_{41}}{210A_3}$	$\frac{6}{7} C^*_{D_{8,1}}$	$\frac{5}{7} C^*_{D_{8,0}}$	$\frac{4m\,A_{48}}{315\pi\,A_3}$	$\frac{7}{8} C^*_{D_{8,3}}$	$\frac{3}{4} C^*_{D_{8,1}}$	$\frac{7}{8} C^*_{D_{8,5}}$
9	$\frac{-3\pi m\,a_6\,c_{42}}{A_3}$	$\frac{16m\,a_6\,A_{28}}{5A_3}$	$\frac{5}{6} C^*_{D_{9,0}}$	$\frac{\pi m\,a_6\,A_{42}}{2A_3}$	$\frac{6}{7} C^*_{D_{9,1}}$	$\frac{5}{7} C^*_{D_{9,0}}$	$\frac{32m\,a_6\,A_{49}}{35A_3}$	$\frac{7}{8} C^*_{D_{9,3}}$	$\frac{3}{4} C^*_{D_{9,1}}$	$\frac{7}{8} C^*_{D_{9,5}}$

8.3 Tabulated $C_{D_{i,j}}^{*}$ Functions

B. Sonic Leading Edges

i \ j	0	1	2	3	4	5	6	7	8	9
0	4.00000	1.69765	2.66667	1.00000	1.27324	2.00000	.67906	.80000	1.01859	1.60000
1	1.33333	.70735	1.00000	.46667	.56588	.80000	.33953	.38889	.47157	.66667
2	2.66667	1.13177	2.00000	.66667	.90541	1.60000	.45271	.55556	.75451	1.33333
3	.66667	.40744	.53333	.28889	.33953	.44444	.21989	.24762	.29103	.38095
4	1.00000	.54891	.80000	.36667	.45742	.66667	.26839	.31429	.39208	.57143
5	2.00000	.86014	1.60000	.51111	.71679	1.33333	.34923	.43810	.61439	1.14286
6	.40000	.26837	.33333	.20000	.23005	.28571	.15729	.17500	.20129	.25000
7	.53333	.33630	.44444	.24127	.28825	.38095	.18478	.21111	.25222	.33333
8	.80000	.45136	.66667	.30476	.38688	.57143	.22439	.26667	.33852	.50000
9	1.60000	.69846	1.33333	.41905	.59868	1.14286	.28825	.36667	.52385	1.00000

8.3 Tabulated $C_{D_{i,j}}{}^*$ Functions

C. Supersonic Leading Edges

i \ j	0	1	2	3	4	5	
0	4	$\frac{8[m^2\Theta+\sqrt{m^2-1}]}{3\pi m\sqrt{m^2-1}}$	$\frac{2}{3}C_{D_{0,0}}{}^*$	$\frac{2m^2+1}{3m^2}$	$\frac{3}{4}C_{D_{0,1}}{}^*$	$\frac{1}{2}C_{D_{0,0}}{}^*$	4[3m … / 1…
1	$\frac{4}{3}$	$\frac{2[m^2 a_{67}\Theta+a_{17}\sqrt{m^2-1}]}{3\pi m(m^2-1)^{3/2}}$	$\frac{3}{4}C_{D_{1,0}}{}^*$	$\frac{6m^2+1}{15m^2}$	$\frac{4}{5}C_{D_{1,1}}{}^*$	$\frac{3}{5}C_{D_{1,0}}{}^*$	2[3m … / 45π…
2	$\frac{8}{3}$	$\frac{2[m^2 k_{15}\Theta+c_{14}\sqrt{m^2-1}]}{3\pi m(m^2-1)^{3/2}}$	$\frac{3}{4}C_{D_{2,0}}{}^*$	$\frac{2(4m^2+1)}{15m^2}$	$\frac{4}{5}C_{D_{2,1}}{}^*$	$\frac{3}{5}C_{D_{2,0}}{}^*$	2[3m … / 45…
3	$\frac{2}{3}$	$\frac{2[3m^2 a_{68}\Theta+b_{36}\sqrt{m^2-1}]}{15\pi m(m^2-1)^{5/2}}$	$\frac{4}{5}C_{D_{3,0}}{}^*$	$\frac{12m^2+1}{45m^2}$	$\frac{5}{6}C_{D_{3,1}}{}^*$	$\frac{2}{3}C_{D_{3,0}}{}^*$	2[3m … / 315…
4	1	$\frac{2[r^2 b_{40}\Theta+b_{41}\sqrt{m^2-1}]}{15\pi m(m^2-1)^{5/2}}$	$\frac{4}{5}C_{D_{4,0}}{}^*$	$\frac{10m^2+1}{30m^2}$	$\frac{5}{6}C_{D_{4,1}}{}^*$	$\frac{2}{3}C_{D_{4,0}}{}^*$	2[m^4 … / 10…
5	2	$\frac{2[m^2 b_{32}\Theta+3b_{33}\sqrt{m^2-1}]}{15\pi m(m^2-1)^{5/2}}$	$\frac{4}{5}C_{D_{5,0}}{}^*$	$\frac{20m^2+1}{45m^2}$	$\frac{5}{6}C_{D_{5,1}}{}^*$	$\frac{2}{3}C_{D_{5,0}}{}^*$	2[3m … / 105…
6	$\frac{2}{5}$	$\frac{[3m^2 a_{70}\Theta+b_{37}\sqrt{m^2-1}]}{45\pi m(m^2-1)^{7/2}}$	$\frac{5}{6}C_{D_{6,0}}{}^*$	$\frac{20m^2+1}{105m^2}$	$\frac{6}{7}C_{D_{6,1}}{}^*$	$\frac{5}{7}C_{D_{6,0}}{}^*$	($3m^6$ … / 420…
7	$\frac{8}{15}$	$\frac{[3m^2 b_{42}\Theta+b_{43}\sqrt{m^2-1}]}{45\pi m(m^2-1)^{7/2}}$	$\frac{5}{6}C_{D_{7,0}}{}^*$	$\frac{4(18m^2+1)}{315m^2}$	$\frac{6}{7}C_{D_{7,1}}{}^*$	$\frac{5}{7}C_{D_{7,0}}{}^*$	[15m … / 126…
8	$\frac{4}{5}$	$\frac{[5m^2 b_{44}\Theta+b_{45}\sqrt{m^2-1}]}{45\pi m(m^2-1)^{7/2}}$	$\frac{5}{6}C_{D_{8,0}}{}^*$	$\frac{2(15m^2+1)}{105m^2}$	$\frac{6}{7}C_{D_{8,1}}{}^*$	$\frac{5}{7}C_{D_{8,0}}{}^*$	[m^4 k… / 420…
9	$\frac{8}{5}$	$\frac{[3m^2 b_{38}\Theta+b_{39}\sqrt{m^2-1}]}{45\pi m(m^2-1)^{7/2}}$	$\frac{5}{6}C_{D_{9,0}}{}^*$	$\frac{4(10m^2+1)}{105m^2}$	$\frac{6}{7}C_{D_{9,1}}{}^*$	$\frac{5}{7}C_{D_{9,0}}{}^*$	[$3m^4$ … / 420…

A

	4	5	6	7	8	9
+1 / 2	$\frac{3}{4} C_{D_{0,1}}^{*}$	$\frac{1}{2} C_{D_{0,0}}^{*}$	$\frac{4[3m^4\Theta + a_{24}\sqrt{m^2-1}]}{15\pi m^3\sqrt{m^2-1}}$	$\frac{4}{5} C_{D_{0,3}}^{*}$	$\frac{3}{5} C_{D_{0,1}}^{*}$	$\frac{4}{5} C_{D_{0,5}}^{*}$
+1 / 2	$\frac{4}{5} C_{D_{1,1}}^{*}$	$\frac{3}{5} C_{D_{1,0}}^{*}$	$\frac{2[3m^4 k_1\Theta + k_2\sqrt{m^2-1}]}{45\pi m^3 (m^2-1)^{3/2}}$	$\frac{5}{6} C_{D_{1,3}}^{*}$	$\frac{2}{3} C_{D_{1,1}}^{*}$	$\frac{5}{6} C_{D_{1,5}}^{*}$
2 +1) / m^2	$\frac{4}{5} C_{D_{2,1}}^{*}$	$\frac{3}{5} C_{D_{2,0}}^{*}$	$\frac{2[3m^4 k_5\Theta + k_6\sqrt{m^2-1}]}{45\pi m^3 (m^2-1)^{3/2}}$	$\frac{5}{6} C_{D_{2,3}}^{*}$	$\frac{2}{3} C_{D_{2,1}}^{*}$	$\frac{5}{6} C_{D_{2,5}}^{*}$
+1 / 2	$\frac{5}{6} C_{D_{3,1}}^{*}$	$\frac{2}{3} C_{D_{3,0}}^{*}$	$\frac{2[3m^4 k_3\Theta + k_4\sqrt{m^2-1}]}{315\pi m^3 (m^2-1)^{5/2}}$	$\frac{6}{7} C_{D_{3,3}}^{*}$	$\frac{5}{7} C_{D_{3,1}}^{*}$	$\frac{6}{7} C_{D_{3,5}}^{*}$
+1 / 2	$\frac{5}{6} C_{D_{4,1}}^{*}$	$\frac{2}{3} C_{D_{4,0}}^{*}$	$\frac{2[m^4 k_{11}\Theta + k_{12}\sqrt{m^2-1}]}{105\pi m^3 (m^2-1)^{5/2}}$	$\frac{6}{7} C_{D_{4,3}}^{*}$	$\frac{5}{7} C_{D_{4,1}}^{*}$	$\frac{6}{7} C_{D_{4,5}}^{*}$
1	$\frac{5}{6} C_{D_{5,1}}^{*}$	$\frac{2}{3} C_{D_{5,0}}^{*}$	$\frac{2[3m^4 k_7\Theta + k_8\sqrt{m^2-1}]}{105\pi m^3 (m^2-1)^{5/2}}$	$\frac{6}{7} C_{D_{5,3}}^{*}$	$\frac{5}{7} C_{D_{5,1}}^{*}$	$\frac{6}{7} C_{D_{5,5}}^{*}$
1	$\frac{6}{7} C_{D_{6,1}}^{*}$	$\frac{5}{7} C_{D_{6,0}}^{*}$	$\frac{(3m^6 b_{26}\Theta + b_{27}\sqrt{m^2-1}]}{420\pi m^5 (m^2-1)^{7/2}}$	$\frac{7}{8} C_{D_{6,3}}^{*}$	$\frac{3}{4} C_{D_{6,1}}^{*}$	$\frac{7}{8} C_{D_{6,5}}^{*}$
+1) / 2	$\frac{6}{7} C_{D_{7,1}}^{*}$	$\frac{5}{7} C_{D_{7,0}}^{*}$	$\frac{[15m^4 k_{13}\Theta + k_{14}\sqrt{m^2-1}]}{1260\pi m^3 (m^2-1)^{7/2}}$	$\frac{7}{8} C_{D_{7,3}}^{*}$	$\frac{3}{4} C_{D_{7,1}}^{*}$	$\frac{7}{8} C_{D_{7,5}}^{*}$
+1) / 2	$\frac{6}{7} C_{D_{8,1}}^{*}$	$\frac{5}{7} C_{D_{8,0}}^{*}$	$\frac{[m^4 k_{62}\Theta + k_{63}\sqrt{m^2-1}]}{420\pi m^3 (m^2-1)^{7/2}}$	$\frac{7}{8} C_{D_{8,3}}^{*}$	$\frac{3}{4} C_{D_{8,1}}^{*}$	$\frac{7}{8} C_{D_{8,5}}^{*}$
+1) / 2	$\frac{6}{7} C_{D_{9,1}}^{*}$	$\frac{5}{7} C_{D_{9,0}}^{*}$	$\frac{[3m^4 k_9\Theta + k_{10}\sqrt{m^2-1}]}{420\pi m^3 (m^2-1)^{7/2}}$	$\frac{7}{8} C_{D_{9,3}}^{*}$	$\frac{3}{4} C_{D_{9,1}}^{*}$	$\frac{7}{8} C_{D_{9,5}}^{*}$

B

8.3 Tabulated $\frac{C^*_{D_{i,j}}}{A}$ Functions

D. Limiting Case, m = 0 (M = 1.0)

i \ j	0	1	2	3	4	5
0	1.57080000	.66666667	1.04720000	.39270000	.50000000	.78540000
1	.66666667	.31830914	.50000000	.20000000	.25464731	.40000000
2	1.57080000	.66666667	1.17810000	.39270000	.53333333	.94248000
3	.39270000	.20000000	.31416000	.13090000	.16666667	.26180000
4	.66666667	.31830914	.53333333	.20000000	.26525762	.44444444
5	1.57080000	.66666667	1.25664000	.39270000	.55555556	1.04720000
6	.26666667	.14147073	.22222222	.69523810	.12126063	.19047619
7	.39270000	.20000000	.32725000	.13090000	.17142857	.28050000
8	.66666667	.31830914	.55555556	.20000000	.27283641	.47619048
9	1.57080000	.66666667	1.30900000	.39270000	.57142857	1.12200000

A

M = 1.0)

2	3	4	5	6	7	8	9
4720000	.39270000	.50000000	.78540000	.26666667	.31416000	.40000000	.62832000
000000	.20000000	.25464731	.40000000	.14147073	.16666667	.21220609	.33333333
810000	.39270000	.53333333	.94248000	.26666667	.32725000	.44444444	.78540000
416000	.13090000	.16666667	.26180000	.09523810	.11220000	.14285714	.22440000
333333	.20000000	.26525762	.44444444	.14147073	.17142857	.22736367	.38095238
664000	.39270000	.55555556	1.04720000	.26666667	.33660000	.47619048	.89760000
222222	.69523810	.12126063	.19047619	.22222222	.08333333	.10610305	.16666667
725000	.13090000	.17142857	.28050000	.09523810	.11453750	.15000000	.24543750
555556	.20000000	.27283641	.47619048	.14147073	.17500000	.23873186	.41666667
00000	.39270000	.57142857	1.12200000	.26666667	.34361250	.50000000	.98175000

B

8.4 **Tabulated $T^*_{i,j}$ Functions**

A. $m \leq 0$

i \ j	0	1	2	3	4	5
0	$-\frac{\pi m\sqrt{1-m^2}}{E^2}$	$-\frac{8m(1-m^2)^{3/2}}{3A_1}$	$-\frac{4\pi m(1-m^2)^{3/2}}{3A_1E}$	$+\frac{2\pi m(1-m^2)^{3/2}A_1}{A_2E}$	$-\frac{2m(1-m^2)^{3/2}A_{50}}{A_2E}$	$-\frac{2\pi m(}{A}$
1	---	$-\frac{2m(1-m^2)^{5/2}E^2}{\pi A_1^2}$	$-\frac{2m(1-m^2)^{5/2}E}{A_1^2}$	$+\frac{16m(1-m^2)^{5/2}E}{5A_2}$	$-\frac{16m(1-m^2)^{5/2}A_{50}E}{5\pi A_1A_2}$	$-\frac{16m(1}{5}$
2	---	----	$-\frac{\pi m(1-m^2)^{5/2}}{2A_1^2}$	$+\frac{8\pi m(1-m^2)^{5/2}}{5A_2}$	$-\frac{8m(1-m^2)^{5/2}A_{50}}{5A_1A_2}$	$-8\pi m($
3	---	----	----	$-\frac{4\pi m(1-m^2)^{5/2}}{3A_2^2}$	$+\frac{8m(1-m^2)^{5/2}A_{50}}{3A_2^2}$	$+8\pi m($
4	---	----	----	----	$-\frac{4m(1-m^2)^{5/2}A_{50}^2}{3\pi A_2^2}$	$-8\pi m($
5	---	----	----	----	----	$-\frac{4\pi m(1}{3}$
6	---	----	----	----	----	
7	---	----	----	----	----	
8	---	----	----	----	----	
9	---	----	----	----	----	

A

	5	6	7	8	9
$)^{3/2}A_{50}$ … E	$-\frac{2\pi m(1-m^2)^{3/2}A_4}{A_2E}$	$-\frac{16m(1-m^2)^{5/2}A_2}{5A_3E}$	$+\frac{8\pi m(1-m^2)^{5/2}C_3}{5A_3E}$	$-\frac{8m(1-m^2)^{5/2}A_{51}}{15A_3E}$	$-\frac{24\pi m(1-m^2)^{5/2}A_5}{5A_3E}$
$^2)^{5/2}A_{50}E$ … A_2	$-\frac{16m(1-m^2)^{5/2}A_4E}{5A_1A_2}$	$-\frac{16m(1-m^2)^{7/2}A_2E}{3\pi A_1A_3}$	$+\frac{8m(1-m^2)^{7/2}C_3E}{3A_1A_3}$	$-\frac{8m(1-m^2)^{7/2}A_{51}E}{9\pi A_1A_3}$	$-\frac{8m(1-m^2)^{7/2}A_5E}{A_1A_3}$
$)^{5/2}A_{50}$ … $_2$	$-\frac{8\pi m(1-m^2)^{5/2}A_4}{5A_2}$	$-\frac{8m(1-m^2)^{7/2}A_2}{3A_1A_3}$	$+\frac{4\pi m(1-m^2)^{7/2}C_3}{3A_1A_3}$	$-\frac{4m(1-m^2)^{7/2}A_{51}}{9A_1A_3}$	$-\frac{4\pi m(1-m^2)^{7/2}A_5}{A_1A_3}$
$)^{5/2}A_{50}$ … ^{2} $_2$	$+\frac{8\pi m(1-m^2)^{5/2}A_1A_4}{3A_2^2}$	$+\frac{32m(1-m^2)^{7/2}A_1}{7A_3}$	$-\frac{16\pi m(1-m^2)^{7/2}A_1C_3}{7A_2A_3}$	$+\frac{16m(1-m^2)^{7/2}A_{51}}{21A_2A_3}$	$+\frac{48\pi m(1-m^2)^{7/2}A_1A_5}{7A_2A_3}$
$^{5/2}A_{50}^2$ … ^{2} $_2$	$-\frac{8\pi m(1-m^2)^{5/2}A_4A_{50}}{3A_2^2}$	$-\frac{32m(1-m^2)^{7/2}A_{50}}{7\pi A_3}$	$+\frac{16m(1-m^2)^{7/2}A_{50}C_3}{7A_2A_3}$	$-\frac{16m(1-m^2)^{7/2}A_{50}A_{51}}{21\pi A_2A_3}$	$-\frac{48m(1-m^2)^{7/2}A_5A_{50}}{7A_2A_3}$
- -	$-\frac{4\pi m(1-m^2)^{5/2}A_4^2}{3A_2^2}$	$-\frac{32m(1-m^2)^{7/2}A_4}{7A_3}$	$+\frac{16\pi m(1-m^2)^{7/2}A_4C_3}{7A_2A_3}$	$-\frac{16m(1-m^2)^{7/2}A_4A_{51}}{21A_2A_3}$	$-\frac{48\pi m(1-m^2)^{7/2}A_4A_5}{7A_2A_3}$
- -	- - - -	$-\frac{4m(1-m^2)^{9/2}A_2^2}{\pi A_3^2}$	$+\frac{4m(1-m^2)^{9/2}A_2C_3}{A_3^2}$	$-\frac{4m(1-m^2)^{9/2}A_2A_{51}}{3\pi A_3^2}$	$-\frac{12m(1-m^2)^{9/2}A_2A_5}{A_3^2}$
- -	- - - -	- - - -	$-\frac{\pi m(1-m^2)^{9/2}C_3^2}{A_3^2}$	$+\frac{2m(1-m^2)^{9/2}A_{51}C_3}{3A_3^2}$	$+\frac{6\pi m(1-m^2)^{9/2}C_3A_5}{A_3^2}$
- -	- - - -	- - - -	- - - -	$-\frac{m(1-m^2)^{9/2}A_{51}^2}{9\pi A_3^2}$	$-\frac{2\pi m(1-m^2)^{9/2}A_5A_{51}}{A_3^2}$
- -	- - - -	- - - -	- - - - B	- - - -	$-\frac{9\pi m(1-m^2)^{9/2}A_5^2}{A_3^2}$

8.4 Tabulated $\frac{T^*_{i,j}}{A}$ Functions

B. Limiting Case, m = 0 (M = 1.0)

i \ j	0	1	2	3	4	5
0	-.78540000	-.16666667	-1.04720000	-.39270000	-.50000000	-.78540000
1	---	-.15915457	-.50000000	-.20000000	-.25464731	-.40000000
2	---	---	-.39270000	-.31416000	-.40000000	-.62832000
3	---	---	---	-.06545000	-.1666667	-.26180000
4	---	---	---	---	-.10610305	-1.04720000
5	---	---	---	---	---	-.26180000
6	---	---	---	---	---	---
7	---	---	---	---	---	---
8	---	---	---	---	---	---
9	---	---	A ---	---	---	---

4	5	6	7	8	9
0000000	-.78540000	-.26666667	-.31416000	-.40000000	-.62832000
5464731	-.40000000	-.14147073	-.16666667	-.21220609	-.33333333
0000000	-.62832000	-.22222222	-.26180000	-.33333333	-.52360000
666667	-.26180000	-.09523810	-.11220000	-.14285714	-.22440000
0610305	-1.04720000	-.12126062	-.14285714	-.18189094	-.28571428
- - -	-.26180000	-.76190476	-.22440000	-.28571428	-.44880000
- - -	- - -	-.03536768	-.08333333	-.10610305	-.16666667
- - -	- - -	- - -	-.04908750	-.12500000	-.19635000
- - -	- - -	- - -	- - -	-.07957729	-.78540000
- - -	- - -	- - -	- - -	- - -	-.19635000

B

8.5 Tabulated Geometric Boundary Condition Functions

Note: These functions are not related to any aerodynamic quantities.

$$A_0 = 12$$

$$A_1 = 12$$

$$A_2 = 12 + 6\, m_1 X_{22}$$

$$A_3 = 12 + 6\, m_1 X_{23}$$

$$A_4 = 12 + 6\, m_1 X_{24}$$

$$A_5 = 12 + 6\, m_1 X_{25} + 4\, m_1^2 X_{55}$$

$$A_6 = 12 + 6\, m_1 X_{26} + 4\, m_1^2 X_{56}$$

$$A_7 = 12 + 6\, m_1 X_{27} + 4\, m_1^2 X_{57}$$

$$A_8 = 12 + 6\, m_1 X_{28} + 4\, m_1^2 X_{58}$$

$$A_9 = 12 + 6\, m_1 X_{29} + 4\, m_1^2 X_{59} + 3\, m_1^3 X_{99}$$

$$B_0 = -6\,n_1$$

$$B_1 = -6\,n_1 + 6\,m_1\,X_{11}$$

$$B_2 = -6\,n_1 + 6\,m_1\,X_{12}$$

$$B_3 = -6\,n_1 + 6\,m_1\,X_{13}$$

$$B_4 = -6\,n_1 + 6\,m_1\,X_{14} + 3\,m_1^2\,X_{44}$$

$$B_5 = -6\,n_1 + 6\,m_1\,X_{15} + 3\,m_1^2\,X_{45}$$

$$B_6 = -6\,n_1 + 6\,m_1\,X_{16} + 3\,m_1^2\,X_{46}$$

$$B_7 = -6\,n_1 + 6\,m_1\,X_{17} + 3\,m_1^2\,X_{47}$$

$$B_8 = -6\,n_1 + 6\,m_1\,X_{18} + 3\,m_1^2\,X_{48} + 2\,m_1^3\,X_{88}$$

$$B_9 = -6\,n_1 + 6\,m_1\,X_{19} + 3\,m_1^2\,X_{49} + 2\,m_1^3\,X_{99}$$

$$C_0 = 0$$

$$C_1 = -2\,n_1\,X_{11}$$

$$C_2 = -2\,n_1\,X_{12} - n_1^2\,X_{22}$$

$$C_3 = -2\,n_1\,X_{13} - n_1^2\,X_{23} + 2\,m_1\,X_{33}$$

$$C_4 = -2\,n_1\,X_{14} - n_1^2\,X_{24} + 2\,m_1\,X_{34}$$

$$C_5 = -2\,n_1\,X_{15} - n_1^2\,X_{25} + 2\,m_1\,X_{35}$$

$$C_6 = -2n_1 X_{16} - n_1^2 X_{26} + 2m_1 X_{36}$$

$$C_7 = -2n_1 X_{17} - n_1^2 X_{27} + 2m_1 X_{37} + m_1^2 X_{77}$$

$$C_8 = -2n_1 X_{18} - n_1^2 X_{28} + 2m_1 X_{38} + m_1^2 X_{78}$$

$$C_9 = -2n_1 X_{19} - n_1^2 X_{29} + 2m_1 X_{39} + m_1^2 X_{79}$$

$$D_0 = 0$$

$$D_1 = 0$$

$$D_2 = 0$$

$$D_3 = -6n_1 X_{33}$$

$$D_4 = -6n_1 X_{34} - 3n_1^2 X_{44}$$

$$D_5 = -6n_1 X_{35} - 3n_1^2 X_{45} - 2n_1^3 X_{55}$$

$$D_6 = -6n_1 X_{36} - 3n_1^2 X_{46} - 2n_1^3 X_{56} + 6m_1 X_{66}$$

$$D_7 = -6n_1 X_{37} - 3n_1^2 X_{47} - 2n_1^3 X_{57} + 6m_1 X_{67}$$

$$D_8 = -6n_1 X_{38} - 3n_1^2 X_{48} - 2n_1^3 X_{58} + 6m_1 X_{68}$$

$$D_9 = -6n_1 X_{39} - 3n_1^2 X_{49} - 2n_1^3 X_{59} + 6m_1 X_{69}$$

$$E_0 = 0$$

$$E_1 = 0$$

$$E_2 = 0$$

$$E_3 = 0$$

$$E_4 = 0$$

$$E_5 = 0$$

$$E_6 = 12 \; X_{66}$$

$$E_7 = 12 \; X_{67} + 6 \, n_1 \, X_{77}$$

$$E_8 = 12 \; X_{68} + 6 \, n_1 \, X_{78} + 4 \, n_1^{\,2} \, X_{88}$$

$$E_9 = 12 \; X_{69} + 6 \, n_1 \, X_{79} + 4 \, n_1^{\,2} \, X_{89} + 3 \, n_1^{\,3} \, X_{99}$$

9.0 ILLUSTRATIVE EXAMPLES

9.1 Design Procedure

Inputs: sonic leading edge: "δ": $m_d = 1,\ C_{L_d} = .136$

"β": $m_d = 1,\ C_{L_d} = .136,\ x_m = .36$

"α": $m_d = 1,\ C_{L_d} = .136,\ x_m = .36,$

$m_1 = .92,\ n_1 = \frac{1}{.85}$

supersonic leading edge: "δ_a": $m_d = 1.323,\ C_{L_d} = .087$

"β_a": $m_d = 1.323,\ C_{L_d} = .087,$

$x_m = .36$

"α_a": $m_d = 1.323,\ C_{L_d} = .087,$

$x_m = .36,\ m_1 = .92,\ n_1 = \frac{1}{.85}$

1. At m_d, compute $C_{D_{i,i}}{}^*$ from section 5.3. Results presented in section 5.3 B. for sonic edge and in Table III for supersonic edge.
2. At m_d, obtain $C_{L_i}{}^*$ from tabulated $C_{D_{i,j}}{}^*$, $C_{L_i}{}^* = C_{D_{i,o}}{}^*$.
3. At m_d, compute $C_{M_i}{}^* = -\frac{3}{2}\ \frac{2+r+s}{3+n+s}\ C_{L_i}{}^*$.
4. Compute $\lambda_{i,j}$, equation (4.22). Results presented in Tables IV A) and B).
5. At m_d, compute X_{ik} from equation (4.31). Results presented in Tables V A) and B).

6. At m_d, compute $(C_L^*)^{(k)}$, $(C_M^*)^{(k)}$, $(C_D^*)^{(k)}$ from equations (4.39), (4.4?), and (4.36). Results presented in Table VI.

7. Solve following matrix, the size of which depends upon the number of terms, n, of the series, for "5" class of wings:

$$\begin{bmatrix} 2(C_D^*)^{(k)} & (C_L^*)^{(k)} \\ (C_L^*)^{(k)} & 0 \end{bmatrix} \begin{Bmatrix} \bar{a}_{kn} \\ \Omega_1 \end{Bmatrix} = \begin{Bmatrix} \{0\} \\ 1.0 \end{Bmatrix}$$

Results for $\bar{a}_{kn}$ and Ω_1 presented in Tables VII A) and B) for n = 0, 1, 2 . . . 9.

8. Solve following 12 × 12 matrix for "β" class of wings:

$$\begin{bmatrix} 2(C_D^*)^{(k)} & (C_L^*)^{(k)} & (C_M^*)^{(k)} \\ (C_L^*)^{(k)} & & \\ & 0 & \\ (C_M^*)^{(k)} & & \end{bmatrix} \begin{Bmatrix} \bar{a}_{kn} \\ \\ \Omega_i \end{Bmatrix} = \begin{Bmatrix} 0 \\ 1.0 \\ -\left(\frac{1+2x_m}{2}\right) \end{Bmatrix}$$

Results for $\bar{a}_{k9}$, Ω_i (k = 0, 1 . . . 9, i = 1, 2) presented in Table VIII.

9. For wing with two straight hinge-lines only compute A_k, B_k, C_k, D_k, E_k, F_k from section 8.5. Results tabulated in following section 10.

10. Solve following 16 × 16 matrix for "α" class of wings:

$$\begin{bmatrix} 2(C_D^*)^{(k)} & (C_L^*)^{(k)} & (C_M^*)^{(k)} & C_k & D_k & F_k & E_k \\ (C_L^*)^{(k)} & & & & & & \\ (C_M^*)^{(k)} & & & & & & \\ C_k & & & & & & \\ D_k & & & 0 & & & \\ F_k & & & & & & \\ E_k & & & & & & \end{bmatrix} \begin{Bmatrix} \bar{a}_{kn} \\ \\ \\ \Omega_i \\ \\ \end{Bmatrix} = \begin{Bmatrix} 0 \\ 1.0 \\ \frac{1+2x_m}{2} \\ 0 \end{Bmatrix}$$

This matrix is presented as Table VIII. The inputs for steps 7 and 8 may be obtained directly therefrom. Results for $\bar{a}_{kn}$, Ω_i (k = 0, 1 ... 9, i = 1, 2 ... 6) presented in Table IX.

11. For subsonic m ($\neq m_d$) only compute $C_{D_{i,j}}{}^*$ from section 8.3 and $\lambda_{i,j}$ and $T_{i,j}$ from section 8.4. Results presented in Tables X and XII. These results will be used later to obtain drag polar for subsonic leading edge speeds.

12. For subsonic m_d with suction only: compute for each k = 0, 1 ... 9 and n = 9

$$q_T X_{kk} \left[\sum_{p=0}^{i} X_{pi} T^*_{p,k} \sum_{i=0}^{k} \bar{a}_{in} + \sum_{p=0}^{i} X_{pi} T^*_{p,k} \right.$$

$$\left. + \sum_{p=k+1}^{i} X_{pi} T^*_{k,p} \left[\sum_{i=k+1}^{n} \bar{a}_{in} \right] \right]$$

where q_T is assumed to be unity. $T^*_{p,k}$ and $T^*_{k,p}$ are obtained from Table XII and X_{ik} is obtained from Table V. This computation will result in a contribution to each term of the 10 × 10 diagonal matrix of steps 7, 8, and 10. The procedures of steps 7, 8, and 10 should be solved with this change for the three wing types. No subsonic design was carried out.

13. At m_d, $\bar{\psi}_{k9}$ are obtained from equation (4.42). Results are presented in Table XIII.

14. For wings with two straight hinge-lines only, compute

$$\zeta_3 = \sum_{k=0}^{9} A_k \bar{a}_{kn}$$

$$\zeta_1 = 0 \; (Z' = 0 \text{ at } x' = y' = 0)$$

$$\zeta_2 = -\zeta_0 = \frac{1}{2} \sum_{k=0}^{9} B_k \bar{a}_{kn} \quad .$$

15. At m_d compute $Z'/\beta C_{L_d}$ from equation (4.44). Results are plotted in figures 5.13 (a) and (b).

This completes the design phase. The following procedure is used to obtain drag polars, pitching-moment versus lift, span and chord loadings.

16. Repeat steps (1) - (3) for each value of m for which the drag polar is required. Repeat step (11) for m < 1.

17. For each wing defined by a set of $\mathcal{J}_{k9}$ retain $\mathcal{J}_{k9}$ for $k \geq 1$. Compute $\mathcal{J}_{o9}$ versus C_L/C_{L_d} :

$$\mathcal{J}_{o9} = \frac{\dfrac{C_L}{C_{L_d}} - \sum_{i=1}^{n=9} \mathcal{J}_{i9}\, C^*_{L_i}}{C^*_{L_o}}$$

where $C^*_{L_i}$ were computed in step 16.

18. Compute $C_D/\beta C_{L_d}^2$

$$C_D/\beta C_{L_d}^2 = \mathcal{J}_{o9}^2\, C^*_{D_{o,o}} + \mathcal{J}_{o9} \sum_{i=1}^{9} \mathcal{J}_{i9}\, \lambda_{o,i}$$

$$+ \frac{1}{2} \sum_{i=1}^{9} \mathcal{J}_{i9}^2\, \lambda_{i,i} + \sum_{i=1}^{9} \mathcal{J}_{i9} \sum_{j=2}^{9} \mathcal{J}_{j9}\, \lambda_{i,j}$$

$$+ \ {}^{1}T \left[\bar{\Psi}_{o9}^{\,2} \ T^{*}_{o,o} + \bar{\Psi}_{o9} \sum_{j=1}^{9} \bar{\Psi}_{j9} \ T^{*}_{o,j} \right.$$

$$\left. + \sum_{i=1}^{9} \bar{\Psi}_{i9} \sum_{j=1}^{9} \bar{\Psi}_{j9} \ T^{*}_{i,j} \right]$$

where the bracketed quantity is used only at $m < 1$ if suction is considered. The results are shown in figures 5.1 to 5.3.

19. Compute $\dfrac{C_{M_{.36\bar{c}}}}{C_{L_d}}$

$$\frac{C_{M_{.36\bar{c}}}}{C_{L_d}} = \bar{\Psi}_{o9} \ C^{*}_{M_o} + \sum_{k=1}^{9} \bar{\Psi}_{k9} \ C^{*}_{M_k}$$

$$+ \left(\frac{1 + 2 \, x_m}{2} \right) \frac{C_L}{C_{L_d}}$$

Results are shown in figures 5.4 to 5.6.

TABLE III

Tabulated $C_{D_{i,j}}^{*}$ for Supersonic Leading Edge Delta Wing (m = 1.3229)

i \ j	0	1	2	3	4	5	6	7	8	9
0	4.00000	1.56682	2.66666	.85714	1.17511	2.00000	.54338	.68571	.94009	1.60000
1	1.33333	.68891	1.00000	.43810	.55112	.80000	.30668	.36508	.45927	.66666
2	2.66666	1.08061	2.00000	.60952	.86449	1.60000	.39725	.50794	.72041	1.33333
3	.66666	.40339	.53333	.27937	.33616	.44444	.20700	.23946	.28813	.38095
4	1.00000	.54116	.80000	.35238	.45097	.66666	.25081	.30204	.38655	.57142
5	2.00000	.83562	1.60000	.48254	.69635	1.33333	.32050	.41360	.59687	1.14285
6	.40000	.26738	.33333	.19592	.22919	.28571	.15104	.17143	.20054	.25000
7	.53333	.33462	.44444	.23563	.28681	.38095	.17691	.20635	.25096	.33333
8	.80000	.44778	.66666	.29660	.38381	.57142	.21374	.25952	.33583	.50000
9	1.60000	.68520	1.33333	.40272	.58732	1.14285	.27123	.35238	.51390	1.00000

TABLE IV

$\lambda_{i,j}$ Functions

A. $m_d = 1.0$

i \ j	0	1	2	3	4	5	6	7	8	9
0	8.00000	3.03098	5.33334	1.66666	2.27324	4.00000	1.07906	1.33333	1.81859	3.20000
1	3.03098	1.41471	2.13177	.87410	1.11479	1.66014	.60792	.72518	.92293	1.36513
2	5.33334	2.13177	4.00000	1.20000	1.70541	3.20000	.78604	1.00000	1.42118	2.66667
3	1.66666	.87410	1.20000	.57778	.70620	.95556	.41989	.48889	.59579	.80000
4	2.27324	1.11479	1.70541	.70620	.91484	1.38345	.49844	.60254	.77896	1.17011
5	4.00000	1.66014	3.20000	.95556	1.38345	2.66667	.63494	.81905	1.18582	2.28572
6	1.07906	.60792	.78604	.41989	.49844	.63494	.31458	.35978	.42568	.53825
7	1.33333	.72518	1.00000	.48889	.60254	.81905	.35973	.42222	.51889	.70000
8	1.81859	.92293	1.42118	.59579	.77896	1.18582	.42568	.51889	.67704	1.02385
9	3.20000	1.36513	2.66667	.80000	1.17011	2.28572	.53825	.70000	1.02385	2.00000

TABLE IV

$\lambda_{i,j}$ Functions

B. m_d = 1.323

i \ j	0	1	2	3	4	5	6	7	8	9
0	8.00000	2.90015	5.33332	1.52380	2.17511	4.00000	.94338	1.21904	1.74009	3.20000
1	2.90015	1.37782	2.08061	.84149	1.09228	1.63562	.57406	.69970	.90705	1.35186
2	5.33332	2.08061	4.00000	1.14285	1.66449	3.20000	.73058	.95238	1.38707	2.66666
3	1.52380	.84149	1.14285	.55878	.68854	.92698	.40292	.47529	.58473	.78367
4	2.17511	1.09228	1.66449	.68854	.90194	1.36301	.48000	.58885	.77036	1.15874
5	4.00000	1.63562	3.20000	.92698	1.36301	2.66666	.60621	.79455	1.16829	2.28570
6	.94338	.57406	.73058	.40292	.48000	.60621	.30208	.34834	.41428	.52123
7	1.21904	.69970	.95238	.47529	.58885	.79455	.34834	.41270	.51048	.68571
8	1.74009	.90705	1.38707	.58473	.77036	1.16829	.41428	.51048	.67166	1.01390
9	3.20000	1.35186	2.66666	.78367	1.15874	2.28570	.52125	.68571	1.01390	2.00000

TABLE V

Orthogonal Weighting Numbers, X_{ik}

A. $m_d = 1.0$

i \ k	0	1	2	3	4	5	6
0	1.00000000	1.00000000	1.00000000	1.00000000	1.00000000	1.00000000	1.0000
1	- - -	-2.63941037	.82019914	-7.63179373	-3.39190044	6.42733122	-14.3882
2	- - -	- - -	-1.96612390	.25590190	-1.77173909	-7.66956789	.8142
3	- - -	- - -	- - -	8.26023442	-3.66137821	-1.17192060	37.4553
4	- - -	- - -	- - -	- - -	7.84446076	-6.59984910	-.86125
5	- - -	- - -	- - -	- - -	- - -	7.59867248	-.43696
6	- - -	- - -	- - -	- - -	- - -	- - -	-25.44035
7	- - -	- - -	- - -	- - -	- - -	- - -	- -
8	- - -	- - -	- - -	- - -	- - -	- - -	- -
9	- - -	- - -	- - -	- - -	- - -	- - -	- -

A

	4	5	6	7	8	9
	1.00000000	1.00000000	1.00000000	1.00000000	1.00000000	1.00000000
	-3.39190044	6.42733122	-14.38826824	-10.59266946	20.04671238	10.94322939
	-1.77173909	-7.66956789	.81422060	-.90779665	-18.22034812	-17.86958396
	-3.66137821	-1.17192060	37.45537664	7.80303914	-121.09680520	12.77278589
	7.84446076	-6.59984910	-.86125165	18.71090866	81.13939664	-61.79588887
	---	7.59867248	-.43696215	-.79416390	17.48320522	47.15048161
	---	---	-25.44035165	12.54795747	14.58624367	-7.79696608
	---	---	---	-27.71630819	107.07197580	-3.08943351
	---	---	---	---	-100.43084140	43.84851317
	---	---	---	---	---	-31.46024774

B

TABLE V

Orthogonal Weighting Numbers, X_{ik}

B. $m_d = 1.323$

i \ k	0	1	2	3	4	5
0	1.00000000	1.00000000	1.00000000	1.00000000	1.00000000	1.000000
1	---	-2.75847801	.89589547	-7.05462078	-3.82783598	4.356023
2	---	---	-1.98717332	.07015240	-1.92307372	-6.365035
3	---	---	---	7.93103641	-4.36241790	.3365584
4	---	---	---	---	9.19729046	-5.7985487
5	---	---	---	---	---	6.3533205
6	---	---	---	---	---	---
7	---	---	---	---	---	---
8	---	---	---	---	---	---
9	---	---	---	---	---	---

A

4	5	6	7	8	9
1.00000000	1.00000000	1.00000000	1.00000000	1.00000000	1.00000000
3.82783598	4.35602319	-15.09206687	-9.22653695	.53550654	9.35385262
1.92307372	-6.36503516	.88371949	-1.74067209	-8.40749262	-12.56021359
4.36241790	.33655847	39.12771452	6.56416860	-45.53044138	7.91130180
9.19729046	-5.79854876	-.08029822	19.12685379	47.95218670	-36.31595856
---	6.35332056	-.69923349	-.07965857	8.16515806	31.65005630
---	---	-27.47050081	15.06332213	.32673792	1.40298368
---	---	---	-30.72531763	50.48045255	-11.67865633
---	---	---	---	-54.10164811	-30.50070508
---	---	---	---	---	-21.23905279

B

TABLE VI

Orthogonalized Lift, Pitching Moment and Drag Coefficients

for Sonic and Supersonic Leading Edge Designs

	$m_d = 1.0$			$m_d = 1.323$		
K	$(C_L{}^*)^{(k)}$	$(C_M{}^*)^{(k)}$	$(C_D\ )^{(k)}$	$(C_L{}^*)^{(k)}$	$(C_M{}^*)^{(k)}$	$(C_D{}^*)^{(k)}$
0	4.00000000	-4.00000000	4.00000000	4.00000000	-4.00000000	4.00000000
1	.450794991	-.0405446	.92777943	.32203852	.13771702	1.24205461
2	-.14980748	.66807296	.76942257	-.10461117	.61767676	.74654546
3	.01355638	.07179736	.31136800	.06831982	.02664484	.33371790
4	.15636365	-.08118241	.24005200	.05702573	-.03583910	.39000779
5	-.07290818	-.00425171	.50189968	-.03296611	.00211309	.34096674
6	.04600996	-.02217679	.13304791	.01219065	.00253886	.29699663
7	.01755929	.02651813	.07615624	.03844958	.00142927	.12737657
8	.10994847	-.10250310	.70934113	-.00517115	-.01094553	.33951706
9	-.06511975	-.00031215	.3940149	-.01309560	.00155441	.13474949

TABLE VII

Tabulated Minimizing Numbers, $\bar{a}_{kn}$ for "δ" Wing

A. $m_d = 1.0$

k \ n	0	1	2	3	4	5
0	.25000000	.23534073	.23374478	.23371254	.22827862	.22772804
1	---	.12195856	.12113150	.12111480	.11829882	.11801350
2	---	---	-.04538887	-.04538261	-.04432744	-.04422053
3	---	---	---	.01017578	.00993919	.00991522
4	---	---	---	---	.14869478	.14833614
5	---	---	---	---	---	-.03308079
6	---	---	---	---	---	---
7	---	---	---	---	---	---
8	---	---	---	---	---	---
9	---	---	---	---	---	---

A

4	5	6	7	8	9
827862	.22772804	.22690588	.22669762	.22582516	.22527764
829882	.11801350	.11758744	.11747952	.11702739	.11674365
432744	-.04422053	-.04406088	-.04402044	-.04385102	-.04374471
993919	.00991522	.00987942	.00987035	.00983237	.00980853
869478	.14833614	.14780061	.14766495	.14709663	.14674002
- -	-.03308079	-.03296136	-.03293111	-.03280437	-.03272483
- -	- - -	.07846745	.07839543	.07809372	.07790438
- -	- - -	- - -	.05226951	.05206835	.05194211
- -	- - -	- - -	- - -	.03500309	.03491822
- -	- - -	- - -	- - -	- - -	-.03723215

B

TABLE VII

Tabulated Minimizing Numbers, $\bar{a}_{kn}$, for "δ_a" Wing

B. $m_d = 1.323$

k \ n	0	1	2	3	4	5
0	.25000000	.24488810	.24401215	.24330830	.24281569	.24262792
1	---	.06349431	.06326719	.06308470	.06295698	.06290829
2	---	---	-.03419269	-.03409406	0.03402503	-.03399872
3	---	---	---	.04222002	.04213454	.04210195
4	---	---	---	---	.03550378	.03547632
5	---	---	---	---	---	-.02345830
6	---	---	---	---	---	---
7	---	---	---	---	---	---
8	---	---	---	---	---	---
9	---	---	---	---	---	---

A

4	5	6	7	8	9
.24281569	.24262792	.24259846	.24191730	.24191270	.24185839
.06295698	.06290829	.06290065	.06272404	.06272285	.06270877
.03402503	-.03399872	-.03399459	-.03389914	-.03389850	-.03389089
.04213454	.04210195	.04209684	.04197864	.04197784	.04196842
03550378	.03547632	.03547201	.03537242	.03537174	.03536380
---	-.02345830	-.02345545	-.02338959	-.02338914	-.02338389
---	---	.00995780	.00992984	.00992965	.00992742
---	---	---	.07302456	.07302318	.07300678
---	---	---	---	-.00368455	-.00368372
---	---	---	---	---	-.01714364

β

8.00000000	0	0	0	0	0	0
0	1.85555888	0	0	0	0	0
0	0	1.53884522	0	0	0	0
0	0	0	.62273594	0	0	0
0	0	0	0	.48010406	0	0
0	0	0	0	0	1.00379952	0
0	0	0	0	0	0	.26609582
0	0	0	0	0	0	0
0	0	0	0	0	0	0
0	0	0	0	0	0	0
4.00000000	.48079499	-.14940748	.01355683	.15636365	-.07290818	.04600996
-4.00000000	-.04088446	.66807296	.07179736	-.08118241	-.00425171	-.02217679
0	6.21037420	.79139665	32.80179484	3.69623449	-6.65238306	101.64567210
0	0	0	-58.30750793	-6.72712108	10.93026568	-399.82233610
0	-29.13909032	-3.71323492	-82.59314638	-9.11514816	17.84475642	-159.67304270
0	0	0	0	0	0	-305.28421980

A

0	0		0	0	4.00000000	-4.00000000	0
0	0		0	0	.48079499	-.04088446	6.21037420
0	0		0	0	-.14940748	.66807296	.79139665
0	0		0	0	.01355688	.07179736	32.80179484
0	0		0	0	.15636365	-.08118241	3.59623449
0	0		0	0	-.07290818	-.00425171	-6.85238306
.26609582	0	0	0	0	.04600996	-.02217679	101.64567210
0	.15231248		0	0	.01755929	.02651818	17.07888942
0	0		1.41868226	0	.10994847	-.10250310	-154.14265690
0	0		0	.78802982	-.06511975	-.00031215	5.75359687
.04600996	.01755929		.10994847	-.06511975	0	0	0
-.02217679	.02651818		-.10250310	-.00031215	0	0	0
101.64567210	17.07888942		-154.14265690	5.75359687	0	0	0
-399.82233610	-60.92149575		541.46899080	-30.16149862	0	0	0
-159.67304270	-30.98012868		271.86849430	-4.90033197	0	0	0
-305.28421980	-45.06894094		374.81864930	-26.29468678	0	0	0

B

TABLE VIII

Tabulated Input Matrix Suitable for Steps 7, 8 and 10

000	0	0	0	0	$\bar{a}_{09}$		0
446	6.21037420	0	-29.13909032	0	$\bar{a}_{19}$		0
296	.79139665	0	-3.71323492	0	$\bar{a}_{29}$		0
736	32.80179484	-58.30750793	-82.59314638	0	$\bar{a}_{39}$		0
241	3.59623449	-6.72712108	-9.11514816	0	$\bar{a}_{49}$		0
71	-0.65238306	10.93026568	17.84475642	0	$\bar{a}_{59}$		0
79	101.64567210	-399.82233610	-159.67304270	-305.28421980	$\bar{a}_{69}$		0
18	17.07888942	-60.92149575	-30.98012868	-45.06894094	$\bar{a}_{79}$	=	0
10	-154.14265690	541.46899080	271.8684943	374.81864930	$\bar{a}_{89}$		0
15	5.75359687	-30.16149862	-4.90033197	-26.29468678	$\bar{a}_{99}$		0
	0	0	0	0	λ_1		1.0
	0	0	0	0	λ_2		-.86
	0	0	0	0	λ_3		0
	0	0	0	0	λ_4		0
	0	0	0	0	λ_5		0
	0	0	0	0	λ_6		0

C

TABLE IX

Tabulated Minimizing Numbers, $\bar{a}_{k9}$, and Lagrangian Numbers, Ω_i

	m = 1.0			m = 1.323		
K	wing "δ"	wing "β"	wing "α"	wing "δ_a"	wing "β_a"	wing "α_a"
0	.22527764	.21832508	.23612771	.24185839	.23755486	.25841132
1	.11674365	.17919850	.03265107	.06270877	.14039856	-.01463731
2	-.04374471	.05151863	.19113832	-.03389089	.11302668	.29026704
3	.00980853	.04764634	.06147854	.04196842	.09257252	-.02396235
4	.14674002	.18584365	.29077364	.03536380	.04629996	.08533328
5	-.03272483	-.05313289	-.04800801	-.02338389	-.04223226	-.02682149
6	.07790438	.10045629	.18240293	.00992742	.0230940	.00440714
7	.05194211	.13097259	-.27335159	.07300678	.13836140	-.07293541
8	.03491822	.03530287	.11296483	-.00368372	-.01372429	-.01944488
9	-.03723215	-.05921872	-.03893320	-.01714364	-.03013857	.00225664
i						
1	---	.71528444	-1.30645055	---	-.9009050	-1.60231635
2	---	.27863429	-.83419513	---	-.42579527	-1.08549372
3	---	---	1.09399773	---	---	.09591424
4	---	---	.31042628	---	---	.05365950
5	---	---	.21485543	---	---	-.00260476
6	---	---	-.15465890	---	---	-.03744934

TABLE X

$C^*_{D_{i,j}}$ at m = .8 (M = 1.72)

i \ j	0	1	2	3	4	5
0	3.54507	1.50457	2.36338	.88627	1.12843	1.77254
1	1.19040	.61840	.89280	.40427	.49472	.71424
2	2.50046	1.06123	1.87534	.62511	.84898	1.50028
3	.59417	.35431	.47534	.24882	.29526	.39611
4	.92124	.49557	.73699	.31906	.41298	.61416
5	1.91332	.81990	1.53066	.486[illegible]5	.68325	1.27555
6	.35087	.23088	.29239	.17073	.19790	.25062
7	.48126	.29753	.40105	.21190	.25502	.34376
8	.74381	.41215	.61986	.27649	.35327	.53129
9	1.53889	.66716	1.28241	.39850	.57186	1.09918

A

4	5	6	7	8	9
12843	1.77254	.60183	.70902	.90274	1.41803
49472	.71424	.29263	.33689	.41227	.59520
84898	1.50028	.42449	.52092	.70749	1.25023
29526	.39611	.18842	.21327	.25308	.33952
41298	.61416	.23957	.27348	.35398	.52642
68325	1.27555	.33156	.41661	.58564	1.09333
19790	.25062	.13370	.14939	.17316	.21929
25502	.34376	.16166	.18541	.22315	.30079
35327	.53129	.20291	.24193	.30911	.46488
57186	1.09918	.27328	.34869	.50038	.96178

B

TABLE XI

Tabulated $\lambda_{i,j}$ Numbers at m = .8 (M = 1.72)

i \ j	0	1	2	3	4	5
0	7.09014	2.69497	4.86384	1.48044	2.04967	3.68586
1	2.69497	1.23680	1.95402	.75858	.99029	1.52414
2	4.86384	1.95402	3.75068	1.10045	1.58597	3.03093
3	1.48044	.75858	1.10045	.49764	.61432	.88216
4	2.04967	.99029	1.58597	.61432	.82596	1.29741
5	3.68586	1.53414	3.03093	.88216	1.29741	2.55110
6	.95270	.52351	.71688	.35915	.43747	.58218
7	1.19028	.63442	.92197	.42517	.52850	.76037
8	1.64655	.82442	1.32733	.52957	.70725	1.11693
9	2.95692	1.26237	2.53264	.73802	1.09828	2.19251

A

4	5	6	7	8	9
2.04967	3.68586	.95270	1.19028	1.64655	2.95689
.99029	1.52414	.52351	.63442	.82442	1.26237
1.58597	3.03093	.71688	.92197	1.32733	2.53264
.61432	.88216	.35915	.42517	.52957	.73802
.82596	1.29741	.43747	.52850	.70725	1.09828
1.29741	2.55110	.58218	.76037	1.11693	2.19251
.43747	.58218	.26740	.31105	.37607	.49257
.52850	.76037	.31105	.37082	.46508	.64948
.70725	1.11693	.37607	.46508	.61825	.96526
.09828	2.19251	.49257	.64948	.96526	1.92361

B

TABLE XII

Tabulated $T^*_{i,j}$ at m = .8 (M = 1.72)

i \ j	0	1	2	3	4	5
0	-.75006849	-.63673496	-.70539762	-.38031133	-.39918064	-.42442730
1	---	-.15202290	-.33683274	-.19370833	-.20331925	-.21617842
2	---	---	-.18657763	-.21459697	-.22524429	-.17831709
3	---	---	---	-.12272945	-.18645017	-.14346646
4	---	---	---	---	-.07081362	-.47307662
5	---	---	---	---	---	-.07992746
6	---	---	---	---	---	---
7	---	---	---	---	---	---
8	---	---	---	---	---	---
9	---	---	---	---	---	---

A

4	5	6	7	8	9
39918064	-.42442730	-.25695068	-.25892735	-.27699598	-.28848687
20331925	-.21617842	-.13738991	-.13737754	-.14696410	-.15306074
22524429	-.17331709	-.15220540	-.15219172	-.16281205	-.16956614
18645017	-.14346646	-.09378370	-.09377525	-.13862131	-.10448077
07081362	-.47307662	-.09843682	-.09842795	-.33079952	-.10966463
---	-.07992746	-.41865029	-.10465315	-.11195612	-.11660050
---	---	-.03492154	-.06933679	-.07471018	-.07780945
---	---	---	-.03491524	-.07470345	-.07780245
---	---	---	---	-.03995823	-.26148074
---	---	---	---	---	-.04334225

B

TABLE XIII

Tabulated Ψ_{k9} Numbers

	m = 1.0			m = 1.323		
K	wing "δ"	wing "β"	wing "α"	wing "δ_a"	wing "β_a"	wing "α_a"
0	.54963286	.83696234	.74724424	.38673144	.70242826	.48287398
1	-2.72871959	-4.80472272	.18278224	-1.72239912	-3.17265221	.643117[illegible]1
2	.12489720	.36703383	-1.47291804	.27911418	.23270134	-.30588421
3	-1.7[illegible]869800	-.47103300	-[illegible].[illegible]7851169	1.07047030	2.60732825	.02553522
4	7.40590117	1[illegible].69653731	8.89786642	2.30238191	3.751[illegible]0880	-1.46939469
5	-1.46898848	-2.72663258	-.[illegible]8814618	-.73320368	-1.35786145	-.25467238
6	-.53052396	.06445776	-6.119[illegible]6543	.84986208	1.47950478	-1.22290327
7	2.41414553	.33282367	19.7[illegible]1[illegible]45[illegible]	-2.2288[illegible]768	-4.5[illegible]202833	1.23302277
8.	-5.13[illegible]44063	-6.14214[illegible]76	-13.05231586	-.32359778	-.17674093	1.12082[illegible]17
[illegible]	1.17133266	1.86303560	1.22484812	.36411467	.54011468	-.047[illegible]28[illegible]0